ICUS REPORT 2007-01

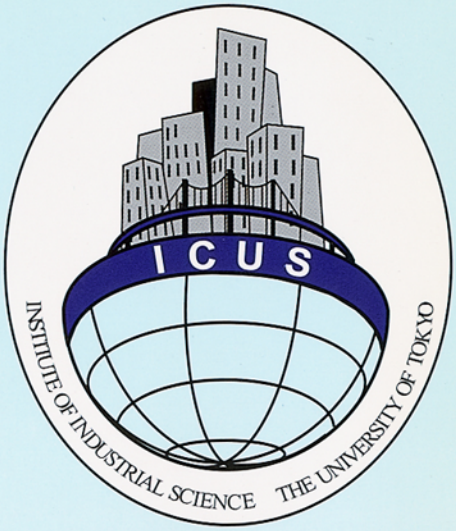

INTERNATIONAL CENTER FOR
URBAN SAFETY ENGINEERING

INSTITUTE OF INDUSTRIAL SCIENCE
THE UNIVERSITY OF TOKYO

REPORT ON INSPECTION OF MARINE REINFORCED CONCRETE STRUCTURES IN THAILAND

Edited by

Pakawat Sancharoen, Raktipong Sahamitmongkol,
Isao Kurashige, Yoshitaka Kato and Taketo Uomoto
ICUS, IIS, The University of Tokyo, Japan

ISBN4-903661-12-1

Serial Number 22

Report on Inspection of Marine Reinforced Concrete Structures in Thailand

Written by

Pakawat Sancharoen, Raktipong Sahamitmongkol,

Isao Kurashige, Yoshitaka Kato and Taketo Uomoto

ICUS Report No. 22

June 2007

International Center for Urban Safety Engineering (ICUS),
IIS, The University of Tokyo, Japan

INSPECTION OF MARINE REINFORCED CONCRETE STRUCTURES IN THAILAND

PAKAWAT SANCHAROEN
Graduate School of Engineering,
The University of Tokyo, Japan
RAKTIPONG SAHAMITMONGKOL
Regional Network for Urban Safety (RNUS),
Asian Institute of Technology, Thailand
ISAO KURASHIGE
Central Research Institute of Electric Power Industry, Japan
YOSHITAKA KATO
International Center for Urban Safety (ICUS),
Institute of Industrial Science, The University of Tokyo, Japan
TAKETO UOMOTO
International Center for Urban Safety (ICUS),
Institute of Industrial Science, The University of Tokyo, Japan

ICUS Report No.22, June 2007

ABSTRACT

Corrosion of reinforcing bar in reinforced concrete structure generally governs the service life of the structure in marine environment. Without the durability design and good construction quality, the RC bridges in eastern Thailand are prone to be subjected to the corrosion earlier than expectation. In this case, good maintenance planning is of crucial importance in order to ensure the safety as well as minimize the maintenance expense.

This project aims to study the condition of traffic RC bridges in eastern part of Thailand. A total of 5 bridges locating in 3 different provinces are inspected. The age of these bridges ranges from 1 year (newly constructed) to 43 years. The usage of fly ash is also included in this study.

The bridges is inspected visually for its overall condition and special techniques are applied to measure its covering depth, chloride diffusion coefficient, surface chloride

content, carbonation depth, and compressive strength. These data is then be analyzed to determined the quality of construction work as well as the ability of concrete to resist aggressive substances.

In the inspection, very large uncertainties in the properties of the structures, especially the covering depth, chloride diffusion coefficient, and concrete quality are found. Mean value of covering depth is mostly lower than the design value. In addition, the variation of surface chloride content can be seen in both of horizontal direction as well vertical direction. Uncertainties are very significant in the actual condition.

The deterioration prediction program is applied to estimate the probability of steel corrosion at any time as well as the time that crack width will reach a maximum allowable limit. These two parameters are key parameters for the maintenance planning. The calculation results show that larger concrete covering depth of reinforcing steel effectively prevents the chloride induced steel corrosion. And, safety of the marine structure can be ensured and maintenance can be minimized, if the properties of actual structure can be controlled and ensured as the designed values during construction.

Table of Contents

INSPECTION OF MARINE REINFORCED CONCRETE STRUCTURES IN THAILAND

PAKAWAT SANCHAROEN
Graduate School of Engineering,
The University of Tokyo, Japan
RAKTIPONG SAHAMITMONGKOL
Regional Network for Urban Safety (RNUS),
Asian Institute of Technology, Thailand
ISAO KURASHIGE
Central Research Institute of Electric Power Industry, Japan
YOSHITAKA KATO
International Center for Urban Safety (ICUS),
Institute of Industrial Science, The University of Tokyo, Japan
TAKETO UOMOTO
International Center for Urban Safety (ICUS),
Institute of Industrial Science, The University of Tokyo, Japan

1. INTRODUCTION

Corrosion of reinforcing steel due to chloride attack is one of main mechanisms deteriorating RC structure. There are great efforts to maintain those deteriorated structures to ensure their safety and serviceability. In 2002, JSCE [1] regulated the durability design to ensure the performance of structure during their service life based on the performance based design concept. In this specification, safety factor is considered to deal with the variation and uncertainties of actual conditions from the designed conditions. This leads to the over-design and higher cost than the actual requirement. In addition, JSCE [2] also regulates the guideline for maintenance the RC structure and has already recommended that structures are periodically inspected in order to ensure their safety and serviceability. Therefore, there are a lot of useful inspection results available. However, they are rarely used to plan an appropriate maintenance program for the structure.

Also coal fly ash concrete is widely utilized in Thailand [12] in order to reduce the cost of concrete as well improve the resistance against chloride induced steel corrosion of marine RC structure. Currently, regulation of some government parties in Thailand required a minimum of 70 mm of covering depth when the structure attaches to marine environment. As well, they regulate to use coal fly ash as a cement replacement material in all marine RC structure a few years ago. They regulate that marine structure has to use pozzalonic material specified ASTM C618 as cement replacement material and has the chloride ion permeation based on ASTM C1202-97 less than 1000 coulombs.

In this study, RC structures attacked by marine environment in Thailand that has been constructed by OPC concrete or coal fly ash concrete were inspected. Inspection results of actual variation of structure properties relating to resistance against chloride induced corrosion are reported. As

well comparison of the performance of OPC RC structure and coal fly ash RC structure are discussed.

2. INSPECTION PROGRAMS

In order to investigate the variation of properties of actual RC structure relating to steel corrosion due to chloride, marine RC structures located in the central and east of Thailand were inspected by both of partially destructive testing and non-destructive testing.

2.1 Site of inspection

All of sites of inspection are road bridges located nearby Bangkok, Thailand as shown in the Fig.1. Totally 5 bridges in 3 provinces which are Samutprakan, Chonburi and Chanthaburi were inspected. Most of them are designed based on the well-known concept of simple span beam column reinforced concrete structure. Except one bridge in Chanthaburi province that was designed to be pre-stressed girder. Not only ordinary Portland cement is used, but other materials such as, sulfate resistant cement, or coal fly ash cement were also used as cementitious materials in some of these bridges in order to retard the corrosion process.

Ages of these structures are range from the minimum 1 year to the maximum 43 years at the time of inspection in November 2006. The visual observation on those structures shows that their deterioration level due to chloride attack can be classified from no damage to severe damage. Concentration of NaCl in surrounding sea water is about 3.0% except the site in Samutprakan province that is surrounded by brackish water which concentration of NaCl is about 0.03%. In order to prevent the deterioration due to chloride, designer specified minimum covering depth, compressive strength, and unit cement content. The location, background information, and surrounding environmental conditions of each structure are shown in Table 1 to 3. Hereinafter, the structure will be named and referred as a bridge No.1 to No.5 as shown in Table 1. General design drawing is shown in Figure 1. Overall and close-up views of each structure are also shown in Figure 2 to 7. Data of weather conditions including monthly average maximum temperature, monthly average relative humidity, and monthly rainfall intensity from year 2004 to 2006 of the area that bridges are located are shown in Figure 8 to 15 [3].

Table 1: Structure name, location and year of construction

Bridge No.	Location			Year of construction
	Province	Latitude	Longtitude	
1	Chanthaburi	13°29′12.81″N	102°03′38.20″E	2005
2	Samutprakan	13°30′05.62″N	100°46′11.05″E	1963
3	Samutprakan	13°30′48.19″N	100°47′19.56″E	1992
4	Samutprakan	13°29′41.84″N	100°51′18.91″E	1976
5	Chonburi	13°22′15.73″N	100°58′34.72″E	2001

Table 2: Material information

Bridge No.	Cementitous material	*Minimum ultimate concrete compressive strength, MPa	Aggregate		Steel
			Coarse	Fine	
1	OPC type 1 and coal fly ash	30	Limestone	River sand	SD30
2	OPC type 1	24			
3	OPC type 1	24			
4	OPC type 1	24			
5	OPC type 5	30			

* Cube specimen with size of 15×15×15cm at 28 days

Table 3: Structural information

Bridge No.	Type of structure	Minimum covering depth, mm
1	Pre-stressed box girder.	75
2	Simple support, cast in place RC structure	50
3	Simple support, case in place RC structure	50
4	Simple support, case in place RC structure	50
5	Simple support, case in place RC structure	70

2.2 Parameters of inspection

Previous research [4] reveals that variable of parameters, including steel covering depth, chloride diffusion coefficient, and surface chloride content, significantly affect the performance of RC structure against chloride attack as well as the prediction result of maintenance planning. Therefore, inspection program conducted in this study mainly focus on the determination of the actual variation of those parameters of each structure and are explained below in the following sections. Please be noted that number of sample points of some structures may be limited due to the limited accessibility of conducting the inspection as well as limit of equipment, budget and time.

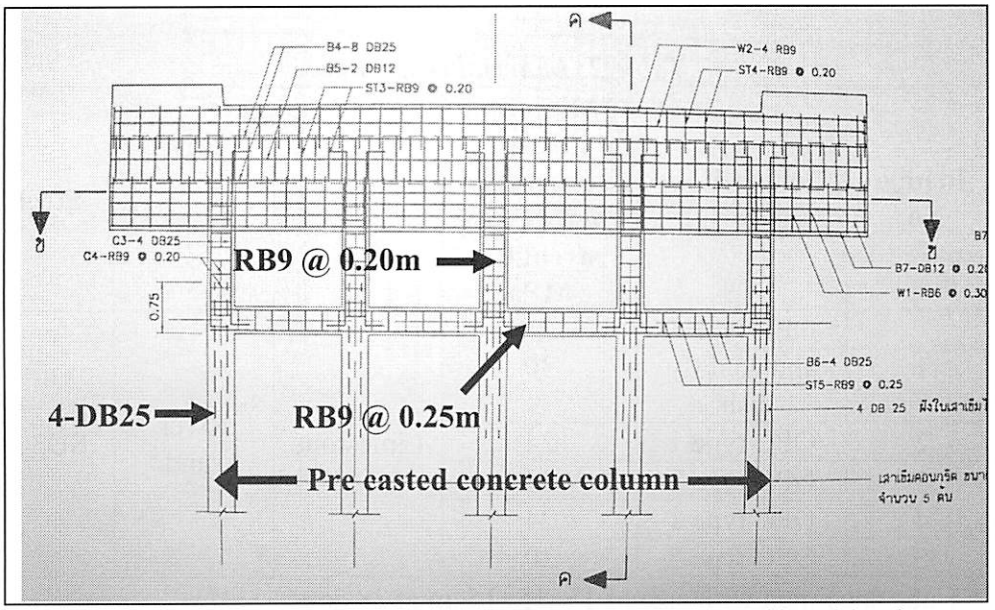

Figure 1: General design drawing of column and beam of local bridge in Thailand

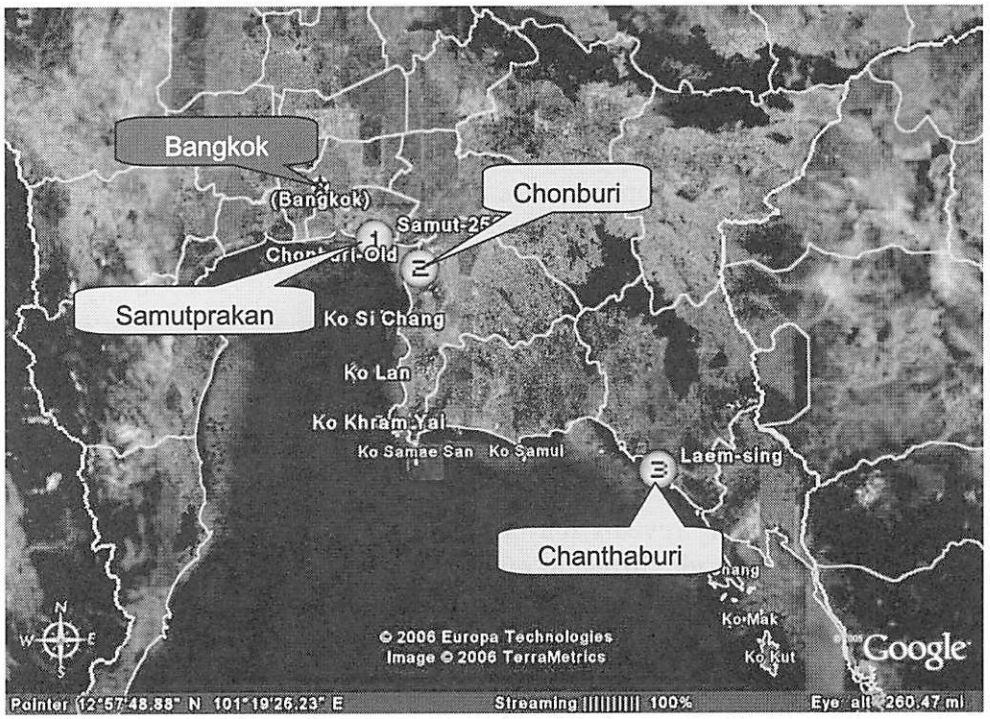

Figure 2: Area of inspection

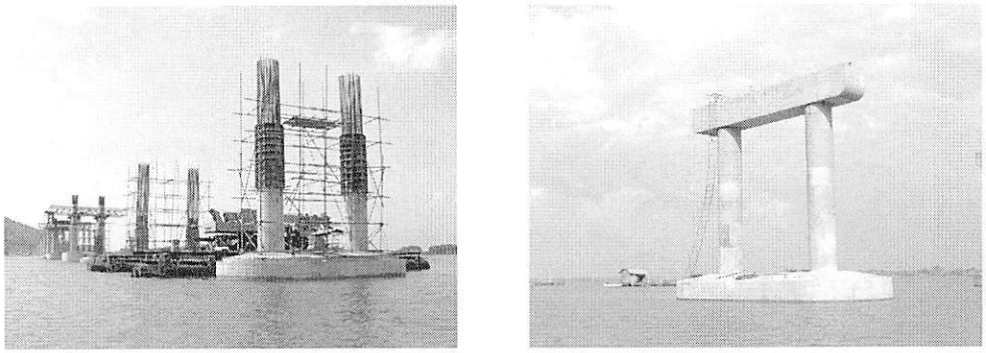

Figure 3: Visual view of Bridge No.1

Figure 4: Visual view of Bridge No.2

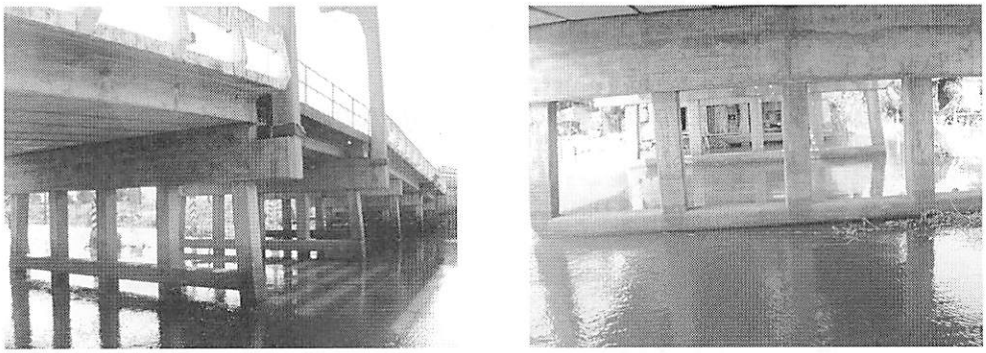

Figure 5: Visual view of Bridge No.3

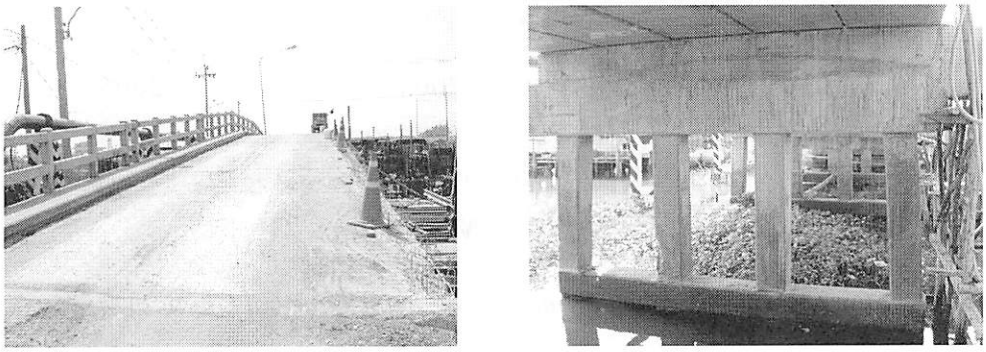

Figure 6: Visual view of Bridge No.4

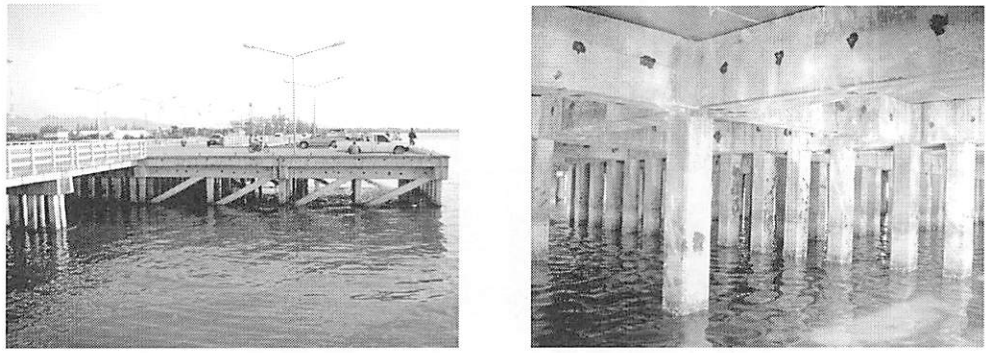

Figure 7: Visual view of Bridge No.5

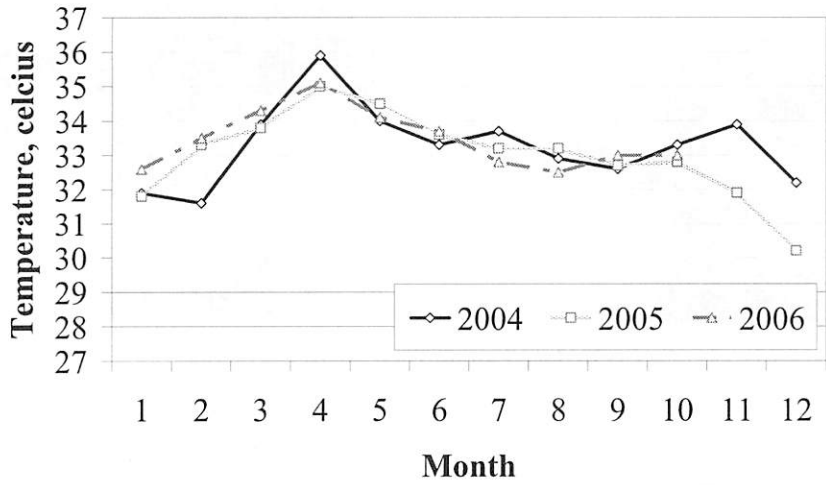

Figure 8: Monthly average maximum temperature of Samutprakan [3]

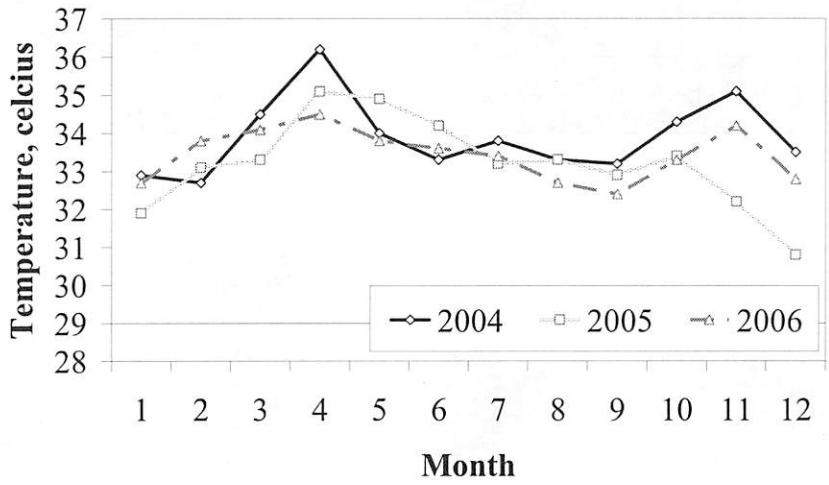

Figure 9: Monthly average maximum temperature of Chonburi [3]

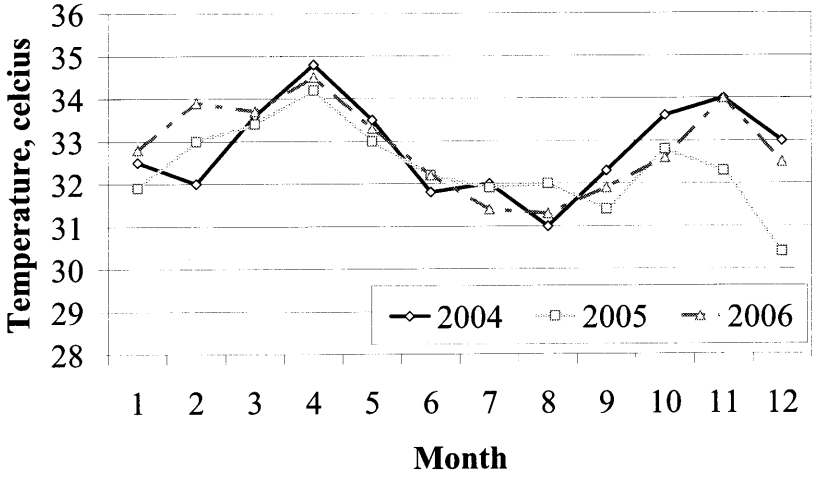

Figure 10: Monthly average maximum temperature of Chanthaburi [3]

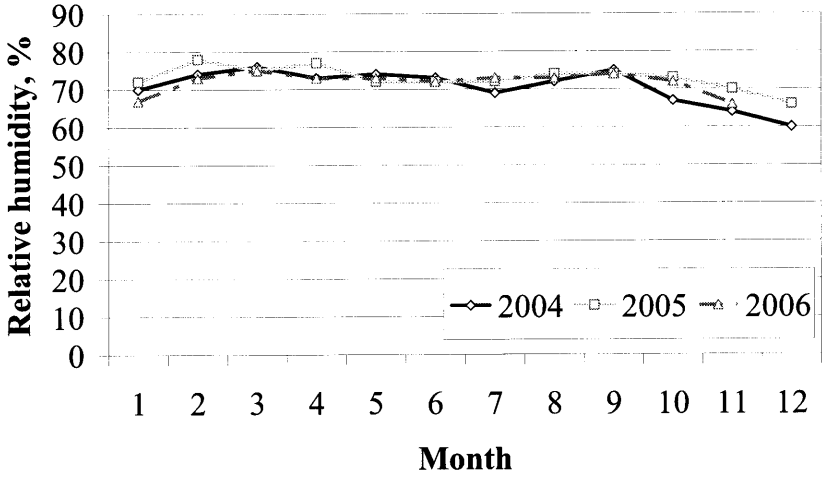

Figure 11: Monthly average relative humidity of Samutprakan [3]

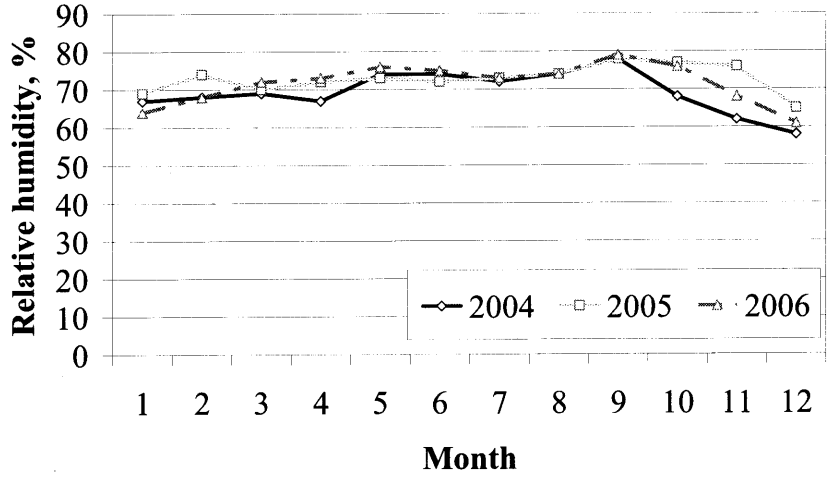

Figure 12: Monthly average relative humidity of Chonburi [3]

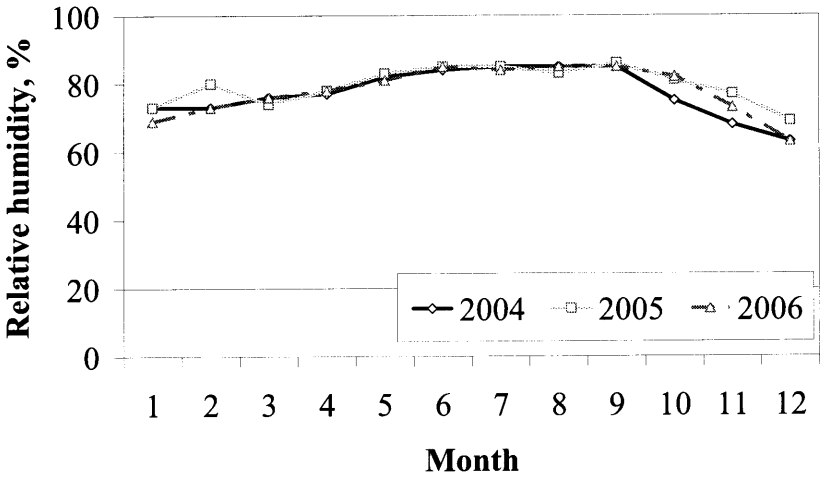

Figure 13: Monthly average relative humidity of Chanthaburi [3]

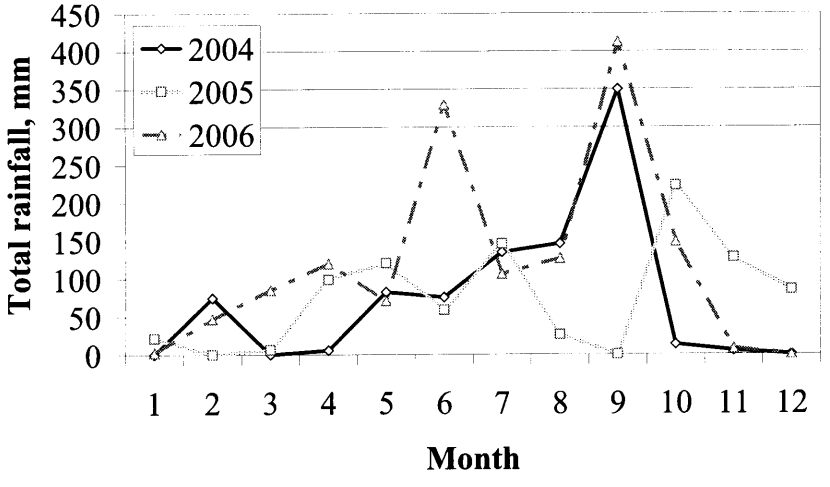

Figure 14: Monthly total rainfall intensity of Samutprakan [3]

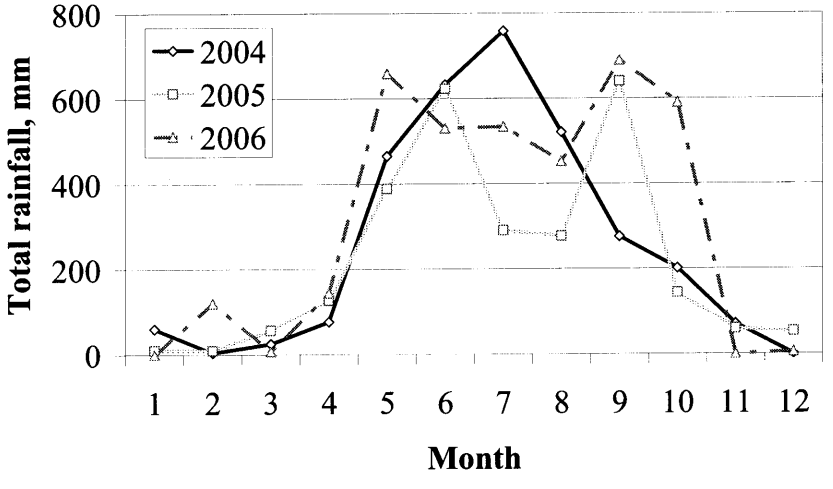

Figure 15: Monthly total rainfall intensity of Chanthaburi [3]

2.2.1 *Visual inspection*

As the first step of the inspection of structure, visual observation was conducted in order to investigate main type and degree of deterioration. Deterioration observed was mostly due to the corrosion of reinforcing steel such as corrosion crack and spalling. Only bridge No. 2 and 4 are severely damaged as shown in Figure 16 to 18. In other bridges, it is possible to observe the rust stain but not the corrosion crack and spalling cannot be observed because they are still in the early stage of their service life.

Figure 16: Visual inspection of deterioration condition of Bridge No.2

2.2.2 *Covering depth of reinforcing steel*

Covering depth of stirrup was measured by a commercial rebar detector of Hilti, model Ferroscan PS200M as shown in Figure 19. Its principle of detecting steel is based on techniques of electromagnetic wave. Scanning was conducted by using Quickscan mode. With concerning of concrete surface and nearby interference metal, only the smooth concrete surface was inspected. Many small sections of member of each structure with the length of each section around 1.5 meters are scanned along the direction perpendicular to the alignment direction of the closet reinforcing steel. Figure 20 and 21 show the method of inspection and transferring the data. Table 4 shows total number of scanned sections, percentage of the whole structure, and measured steel of each structure. Scanned result is processed by software named PS200. The covering depth can be calculated by this software based on the specified diameter of steel as specified in the design drawing of each structure. The example of processing the raw data by PS200 software is shown in Figure 22. Later, all of data is combined together for each structure to finalize its random variable and probability

distribution by distribution statistic software and will be explained later in Section 2.3.

Figure 17: Visual inspection of deterioration condition of Bridge No.4

Figure 18: Visual inspection of deterioration condition of Bridge No.4

Figure 19: Hilti model Ferroscan PS200M

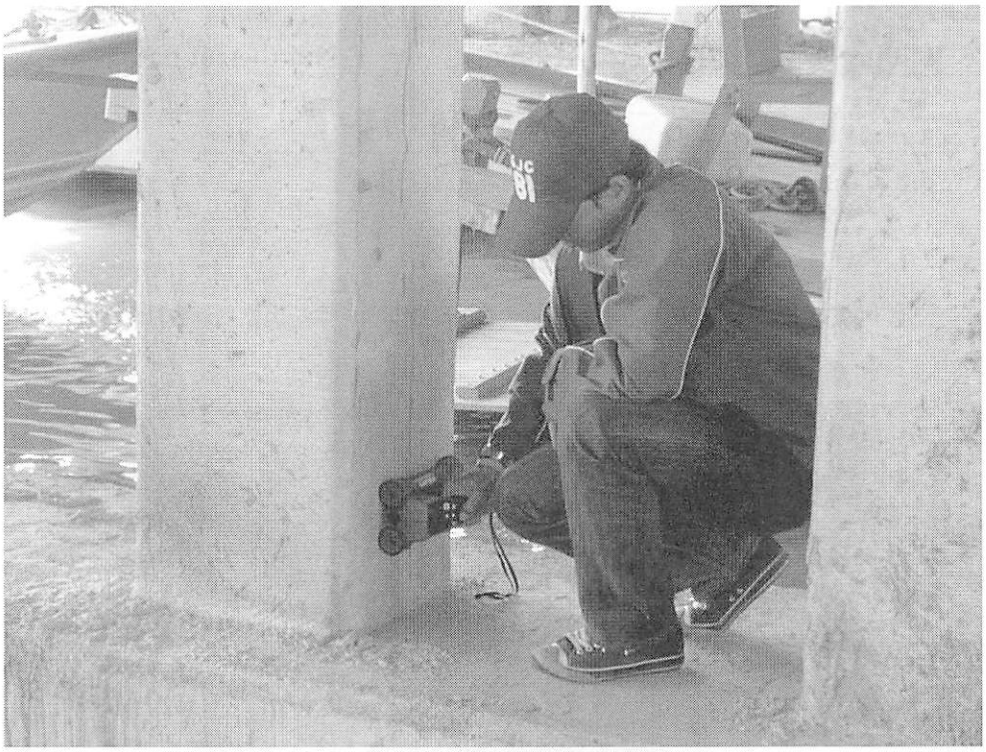

Figure 20: Measuring the covering depth of reinforcing steel

Figure 21: Transferring measured data of covering depth

Table 4: Number of data for covering depth

Bridge No.	Inspected section	Number of data
1	33	192
2	61	918
3	68	357
4	25	129
5	76	1254

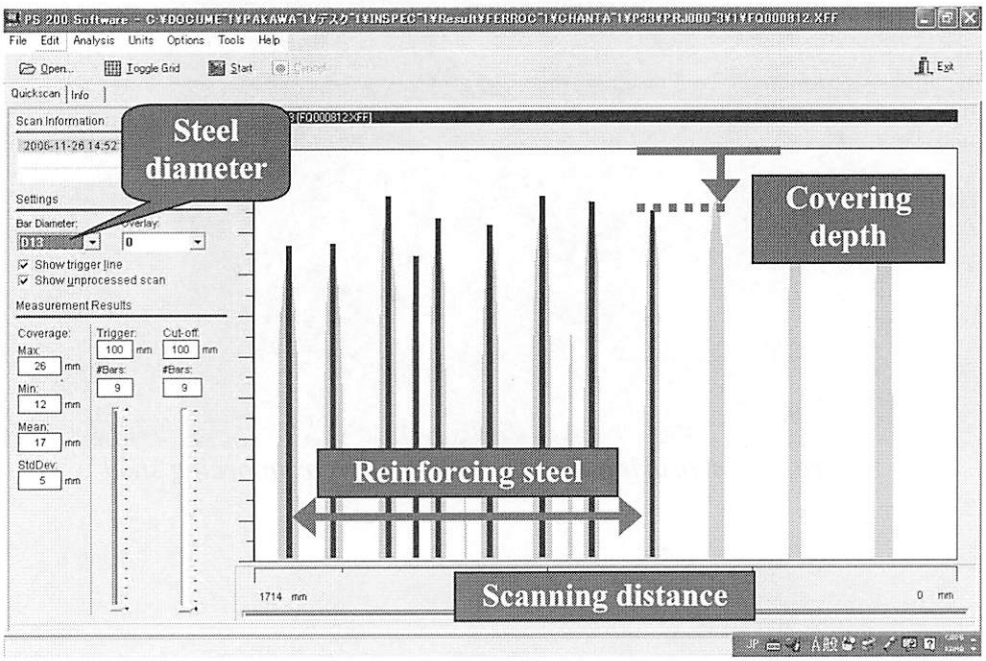

Figure 22: Processing result of covering depth

2.2.3 *Chloride diffusion coefficient and surface chloride content*

Chloride diffusion coefficient and surface chloride content were calculated from the measured profile of chloride content based on JSCE G573 [5]. Sample of concrete powder was collected on site by Hilti, portable drilling machine with the diameter of drilling bit of 14mm as shown in Figure 23. Sample powder was collected from three to four adjacent holes to minimize the effect of aggregate size with the depth of 0-2cm, 2-4cm, 4-6cm, 6-8cm, and 8-10cm from the surface. However, Bridge No.1 has been constructed in 2005 and was expected low amount of chloride penetration. Therefore, the sample was collected from the depth of 0-1cm, 1-2cm, 2-3cm, 3-4cm, and 4-5cm in case of Bridge No.1. Noted that sample was collected not only at the sea water level but also at different heights in order to determine the effect of height from the sea level as shown in Figure 24. After collecting the sample, the drilled holes were filled by waterproof epoxy or non-shrink cement mortar in order to prevent the further deterioration of that structure. Figure 25 to 29 show drilling method, adjacent drilled holes, set of collected sample powder, and chloride measurement method. Table 5 shows number of set of samples for chloride analysis. Due to many limitations such as accessibility, equipment capacity, or permission from the responsible party, the number of samples is limited. Total chloride content in powder was measured based on method of JCI SC5 [6]. This method uses boiled nitric acid to extract all of chloride in the sample and titrates by using silver nitrate solution. The auto titration machine is used in this study. Then chloride diffusion coefficient and surface chloride content were calculated that will minimize the different between measured and calculated chloride content. Fick's diffusion law is used to calculate profile of chloride content as shown in Equation 1. The example of actual measured chloride profile and calculated chloride profile are compared in Figure 30.

$$C_x = C_0 \times \left[1 - erf\left(\frac{0.1 \cdot c}{2\sqrt{D_{cl} \cdot t}}\right)\right] \quad (1)$$

where C_x is chloride content (kg/m^3) at depth c from the surface, C_0 is surface chloride content (kg/m^3), c is depth from the surface (mm), D_{cl} is chloride diffusion coefficient (cm^2/year), t is exposure time (year).

Table 5: Number of collected data for chloride analysis

Bridge No.	Inspected section	Number of data
1	6	6
2	3	3
3	5	5
4	5	5
5	19	19

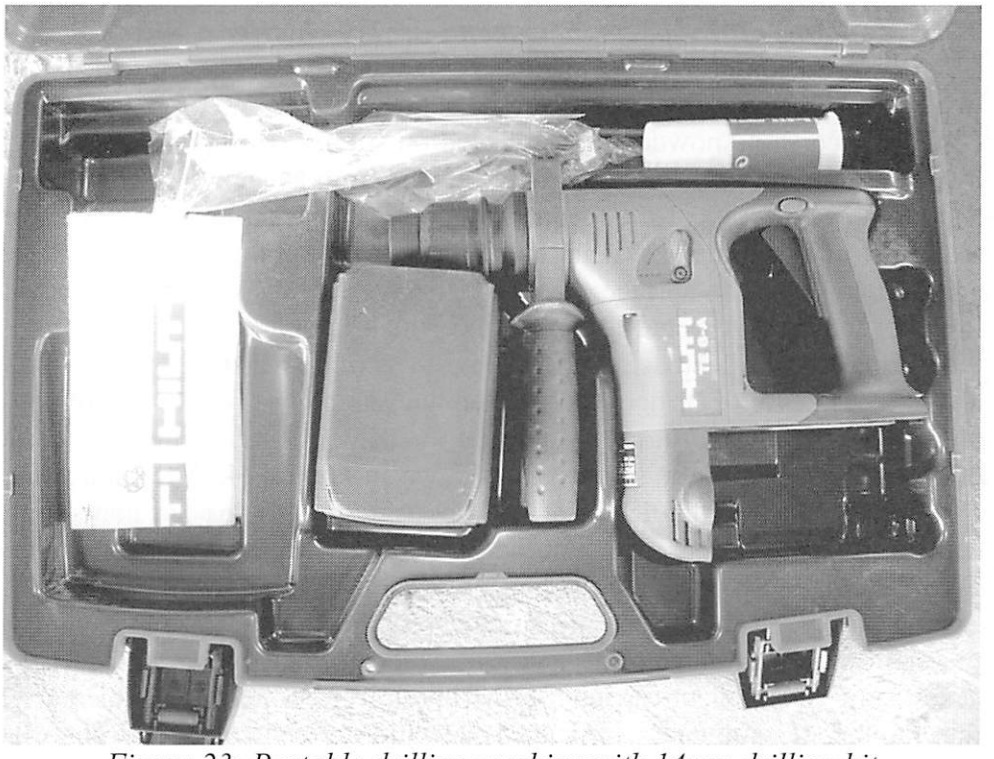

Figure 23: Portable drilling machine with 14mm drilling bit

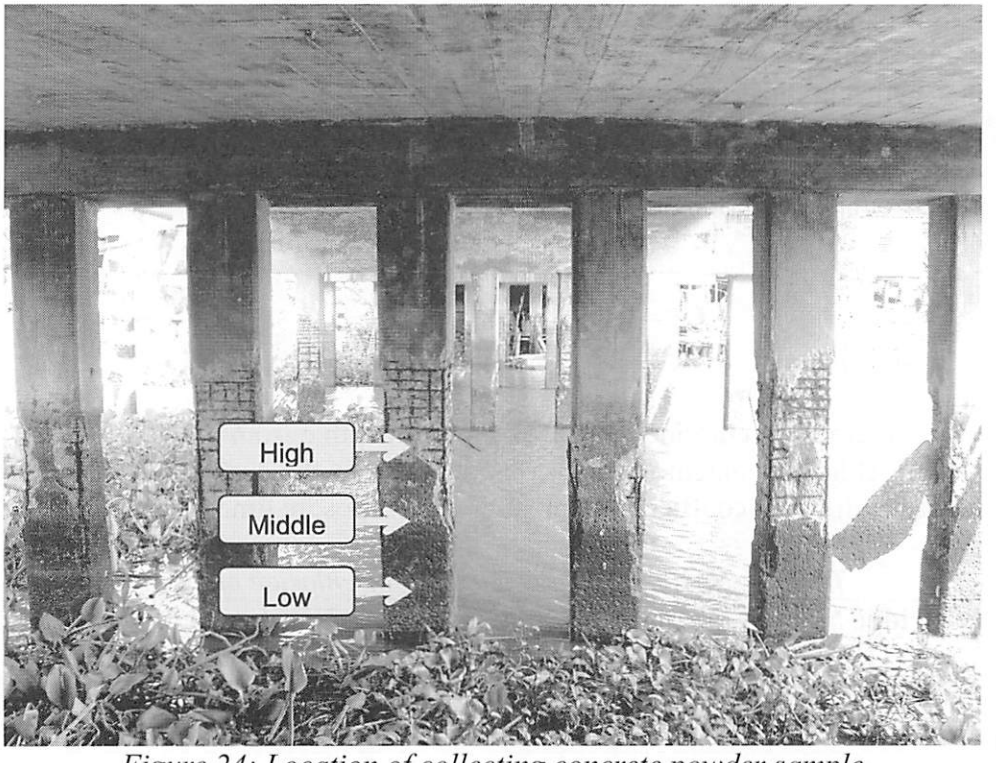

Figure 24: Location of collecting concrete powder sample

Figure 25: Collecting concrete powder sample

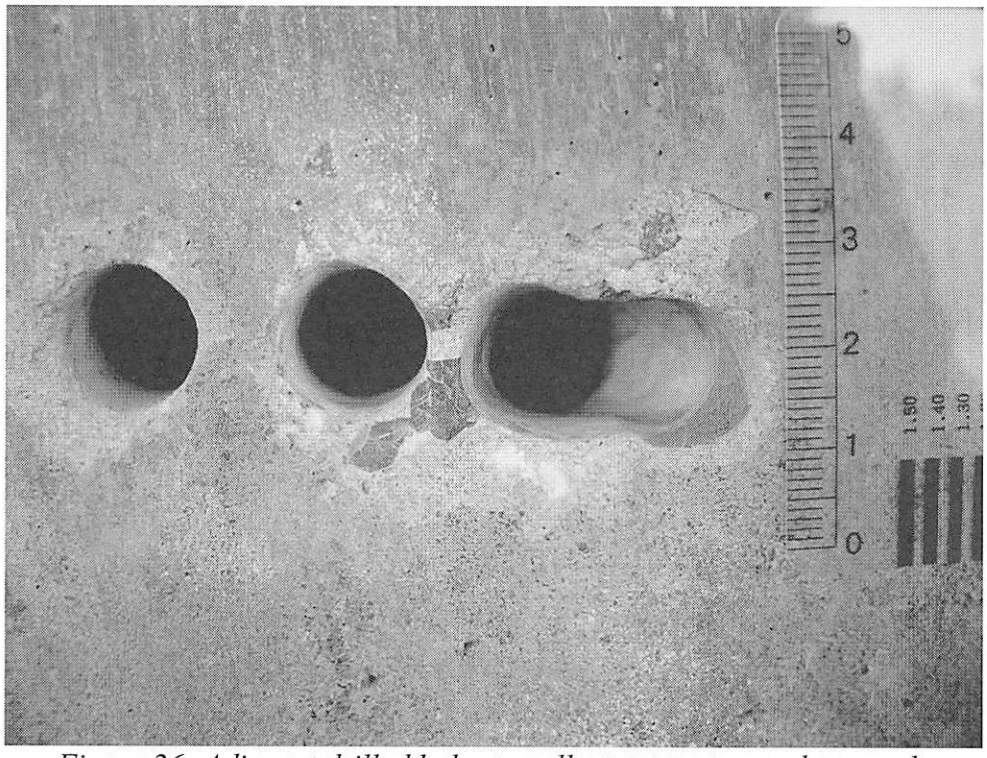

Figure 26: Adjacent drilled holes to collect concrete powder sample

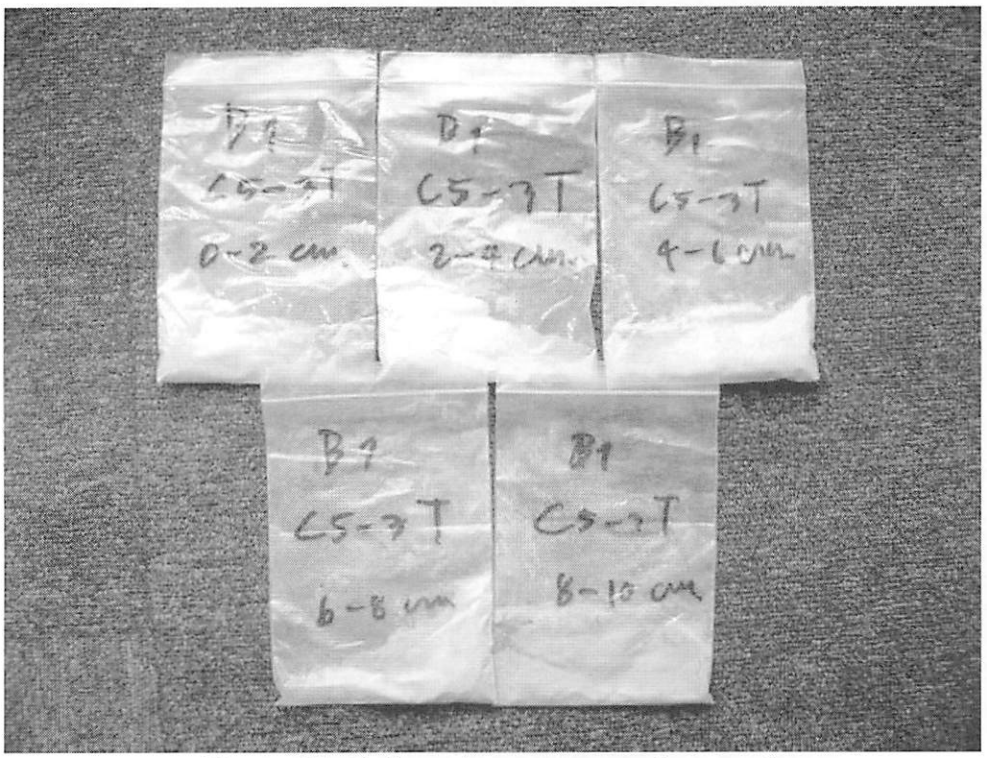

Figure 27: Collected concrete powder sample

Figure 28: Epoxy filled hole after collecting the sample

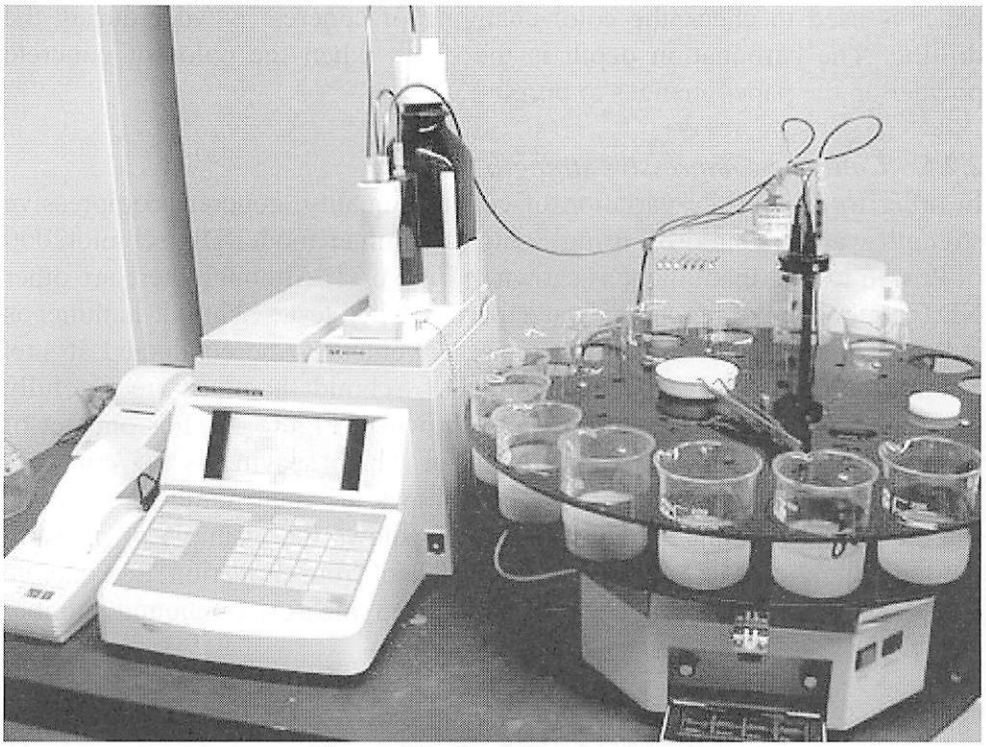

Figure 29: Titration machine

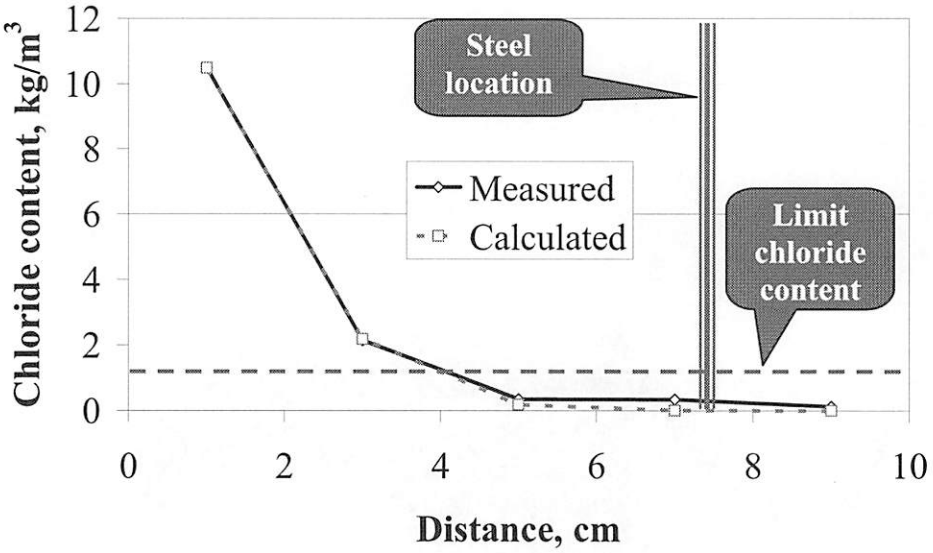

Figure 30: Example of comparison between measured and calculated chloride content

2.2.4 Carbonation depth

As carbonation is also one of main reasons of reinforcing steel corrosion, its depth is measured by spraying of phenolphthalein solution. Two methods were used to measure carbonation depth. The first, concrete powder was cleaned from the drilled hole after collecting concrete powder sample. Then the hole was sprayed by phenolphthalein solution. The carbonation depth is measured as the depth that the concrete color is not changed. The second method uses the filter paper soaked with phenolphthalein solution. Soaked

paper is used to check the color changing of concrete powder during the drilling. The carbonation depth is the depth when the color of concrete powder on the paper changes to purple.

2.2.5 Concrete compressive strength

In order to inspect the variation of concrete quality, concrete compressive strength was measured by using Schmidt hammer model Digischmidt2000 of Proceq testing instrument as shown in Figure 31. Although there are other NDT methods such as air or water permeability test., Schmidt hammer is still one of the methods that are most convenient to be conducted at site. Smooth concrete surface and direction of Schmidt hammer are carefully controlled during the measurement as shown in Figure 32. For one set of sample, the minimum of twenty points of which spacing is 2.5 cm were measured its rebound number. Table 6 shows the total number of sample sets measured rebound number. Figure 33 shows the example of measure rebound number for 1 set of sample. Then from Equation 2, concrete compressive strength can be calculated from measured rebound number (JSCE [7]).

$$f_c^{'} = -18 + (1.27 \times RN) \tag{2}$$

where, fc' is concrete compressive strength (MPa), and RN is rebound number.

Figure 31: Schmidt hammer

Figure 32: Method of conducting Schmidt hammer

Table 6: Number of data of Schmidt hammer

Bridge No.	Scanned section	Number of data
1	65	1493
2	23	253
3	32	360
4	10	150
5	40	839

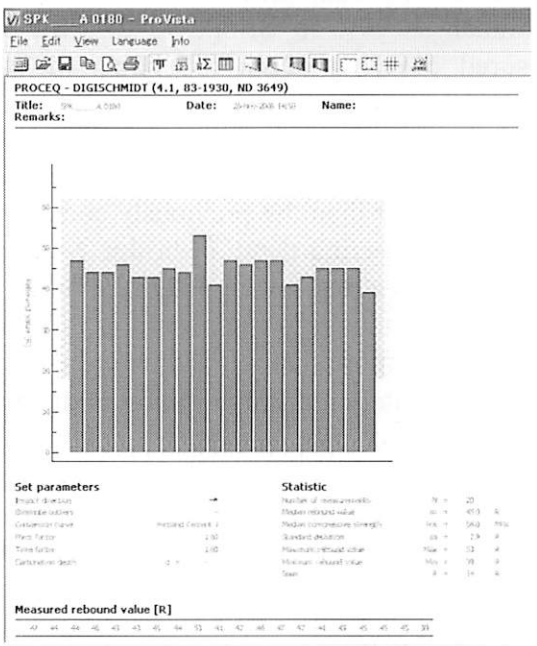

Figure 33: Example of a set of Schmidt hammer result

2.3 Distribution fitting

As explained in the previous section, inspections were conducted at many locations on each structure. In order to conclude the distribution of all inspected data, they are combined together for each structure as one set of

data. Then distribution fitting program called "Bestfit 4.5" was used to select the most fitting distribution from the total list of 38 distribution types to our set of data. The most suitable distribution type and its parameters to our data are selected based on chi-square goodness of fit test. Distribution type, its parameters, mean value, and coefficient of variation are reported in this study. The example of distribution fitting is shown in Figure 34. Appendix A discusses more detail about distribution fitting method.

3. INSPECTION RESULTS

In order to determine the distribution and random variable of properties of structures, processed inspection results are reported.

3.1 Covering depth of reinforcing steel

Results of scanning at different locations of structure are combined together and the distribution fitting is conducted. The results of type of distribution, and random variable are concluded in Table 7 and 8 as well as the specified covering depth. Figure 35 to 39 shows the comparison between distribution of actual inspection result and the fitting distribution of each bridge. Please be noted that most of measured covering depths are significantly less than those specified in the design. Only Bridge No.1 of which ratio of data which is not satisfied the specified depth is 15% because this bridge was strictly controlled the quality during construction. Ratio of other bridges is more than 50% and as much as 90% in Bridge No.2. Also there is very high variation of measured covering depth as shown in Table 7 that their coefficients of variation are more than 20%. Since the current specification in Thailand for RC structures requires larger covering depth for marine structure compared to normal RC structure, the specified covering depth of Bridge No. 4 and 5 are larger than the previously constructed bridge No. 1, 2 and 3. However, actual covering depth of bridge No. 4 is still lower than the required value and this causes severe deterioration as will be discussed in the Section 4. From result, very high variation of measured covering depth can also be observed more than 20%. Please be noted that this result possibly includes approximately ±5% of variation of the machine itself.

As shown in Table 8, distribution type of covering depth is different for each structure. This result is obtained from the best fitting type of distribution from the chi square goodness of fit test. This fitting distribution can be used as the most suitable distribution to represent the actual inspected data. The same mean of covering depth but different type of distribution is possible to cause different resistance against chloride induced corrosion. For example, comparison between Figure 36 and 37 shows that they have similar mean of covering depth. However, Figure 37 shows that covering depth of Bridge No.3 has a large number of large covering depth than Bridge No.2 as shown in Figure 36. Therefore, the resistance against chloride induced corrosion of Bridge No.3 is expected to larger than Bridge No.2 as shown in Section 4.1.1.

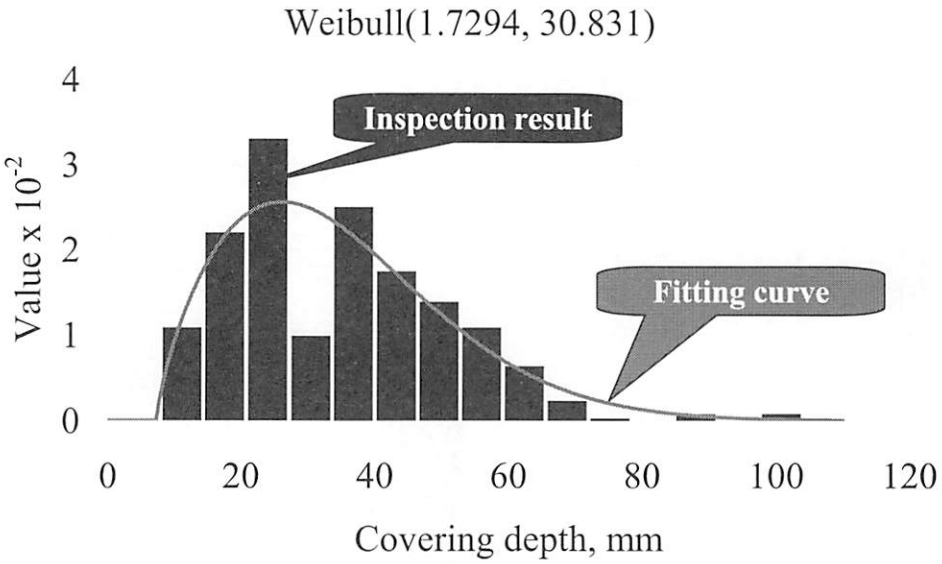

Figure 34: Example of actual distribution and fitting distribution of inspection result

Table 7: Comparison between specified and actual covering depth

Bridge No.	Specified depth, mm	Ratio of number of data not satisfied the specified depth, %	Actual depth	
			Mean, mm	COV, %
1	75	15	88.34	22.30
2	50	90	24.21	38.69
3	50	55	27.03	44.43
4	50	78	33.11	64.78
5	70	85	41.61	46.45

Table 8: Distribution type and parameter of actual covering depth

Bridge No.	Distribution type	Parameter	
		A	B
1	Weibull	$\lambda = 6.6890$	$\beta = 120.47$
2	Inverse Gaussian	$\mu = 18.469$	$\lambda = 71.958$
3	Inverse Gaussian	$\mu = 22.406$	$\lambda = 77.984$
4	Pearson5	$\lambda = 4.0887$	$\beta = 95.750$
5	Inverse Gaussian	$\mu = 52.904$	$\lambda = 396.427$

3.2 Chloride diffusion coefficient and surface chloride content

Powder of concrete sample was collected and analyzed for chloride content. However, the number of samples is limited due to difficulties of sample collection. Therefore, it is difficult to reliably determine their random variable. As a result, only actual variations of the data are shown in Table 9. There are very high variations in both of surface chloride content and chloride diffusion coefficient. Local effects of chloride attack due to location of members, wind direction, etc., can be seen from this result.

Variation of the concrete permeation due to effects of casting and curing can be seen from the result as well.

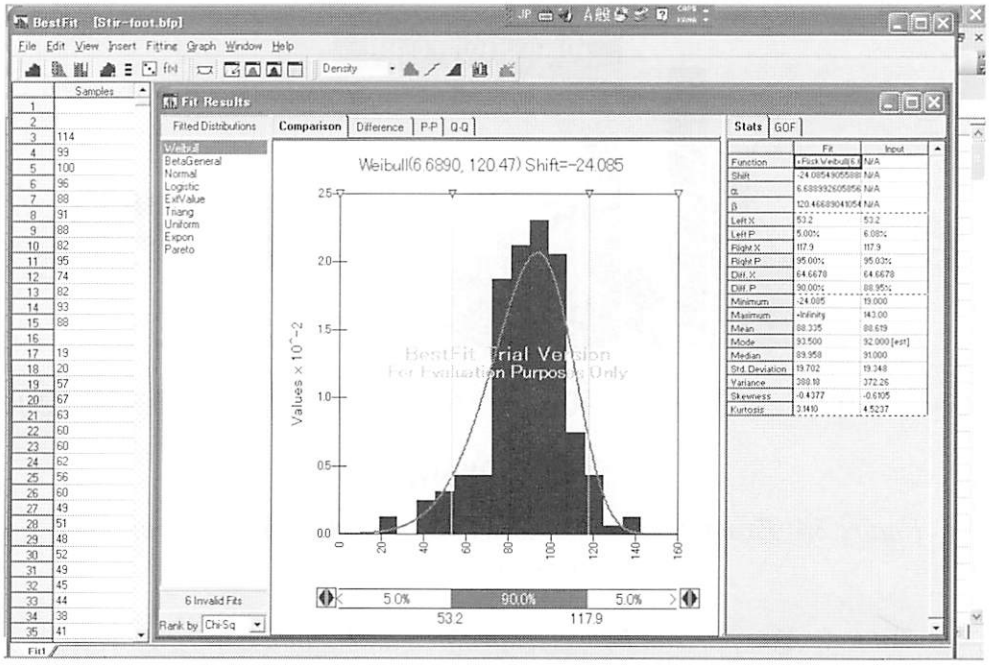

Figure 35: Actual distribution and fitting distribution of covering depth of Bridge No.1

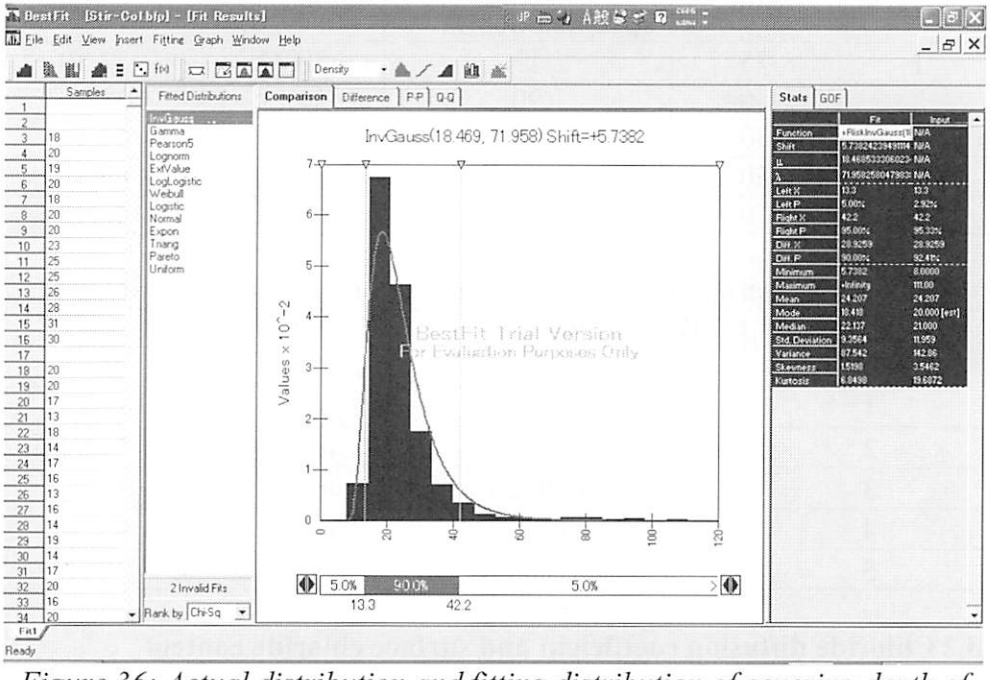

Figure 36: Actual distribution and fitting distribution of covering depth of Bridge No.2

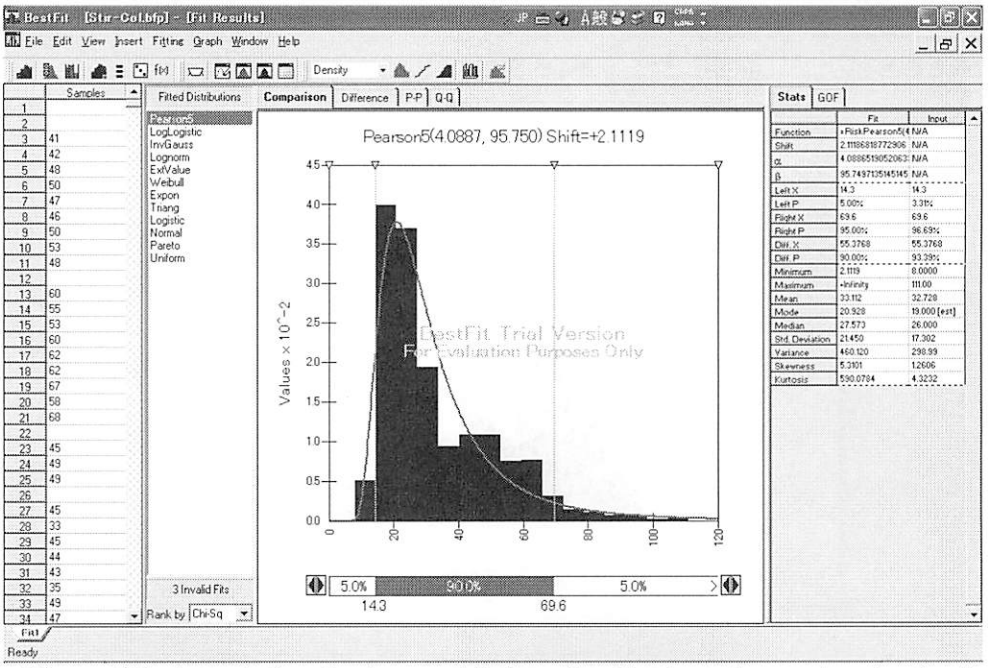

Figure 37: Actual distribution and fitting distribution of covering depth of Bridge No.3

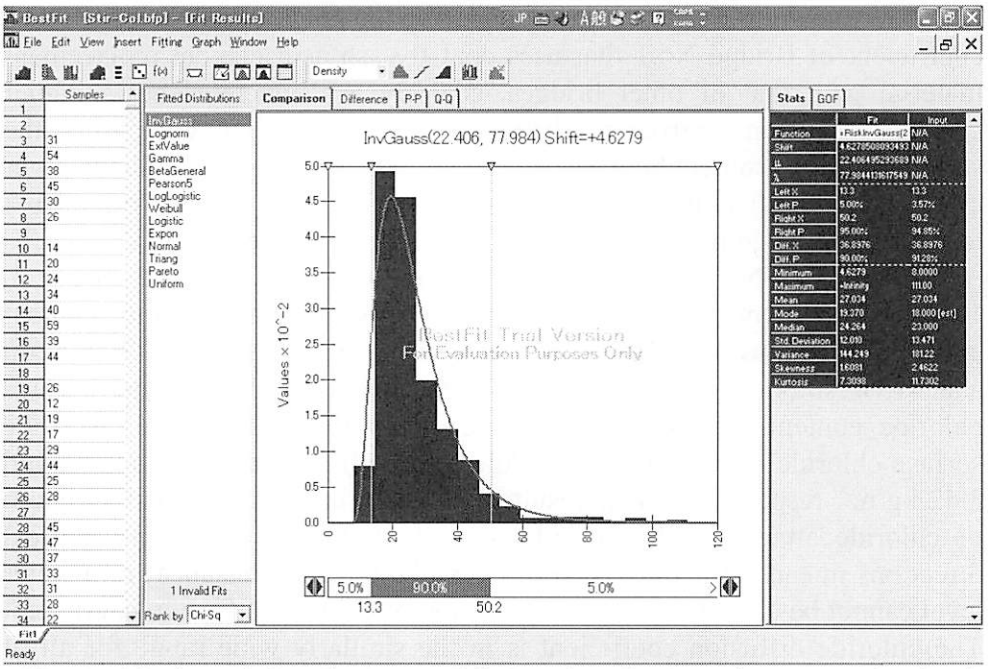

Figure 38: Actual distribution and fitting distribution of covering depth of Bridge No.4

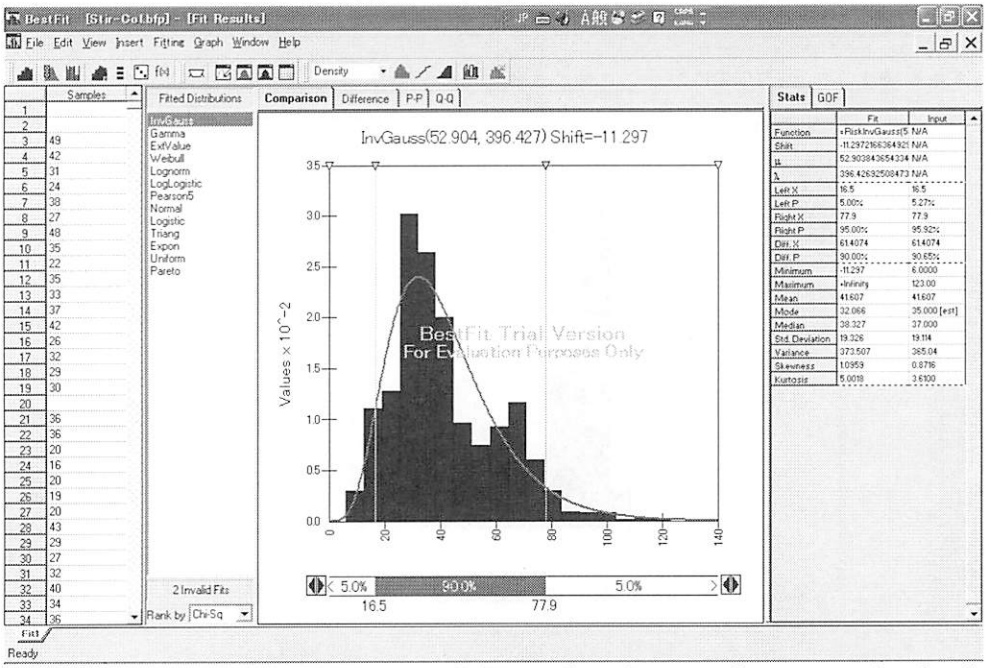

Figure 39: Actual distribution and fitting distribution of covering depth of Bridge No.5

As shown in Table 9, when comparing the result of chloride diffusion coefficient of Bridge No.1 that uses coal fly ash as a cement replacement material with that of other bridges, coal fly ash concrete shows higher chloride diffusion coefficient than other bridges. When comparing the surface chloride content between each bridge, Bridge No. 2 to 4 show lower chloride content than that of Bridge No. 1 and 5. This is due to Bridge No.2 to 4 are surrounded by brackish water that has lower concentration of NaCl.

On bridge No.5, concrete samples were collected at height of 50cm, 100cm, and 150cm from the water level. Results of surface chloride content and chloride diffusion coefficient at different height are shown in Figure 40 and 41. Results of samples closer to the water level show higher surface chloride content than samples collected from the higher level. Average surface chloride content of low, middle, and high level are 15.33, 9.40, and 3.42 kg/m^3, respectively. This result shows that the effect of local variation of chloride attack can be considered in both of horizontal and vertical directions in each structure. Nevertheless, the effect of distance from water level cannot be clearly seen on the variation of chloride diffusion coefficient. The chloride diffusion coefficient is in the similarly wide range for all of three levels of measurements. It can thus be concluded that chloride diffusion coefficient is mainly affected by the variation of concrete quality itself.

Table 9: Results of surface chloride content (C_s) and chloride diffusion coefficient (D_{cl})

Bridge No.	Parameter	No.		
1	No.	1	2	3
	C_s, kg/m^3	8.60	5.58	14.39
	D_{cl}, cm^2/year	0.35	0.73	0.75
	No.	4	5	6
	C_s, kg/m^3	6.52	3.95	11.13
	D_{cl}, cm^2/year	1.01	1.32	1.38
2	No.	1	2	3
	C_s, kg/m^3	11.17	7.82	7.14
	D_{cl}, cm^2/year	0.82	2.00	1.19
3	No.	1	2	3
	C_s, kg/m^3	4.64	1.61	3.33
	D_{cl}, cm^2/year	0.18	1.11	0.26
	No.	4	5	
	C_s, kg/m^3	2.56	2.04	
	D_{cl}, cm^2/year	1.08	0.45	
4	No.	1	2	3
	C_s, kg/m^3	3.22	5.94	3.73
	D_{cl}, cm^2/year	0.54	0.22	0.36
	No.	4	5	
	C_s, kg/m^3	6.72	3.10	
	D_{cl}, cm^2/year	0.24	0.40	
5	No.	1	2	3
	C_s, kg/m^3	10.58	14.05	17.14
	D_{cl}, cm^2/year	0.75	0.58	0.39
	No.	4		
	C_s, kg/m^3	19.45		
	D_{cl}, cm^2/year	0.36		

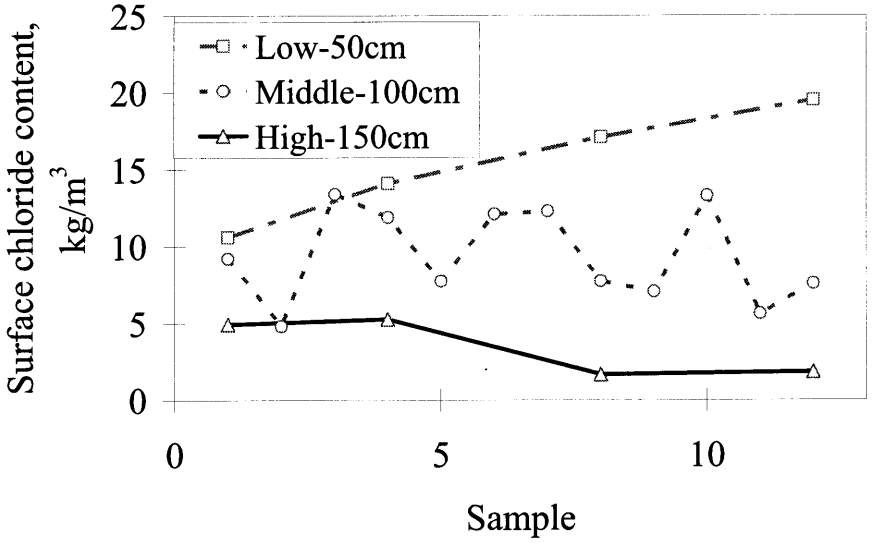

Figure 40: Variation of surface chloride content of Bridge No.5 at different height

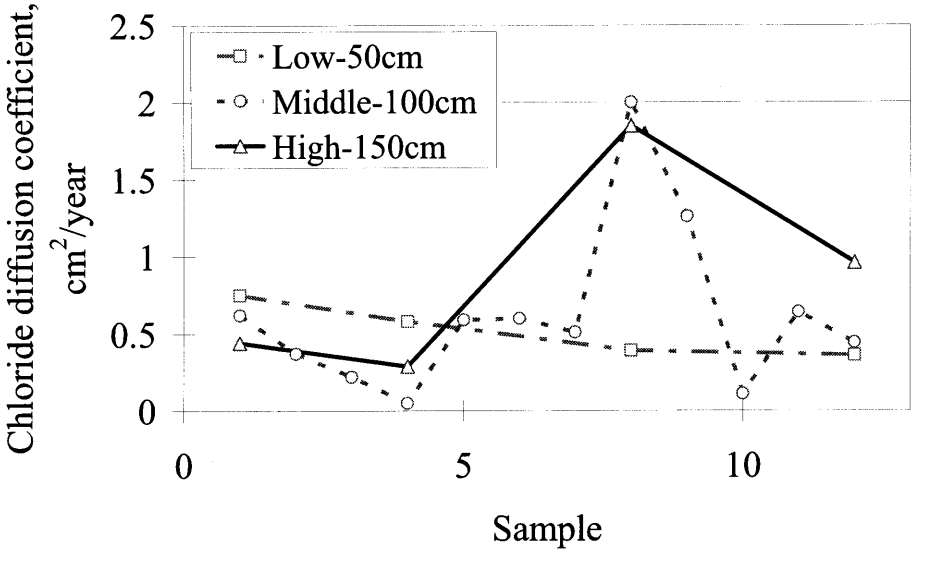

Figure 41: Variation of chloride diffusion coefficient of Bridge No.5 at different height

3.3 Carbonation depth

Carbonation depth was measured mainly by two methods during the collection of concrete powder sample for chloride analysis. The measured carbonation depth was very small and can be negligible from a possible cause of steel corrosion in these bridges. Figure 42 shows the example of the measuring of carbonation depth by drilling method. As shown in Figure 42, there was not significant carbonation even at the depth very close to the concrete surface.

Figure 42: Observation of carbonation at very small distance from surface

3.4 Concrete compressive strength

Due to handiness of Schmidt hammer, the measurement of concrete strength was conducted on a large number of members to determine the variation of the concrete compressive strength used to represent the concrete quality. The results of the calculated concrete compressive strength by Equation 2 are shown in Table 10 together with the specified minimum concrete compressive strength in design drawing. It can be seen that all of measured compressive strength is higher than specified value. However, there are some measured data that their values are less than the specified strength as also shown in Table 10. However, this ratio is significantly lower than that of covering depth as shown in Table 7. This is because the specified value is based on compressive strength at 28days but the inspection was conducted on the structure that has already been in service for more than 1 year after the casting. Besides, concrete quality shows variation in the range of 10 to 20%. However, these variations are significantly lower than that of covering depth. Please be noted that this result still includes the variation due to the machine and inspector that may be up to ±20%. Table 11 shows the conclusion of distribution type and its parameters of rebound number of each structure. Figure 43 to 47 show the actual distribution and fitting distribution of result of rebound number.

Due to difficulties in collecting the concrete powder sample for chloride analysis, the variation of concrete compressive strength is considered to be used as the variation of chloride diffusion coefficient. However, this implementation is needed to be confirmed their appropriate in the future. Due to easiness of Schmidt hammer, it will be very useful, if

variation of their inspection result can be used as a variation of chloride diffusion coefficient.

Table 10: Comparison between specified and actual compressive strength

Bridge No.	Specified strength, MPa	Ratio of number of data not satisfied the specified strength, %	Actual strength	
			Mean, MPa	COV, %
1	30	22.0	34.97	19.89
2	24	6.0	34.30	18.35
3	24	4.7	42.31	17.79
4	24	0.0	39.30	20.53
5	30	0.2	43.39	10.70

Table 11: Distribution type and parameter of rebound number

Bridge No.	Distribution type	Parameter	
		A	B
1	Extreme Value	$\lambda = 39.3467$	$\beta = 6.5968$
2	Extreme Value	$\lambda = 38.0951$	$\beta = 5.5787$
3	Weibull	$\lambda = 17.048$	$\beta = 119.31$
4	Beta General	$\alpha 1 = 22.406$	$\alpha 2 = 77.984$
5	Weibull	$\lambda = 8.2688$	$\beta = 38.126$

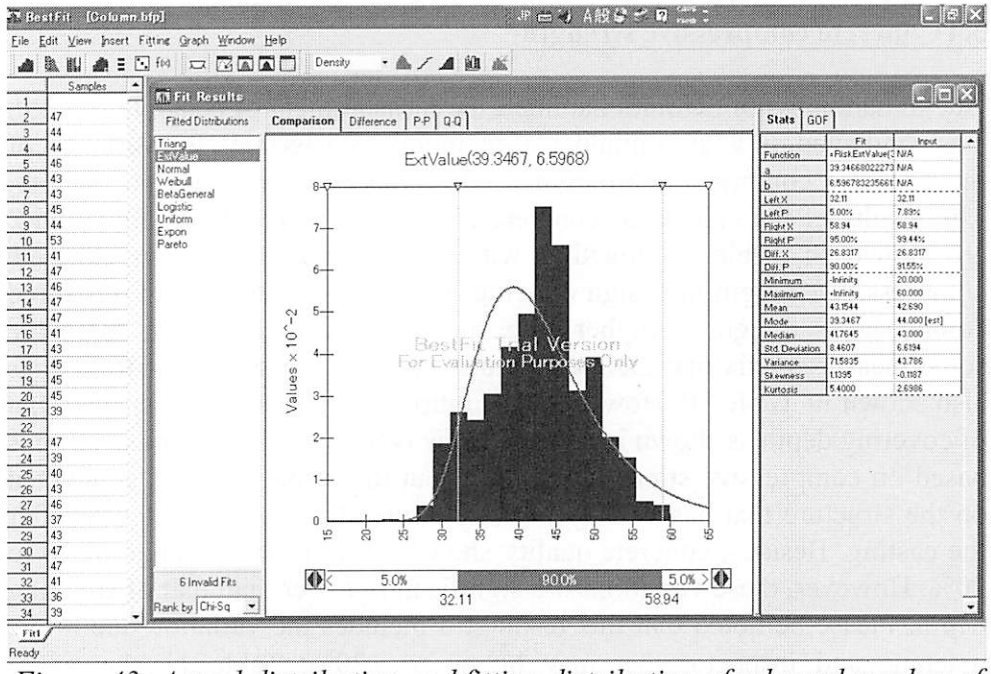

Figure 43: Actual distribution and fitting distribution of rebound number of Bridge No.1

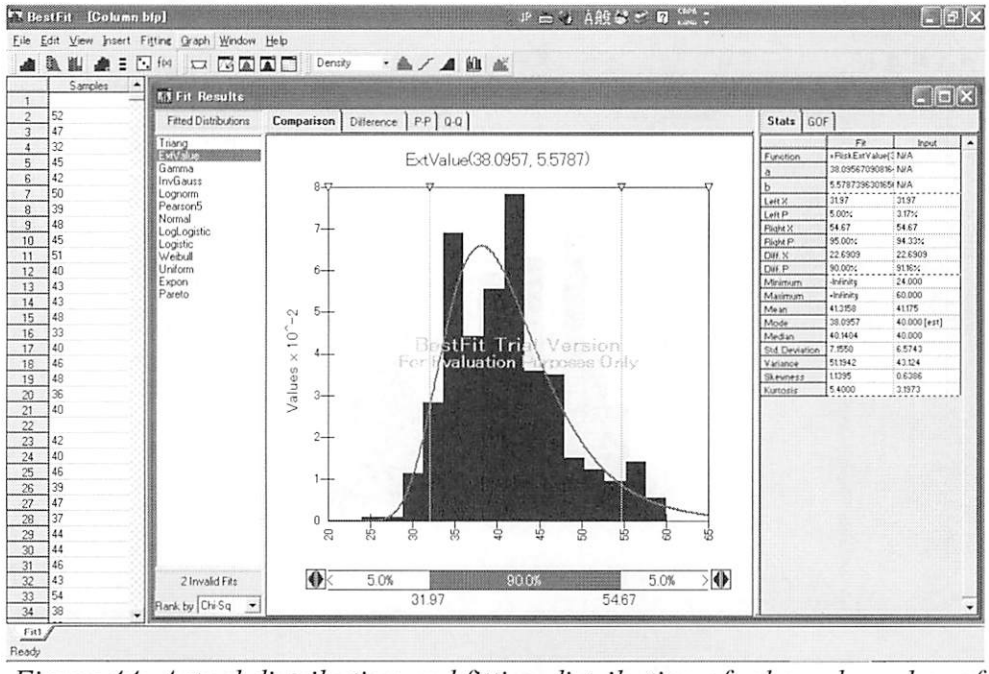

Figure 44: Actual distribution and fitting distribution of rebound number of Bridge No.2

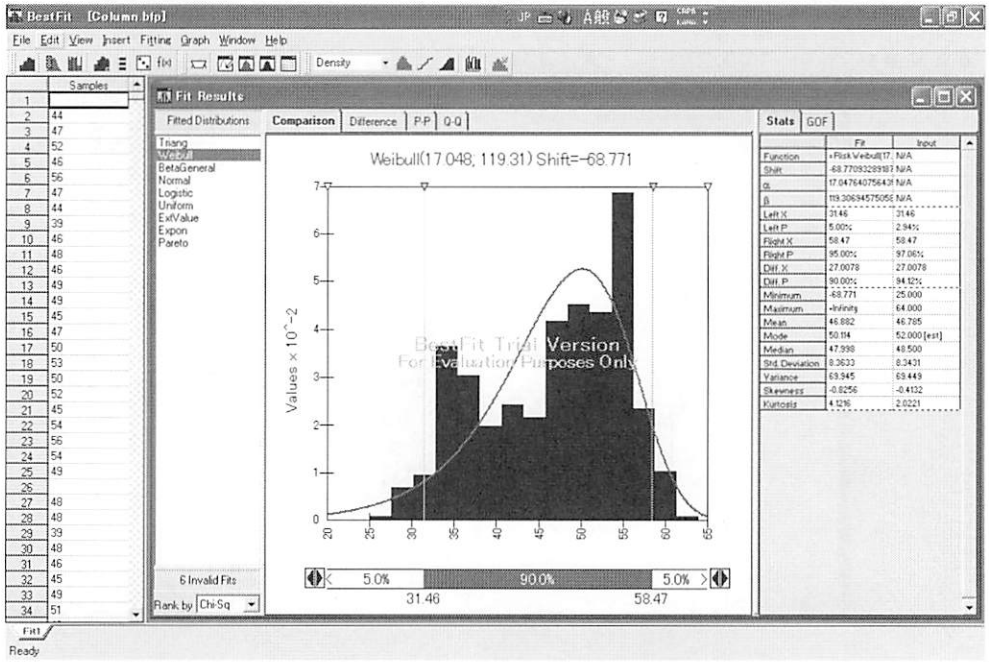

Figure 45: Actual distribution and fitting distribution of rebound number of Bridge No.3

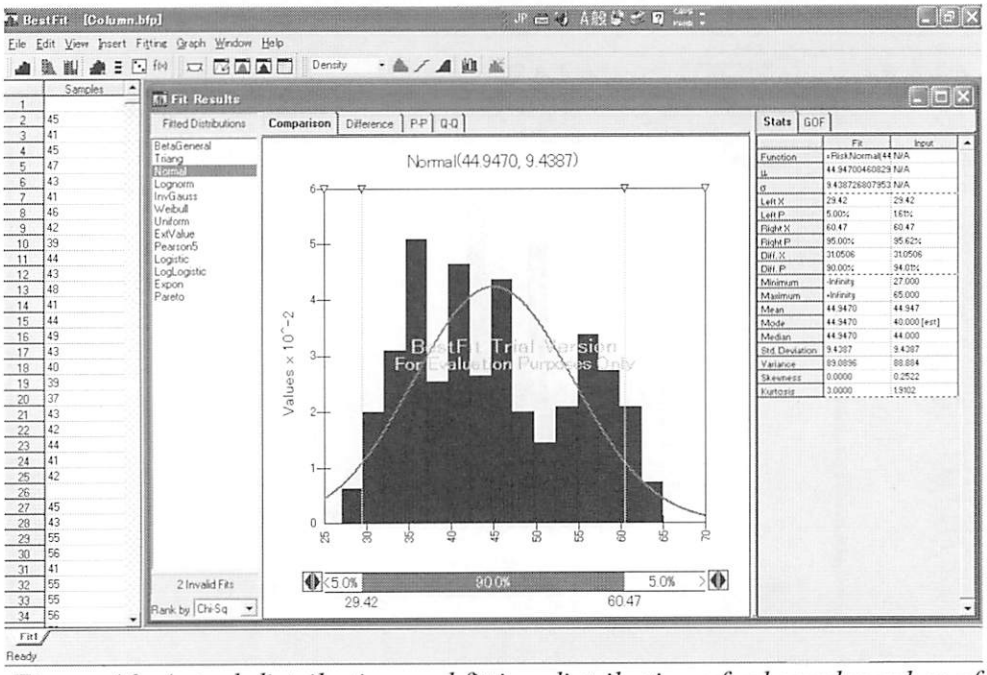

Figure 46: Actual distribution and fitting distribution of rebound number of Bridge No.4

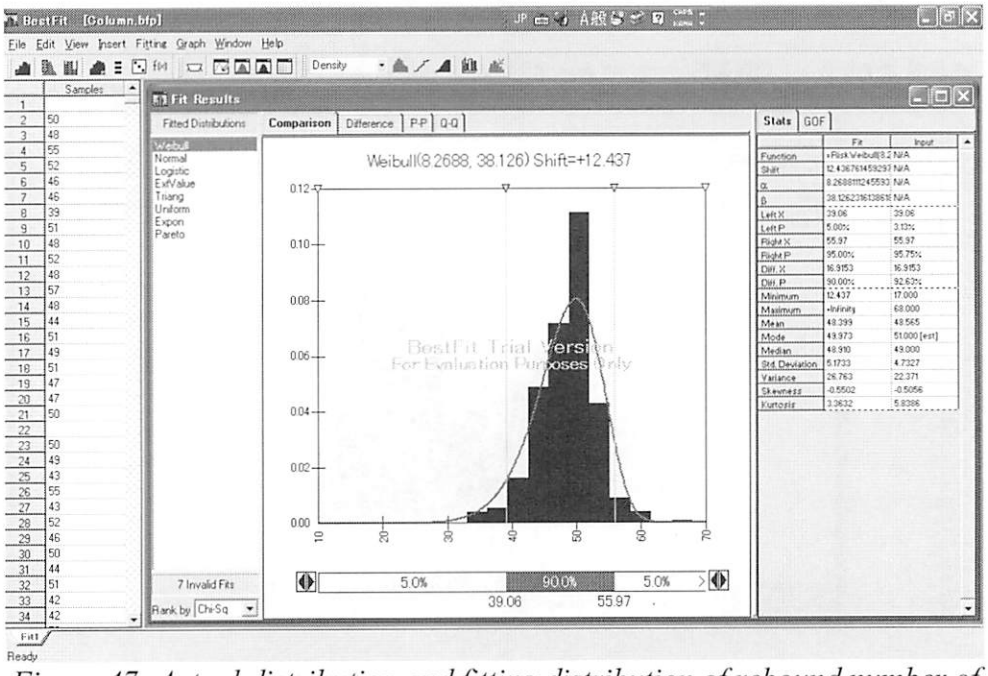

Figure 47: Actual distribution and fitting distribution of rebound number of Bridge No.5

4. MAINTENANCE PROGRAM PLANNING

From the actual inspection results shown in the last section, deterioration of each structure due to chloride attack is predicted. Mainly, distribution of corrosion initiation time and time until corrosion crack width exceeded the limit are reported.

4.1 Required number of sample

In order to get the reliable inspection result, the enough number of samples is very important to accurately represent the population. Based on the expected level of confidence, margin of error, and variation of the data, the minimum requirement of the number of samples can be determined as shown in Equation 3. However, in the beginning of this study, there is limited information about the variation of the properties of marine RC structure in Thailand. Therefore, a large number of data as explained in Section 3 were collected in our study to ensure that the sampled data is suitable to be used as a representative for a whole structure.

$$n = \left(\frac{z_{\frac{\alpha}{2}} \cdot \sigma}{E} \right)^2 \tag{3}$$

where, n is minimum number of required sample, $Z_{\alpha/2}$ is correspond z-value at the confidence level α %, σ is standard deviation of the population, and E is a margin of error.

Based on Equation (3) and the variation of the inspection result as shown in Section 3, the minimum number of required sample for marine RC structure in Thailand is recommended as below. If the number of inspected samples is less than the minimum requirement, inspected samples may not be able to accurately represent the value of the whole structure within the required level of confidence, and acceptable margin of error.

Table 12: Minimum number of required sample

Parameters	Confidence level	Margin of error	COV	Number of required sample
Covering depth	95%	5%	50%	385
Surface chloride content	95%	5%	10%*	16
Chloride diffusion coefficient	95%	5%	20%**	62
Schmidt hammer	95%	5%	20%	62

* From previous research [11]

** Assumed to be same as variation of Schmidt hammer

4.2 Inspection of surface chloride content

As shown in the result of chloride analysis, surface chloride content shows a large variation not only in horizontal direction but also in vertical direction of the structure. Therefore, it is necessary to inspect the surface chloride content of the structure at different location of the structure as well at

different height from the sea level. However, it is not required to consider the distribution of surface chloride content separately by height of the inspection. For easiness, all of the data can be combined together and determined their distribution as for the whole structure. Result of prediction of deterioration of the structure by using distribution of overall data is similar to that of using distribution of separated data. Table 13 shows the example of comparison between considering separate distribution and overall distribution of surface chloride content. Figure 48 and Table 14 shows the result of prediction of distribution surface chloride content at the 50mm from the surface of concrete after 20 years that its chloride diffusion coefficient is 0.2cm^2/year. No significant different of the prediction result can be observed between considering distribution overall and separately.

4.3 Deterioration prediction model

Although RC structure is deteriorated by many mechanisms, this study mainly focuses on chloride attack. JSCE [2] described four stages of the deterioration mechanisms of chloride attack as corrosion initiation, corrosion propagation, corrosion acceleration and deterioration stage. Detail of each stage is explained in Table 15. Deterioration prediction models must usually be selected to suit with each stage of deterioration. In this study, model to predict diffusion of chloride ion based on Fick's diffusion law is used for corrosion initiation stage as shown in Equation 4. After chloride content at the steel surface reached the limit content to initiate the corrosion which is regulated by JSCE [1] as 1.2 kg/m^3, corrosion starts. Then the model used to predicted corrosion amount, corrosion cracking time, and corrosion crack propagation are used and shown in Equation 5 [8]. Sancharoen and Uomoto [9], and Sancharoen et al. [2] proposed the method to consider variation of parameters on the prediction results including probability of failure, probability of repairing, and cost of repairing by Monte Carlo simulation and event tree analysis.

Table 13: Example condition of variation of surface chloride content with height from sea level

Height of inspection from sea level	Surface Chloride Content (kg/m^3)			
	Distribution type*	Mean*	COV*	Sigma*
20cm	Normal	12	0.1	1.2
40cm	Normal	10	0.1	1
60cm	Normal	8	0.1	0.8
80cm	Normal	6	0.1	0.6
100cm	Normal	4	0.1	0.4
Overall	Normal	8	0.375	3

*All are assumed value for a demonstration purpose

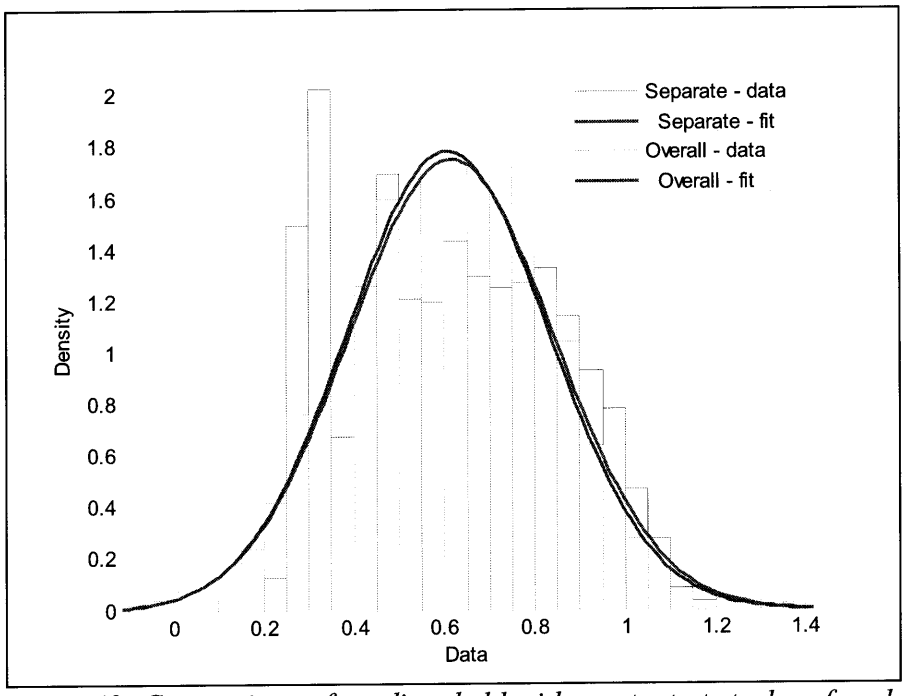

Figure 48: Comparison of predicted chloride content at steel surface by using data from inspection surface chloride content separately with height from the sea level and overall inspection

Table 14: Random variable of predicted chloride content

Method of inspection	Random variable		
	Distribution type	Mean	Sigma
Separately inspection	Normal	0.62	0.23
Overall inspection	Normal	0.61	0.23

Random variables of parameters including covering depth, chloride diffusion coefficient, surface chloride content, and concrete compressive strength are used from the actual inspection results reported in the last section for each bridge. However, other parameters required in the prediction and were not inspected at site are assumed as rationally as possible based on the literature review as shown in Table 16. Please be noted that due to the limit number of data, distribution of surface chloride content is assumed to be uniform within the minimum and maximum range as shown in Table 17. Mean value of chloride diffusion coefficient is used as the actual result of chloride analysis. However, its distribution is used from the result of rebound number of the Schmidt hammer that represents the variation of concrete quality.

Table 15: Deterioration process due to chloride induced corrosion [2]

Deterioration process	Definition	Major factors determining duration
Initiation stage	Up to time when the chloride ions content at the cover depth reaches the threshold value for corrosion of reinforcing steel	Diffusion of chloride ions Content of initially included chloride ions
Propagation stage	From the beginning of corrosion of steel reinforcement to the onset of corrosion induced cracking	Corrosion rate of reinforcing steel
Acceleration stage	Period during which corrosion is accelerated by corrosion induced cracking	Corrosion rate of reinforcing steel with cracking in concrete
Deterioration stage	Period in which the load-bearing capacity is significantly reduced by the increase in corrosion	

$$t_i = \frac{(0.1x)^2}{4D_{cl}}\left[erfc^{-1}\left(\frac{C_{\lim}}{C_s}\right)\right]^{-2} \quad (4)$$

where, t_i is corrosion initiation time (year), x is steel covering depth (mm), D_{cl} is chloride diffusion coefficient (cm^2/year), C_{lim} is threshold chloride content that corrosion will be initiated (% by weight of concrete), C_s is the chloride content at concrete surface (% by weight of concrete).

$$w_c = \frac{4\pi d_s(t)}{(1-\upsilon_c)\left(\frac{a}{b}\right)^{\sqrt{\alpha}} + (1+\upsilon_c)\left(\frac{b}{a}\right)^{\sqrt{\alpha}}} - \frac{2\pi b f_t}{E_{ef}} \quad (5)$$

where, w_c is crack width (mm), υ_c is concrete Poisson's ratio, α is stiffness reduction factor, f_t is concrete tensile strength (MPa), E_{ef} is effective modulus of concrete equals to $E_c/(1+\varphi_{cr})$ (MPa), E_c is elastic modulus of concrete (MPa), φ_{cr} is concrete creep coefficient, $d_s(t)$ can be determined from Eq. (6) [10].

$$d_s(t) = \frac{W_{rust}(t)}{\pi(D+2d_0)}\left(\frac{1}{\rho_{rust}} - \frac{\alpha_{rust}}{\rho_{st}}\right) \quad (6)$$

where, $W_{rust}(t)$ is a mass of rust product (mg/mm), ρ_{rust} is density of corrosion products, ρ_{st} is density of steel, α_{rust} is coefficient related to types of rust products. $W_{rust}(t)$ can be determined from Eq. (7) [10].

$$W_{rust}(t) = \sqrt{2\int_{t_i}^{t}\left(\frac{0.105\pi D i_{corr}(t)}{\alpha_{rust}}\right)dt} \quad (7)$$

where, t is the considering point of time (year), i_{corr} is annual mean corrosion rate ($\mu A/cm^2$).

Table 16: Random variables of other parameters

Parameters	Mean	Coefficient of variation (Distribution Type)
C_{lim}, [11]	0.05 % by mass of concrete	0.10 (Log normal)
D	1.6 cm	0.015 (Normal)
i_{corr}, [10]	2 $\mu A/cm^2$	Constant
d_0, [10]	12.5 μm	Constant
α_{rust}, [10]	0.57	Constant
ρ_{rust}, [10]	3600 kg/m^3	Constant
ρ_{st}, [10]	7850 kg/m^3	Constant
f_t', [1]	$0.23 f_c'^{2/3}$	-
E_c, [1]	30.1 GPa	Constant
φ_{cr}, [1]	1.1	Constant
υ_c, [1]	0.20	Constant

4.3.1 Corrosion initiation time

The first stage of deterioration of RC structure due to chloride induced corrosion is from the starting of diffusion of chloride ion into the structure until the corrosion of reinforcing steel is initiated. This initiation time is commonly defined by the limit of chloride ion at the steel surface (1.2 kg/m^3 [1]) and can be calculated as shown in Equation 4. By considering the variation of the parameters including covering depth, chloride diffusion coefficient, and surface chloride content obtained from the actual inspection, the distribution of expected corrosion initiation time can be predicted alone the service life of structure. Figure 49 to 53 show the probability of corrosion initiation time of each structure along their service life.

Table 17: Assumed distribution of surface chloride content

Bridge No.	Distribution	Surface chloride content, kg/m^3	
		Minimum	Maximum
1	Uniform	7.14	11.17
2	Uniform	1.61	4.64
3	Uniform	3.1	6.72
4	Uniform	10.58	19.45
5	Uniform	3.95	14.39

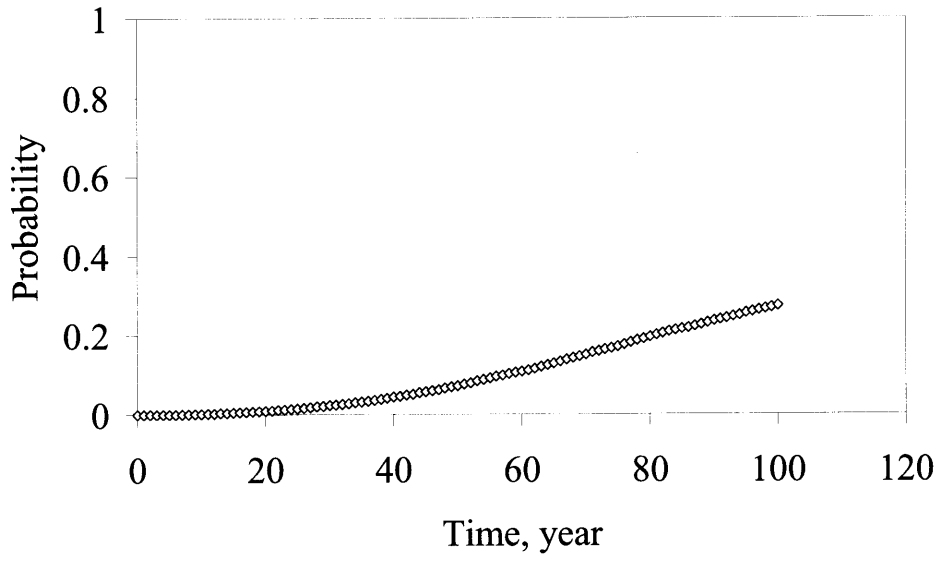

Figure 49: Probability of steel corrosion to be initiated along the service life of Bridge No.1

Figure 49 shows the probability that corrosion will be initiated during each year along service life of Bridge No.1 that use coal fly ash as a cement replacement material. As shown, there is low probability of corrosion to be initiated even at the end of expected service life of structure. Even at 100 years after service, the corrosion is expected to be observable in only 30% of total structure area. This is due to the design specification of this bridge requires minimum covering depth as 75mm and the inspection result shows actual covering depth of Bridge No.1 is larger than the minimum requirement. When comparison the probability of corrosion initiation shown in Figure 49 with Figure 50 to 53 is made, Figure 49 shows low probability of corrosion in the beginning. The main reason is that the larger covering depth of Bridge No.1 causes a small number of low covering depth concrete. Therefore, the corrosion initiation starts slowly. However, the benefits of utilizing coal fly ash as a partial cement replacement material to decrease chloride diffusion coefficient of structure cannot be seen in the result of inspection as shown in Table 9. However, in the long term performance, coal fly ash concrete is expected to show higher performance against chloride penetration. As a result, the overall resistance of concrete against steel corrosion of this bridge is expected to be very high.

Figure 50 shows the probability that corrosion is initiated during each year along service life of Bridge No.2 which is the oldest bridge in this study. Even though marine environment of this bridge is not so severe, but inspection result reveals that its covering depth is very low. Therefore, corrosion is expected to be initiated approximately 80% of the total structure within the first 10 years after construction. This agrees well with the visual observation of deterioration degree as shown in Figure 16. Severe damage and spalling of concrete can be observed on the whole structure.

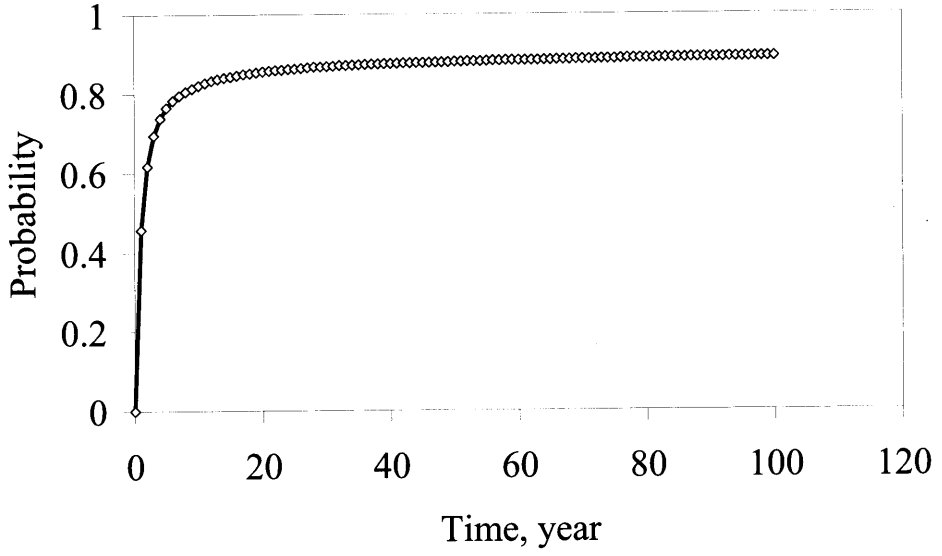

Figure 50: Probability of steel corrosion to be initiated along the service life of Bridge No.2

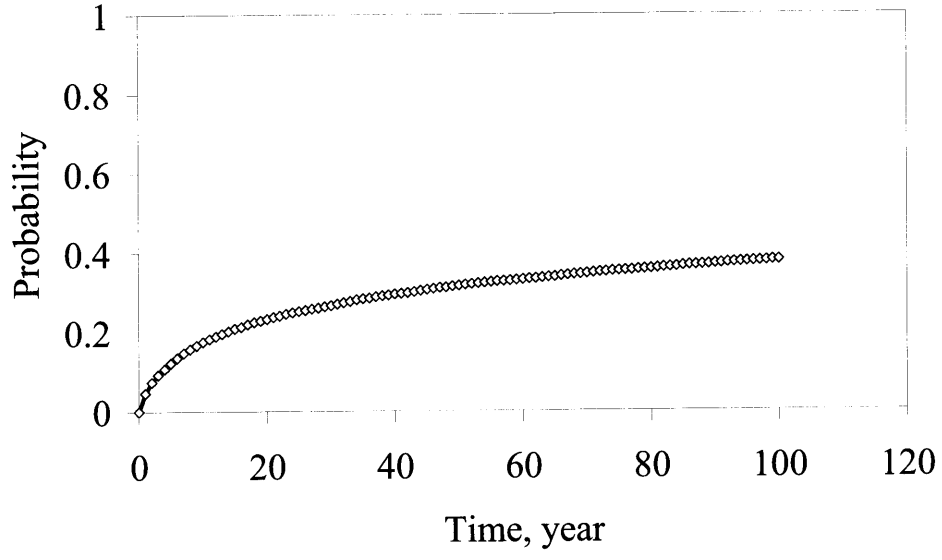

Figure 51: Probability of steel corrosion to be initiated along the service life of Bridge No.3

Figure 51 shows the probability that corrosion is initiated during each year along service life of Bridge No.3. Because covering depth of Bridge No.3 is larger than that of Bridge No.2, steel corrosion is also expected to be slower. As shown, corrosion will be observed only 40% of structure at the 100 years after the service.

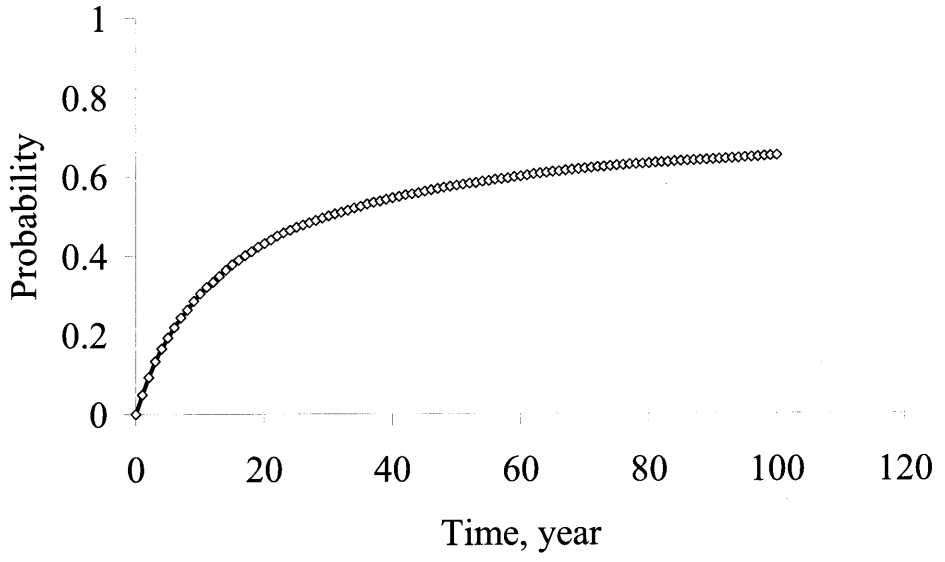

Figure 52: Probability of steel corrosion to be initiated along the service life of Bridge No.4

Corrosion of Bridge No. 4 is also expected to start early. The main reason is still that the covering depth is significantly smaller than design value. As shown in Figure 52, corrosion is expected to be in active more than 60% of structure at the end of year 100th after the service.

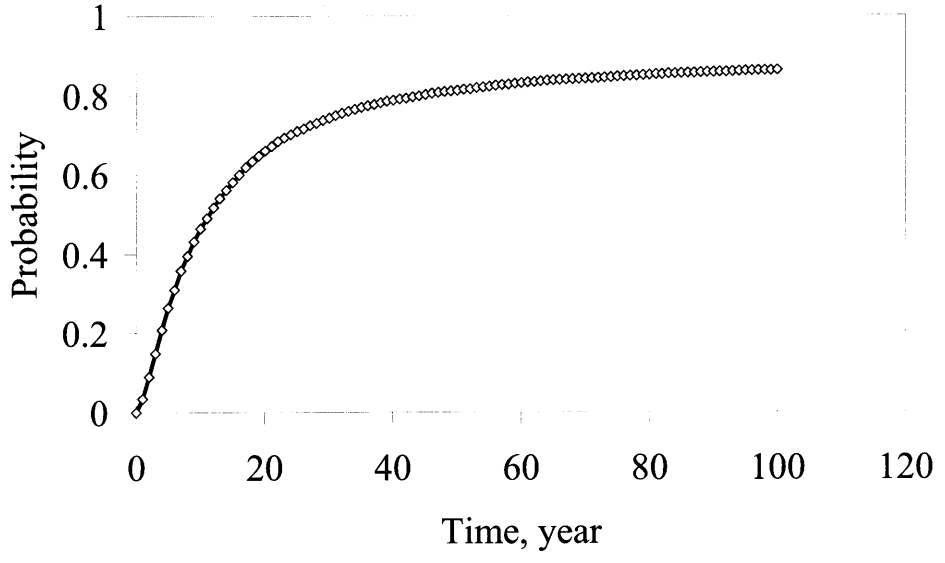

Figure 53: Probability of steel corrosion to be initiated along the service life of Bridge No.5

Figure 53 shows the probability of corrosion initiation during each year along service life of Bridge No.5 that use the sulfate resistance cement. The prediction result shows that after 40 years in service, probability of corrosion initiation can be observed more than on 80% of structure. Even though this structure specified to use larger covering depth and sulfate resistance cement, the mean value of actual covering depth of this structure

is only 41 mm that is lower than the design value. Also using sulfate resistance cement for marine RC structure is a misunderstanding because the lower calcium aluminate content degrades chloride binding capacity hydrated products. The severe marine condition of Bridge No.5 as revealed from the surface chloride content is another cause of the rapid deterioration of this structure.

4.3.2 Time to reach allowable crack width

After corrosion crack has been generated, the corrosion process is still active and even faster. As a result, the internal pressure will be continuously generated and causes the expansion of the corrosion crack width as calculated by Equation 5. Normally, corrosion crack width is limited in order to prevent the ingression of harmful material from outside as well other safety reasons. Guideline of limit crack width is shown in Table 18.

Table 18: Permissible crack width [6]

Type of reinforcement	Environmental condition		
	Normal	Corrosive	Severely corrosive
Deformed and plain bars	0.005x	0.004x	0.0035x
Prestressing steel	0.004x	-	-

where x is the covering depth (mm)

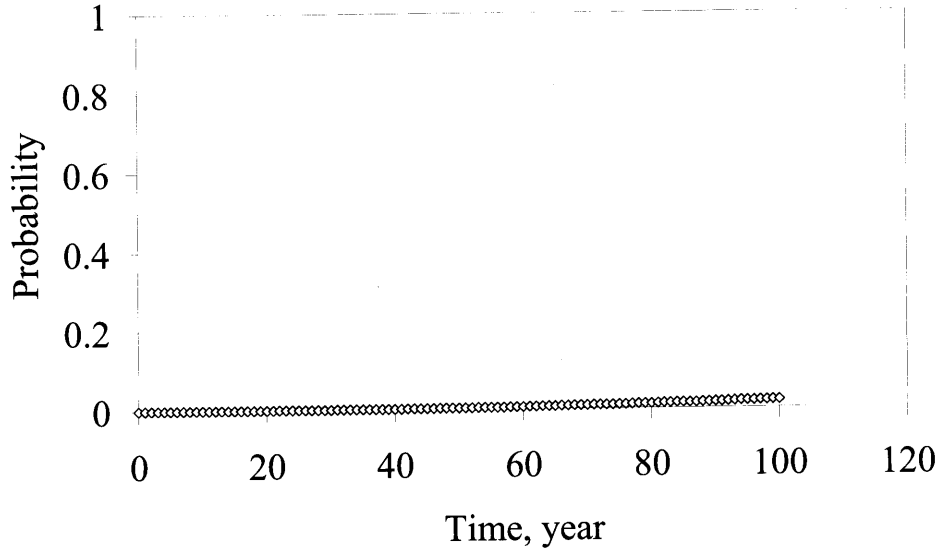

Figure 54: Probability of corrosion crack width exceed the limit along the service life of Bridge No.1

Figure 54 shows the result of the prediction of time required for corrosion crack width will propagate to the limit width of the Bridge No.1. Due to its large covering depth, there is very low probability that the corrosion crack width will reach the limit during its service life of 100 years. As a result, the future maintenance cost of this structure can be expected to be very low while the safety is still high.

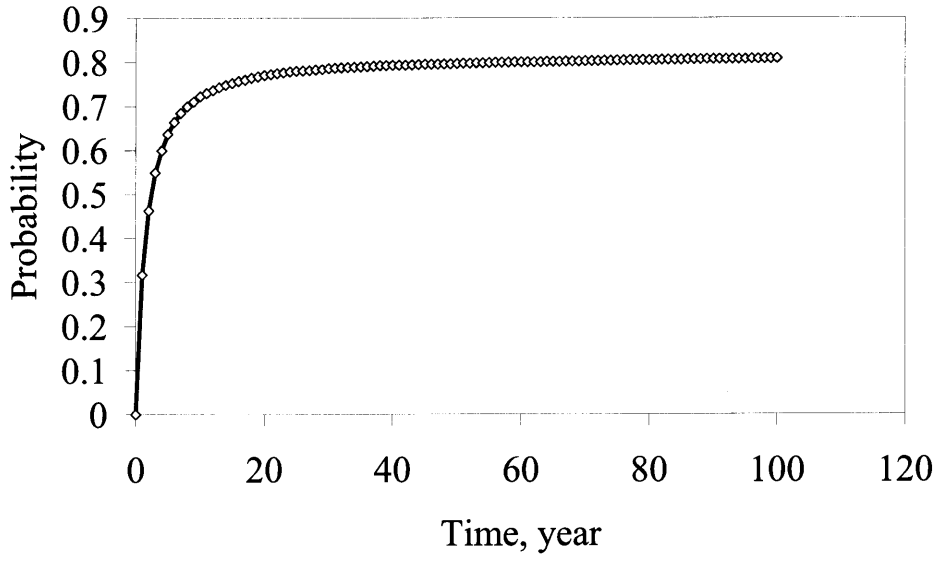

Figure 55: Probability of corrosion crack width exceed the limit along the service life of Bridge No.2

Figure 55 shows that the bridge No.2 shows very high probability that the corrosion crack width will reach the service during its service life. As shown, 80% of total structure is expected to show the corrosion crack with in the first 40 years after being in service. This agrees well with the actual visual inspection of the current condition as shown in Figure 19.

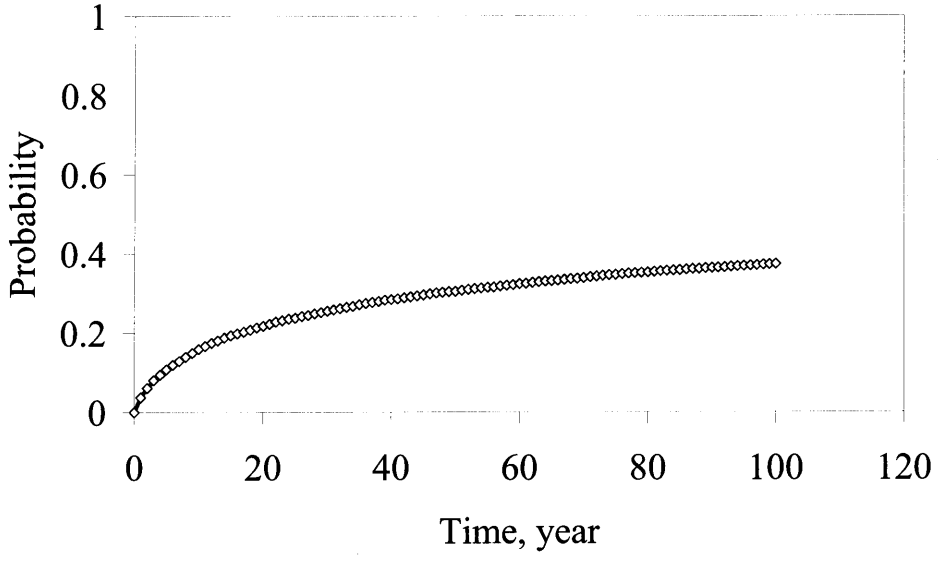

Figure 56: Probability of corrosion crack width exceed the limit along the service life of Bridge No.3

Compared to Bridge No.2, Bridge No.3 shows lower probability of exceeding the limit of corrosion crack width during the service life because of its larger covering depth. Only 40 % of the total structure is expected to show the larger crack width than the acceptable value.

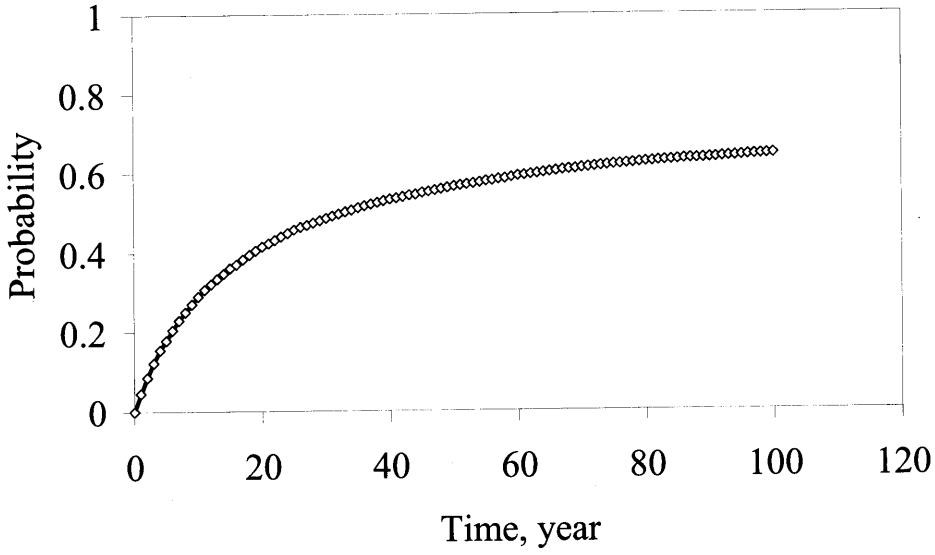

Figure 57: Probability of corrosion crack width exceed the limit along the service life of Bridge No.4

Figure 57 shows the probability that corrosion crack width of Bridge No.4 will exceed the limit. As shown, 60% of structure is expected to be observed that its crack width is larger than the limited width at the end of service life of 100 years.

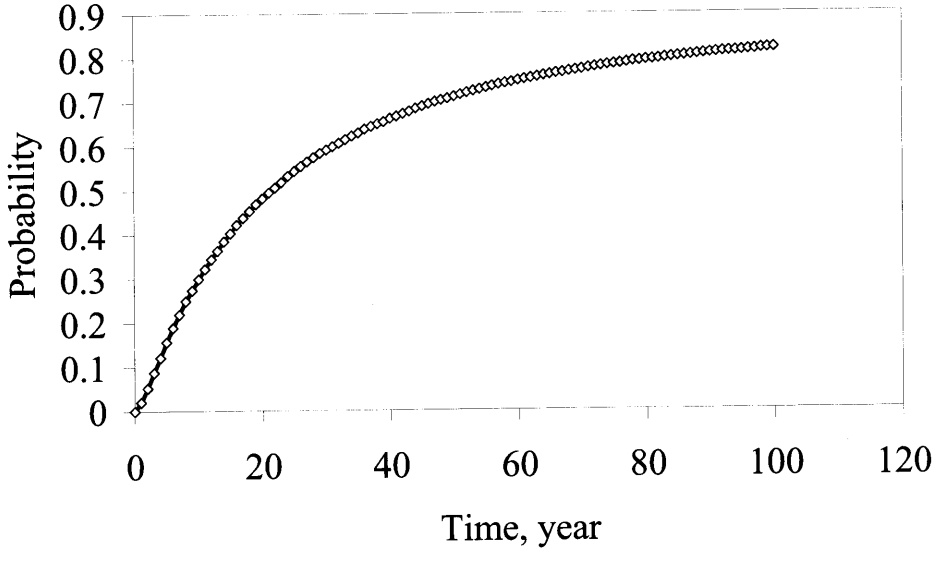

Figure 58: Probability of corrosion crack width exceed the limit along the service life of Bridge No.5

Figure 58 shows that there is high probability that Bridge No.5 will show corrosion crack width larger than the limit. Even though, Bridge No.5 regulates minimum covering depth same to that of Bridge No.1, the actual inspection result reveals that covering depth of Bridge No.5 is only half of that of bridge No.1. Also the result of chloride analysis reveals that surface

chloride content of Bridge No.5 is the highest of the result from every Bridges. As a result, the probability that corrosion crack width of Bridge No.5 will larger than limit value is more than 80% at the end of service life of 100 years.

5. CONCLUSIONS

In this study, the inspection was conducted on five marine RC structures in Thailand both of OPC RC structure and coal fly ash RC structure. From the results, it was revealed that there are very large uncertainties in the properties of the structures, especially the covering depth, chloride diffusion coefficient, and concrete quality. Mean value of covering depth is mostly lower than the design value. The reason can be lack of quality control, knowledge, or mistake of construction lead to large variation of the result. However, not only the quality of construction but also environment causes uncertainties in durability of RC structure. As shown, the variation of surface chloride content can be seen in both of horizontal direction as well vertical direction. Uncertainties are very significant in the actual condition.

Deterioration prediction result shows that larger concrete covering depth of reinforcing steel effectively prevents the chloride induced steel corrosion. However, the benefit of utilizing of coal fly ash to increase resistance against chloride penetration cannot be clearly seen in this study. This may be due to the inspected structure are exposed to different environmental condition and coal fly ash RC structure is still very young compare to other inspected structures. Safety of the marine structure can be ensured and maintenance can be minimized, if the properties of actual structure can be controlled and ensured as the designed values during construction.

ACKNOWLEDGEMENT

This study was financially supported by the Central Research Institute of Electric Power Industry: Organization and Activities. The kind cooperation from the officers of Department of Rural Roads and Department of Public Works and Town & Country Planning, Thailand was also highly appreciated. The authors would also like to pay a profound gratitude to Hilti (Thailand) Ltd. for a kind support of equipments. The special thank is extended to Mr. Nanayakara Ominda, a current doctoral student of Graduate School of Civil Engineering, The university of Tokyo as well as 4th year students of Rachamangala Institute of Technology.

REFERENCES

[1] JSCE, "Standard Specifications for Concrete Structures-2002 "Structural Performance verification"," JSCE, 2005

[2] JSCE, "Standard Specifications for Concrete Structures-2001 "Maintenance"," JSCE, 2005

[3] Thai Meteorological Department, "Daily Weather Information", Information Service Department, Thai Meteorological Department, 2007

[4] Sancharoen, P., Kato, Y., and Uomoto, T., "Effect of Variation of Parameters Used in the Deterioration Prediction Model on the R&M Plan," Proceedings of the second ACF International Conference (ACF2006), Bali, Indonesia, 2006

[5] JSCE, "JSCE-G573: Measurement Method for Distribution of Total Chloride Ion in Concrete Structure," JSCE, 2003

[6] JCI SC5, "Abbreviated analysis method of all salinity which is included in the hardening concrete, Standard Method of Examination Regarding the Corrosion and Corrosion Protection of Concrete Structure," Japan Concrete Institute, Tokyo, 1987

[7] JSCE, "Guideline for Experiment on Materials of Civil Works," JSCE, 2005.

[8] Li, C. Q., Melchers, R. E., and Zheng, J. J., "Analytical Model for Corrosion-Induced Crack Width in Reinforced Concrete Structures," *ACI Structural Journal*, Vol.11, No.4, 2006, pp.479-487

[9] Sancharoen, P., and Uomoto, T., "Life Cycle Repairing Cost Considering Uncertainties of Deterioration Prediction Model," Proceedings of the Annual Convention of Japan Concrete Institute, 2006, 1639-1644

[10] Liu, Y. and Weyers, R. E., "Modeling the Time-to-Corrosion Cracking in Chloride Contaminated Reinforced Concrete Structures," ACI Materials Journal, Vol.95, No.6, Nov.-Dec., 1998, pp.675-681

[11] Enright, M. P. and Frangapol, D. M., "Condition Prediction of Deteriorating Concrete Bridges Using Bayesian Updating," J. of Structural Div., ASCE, Vol.125, No.10, Oct., 1999, pp.1118-1125

[12] Sahamitmongkol, R., Kato, Y., Kurashige, I., Tangtermsirikul, S., and Uomoto, T., "Report on Application of Fly Ash as Concrete ingredient in Thailand and Japan -Development and Current Situation-," ICUS Report 2006-05, International Center for Urban Safety Engineering, Institute of Industrial Science, The University of Tokyo, 2006.

APPENDIX A

A.1 PROBABILITY DENSITY FUNCTION

In mathematics and statistics, a probability density function describes how probabilities are distributes on events. Informally, a probability density function can be seen as a "smoothed out" version of a histogram: if one empirically samples enough values of a continuous random variable, producing a histogram depicting relative frequencies of output ranges, then this histogram will resemble the random variable's probability density, assuming that the output ranges are sufficiently narrow.

A probability density function is any function f(x) that describes the probability density in terms of the input variable x in a manner described below.

- f(x) is greater than or equal to zero for all values of x
- The total area under the graph is 1 as shown in Equation A-1

$$\int_{-\infty}^{+\infty} f(x)dx = 1.0 \qquad \text{(A-1)}$$

A distribution is called discrete if its cumulative distribution function only increases in jumps, or equivalently that it belongs to a discrete random variable, a random variable which is fully characterized by the probabilities it assigns to a certain finite or countable set of values. By one convention, a distribution is called continuous if its cumulative distribution function is continuous, which means that it belongs to a random variable X for which Pr[X = x] = 0 for all x in R

Several probability distributions are so important in theory or applications that they have been given specific names as below.

A.1.1 Discrete distributions

A.1.1.1 With finite support

- The Bernoulli distribution, which takes value 1 with probability p and value 0 with probability q = 1 − p.
- The Rademacher distribution, which takes value 1 with probability 1/2 and value − 1 with probability 1/2.
- The binomial distribution describes the number of successes in a series of independent Yes/No experiments.
- The degenerate distribution at x0, where X is certain to take the value x0. This does not look random, but it satisfies the definition of random variable because although its output is determinate, its

input is random. This is useful because it puts deterministic variables and random variables in the same formalism.

- The discrete uniform distribution, where all elements of a finite set are equally likely. This is supposed to be the distribution of a balanced coin, an unbiased die, a casino roulette or a well-shuffled deck. Also, one can use measurements of quantum states to generate uniform random variables. All these are "physical" or "mechanical" devices, subject to design flaws or perturbations, so the uniform distribution is only an approximation of their behaviour. In digital computers, pseudo-random number generators are used to produce a statistically random discrete uniform distribution.
- The hypergeometric distribution, which describes the number of successes in the first m of a series of n Yes/No experiments, if the total number of successes is known.
- Zipf's law or the Zipf distribution. A discrete power-law distribution, the most famous example of which is the description of the frequency of words in the English language.
- The Zipf-Mandelbrot law is a discrete power law distribution which is a generalization of the Zipf distribution.

A.1.1.2 With infinite support

- The Boltzmann distribution, a discrete distribution important in statistical physics which describes the probabilities of the various discrete energy levels of a system in thermal equilibrium. It has a continuous analogue. Special cases include:
- The Gibbs distribution
- The Maxwell-Boltzmann distribution
- The Bose-Einstein distribution
- The Fermi-Dirac distribution
- The geometric distribution, a discrete distribution which describes the number of attempts needed to get the first success in a series of independent Yes/No experiments.
- The logarithmic (series) distribution
- The negative binomial distribution, a generalization of the geometric distribution to the nth success.
- The parabolic fractal distribution
- The Poisson distribution as shown in Equation A-2 and Figure A-1, which describes a very large number of individually unlikely events that happen in a certain time interval.

$$f(k,\lambda) = \frac{e^{-\lambda}\lambda^{k}}{k!} \qquad \text{(A-2)}$$

where, e is is the base of the natural logarithm, k is the number of occurrences of an event - the probability of which is given by the function, and λ is a positive real number, equals to the expected number of occurrences that occur during the given interval. For instance, if the events occur on average every 4 minutes, and you are interested in the number of

events occurring in a 10 minute interval, you would use as model a Poisson distribution with $\lambda = 10/4 = 2.5$.

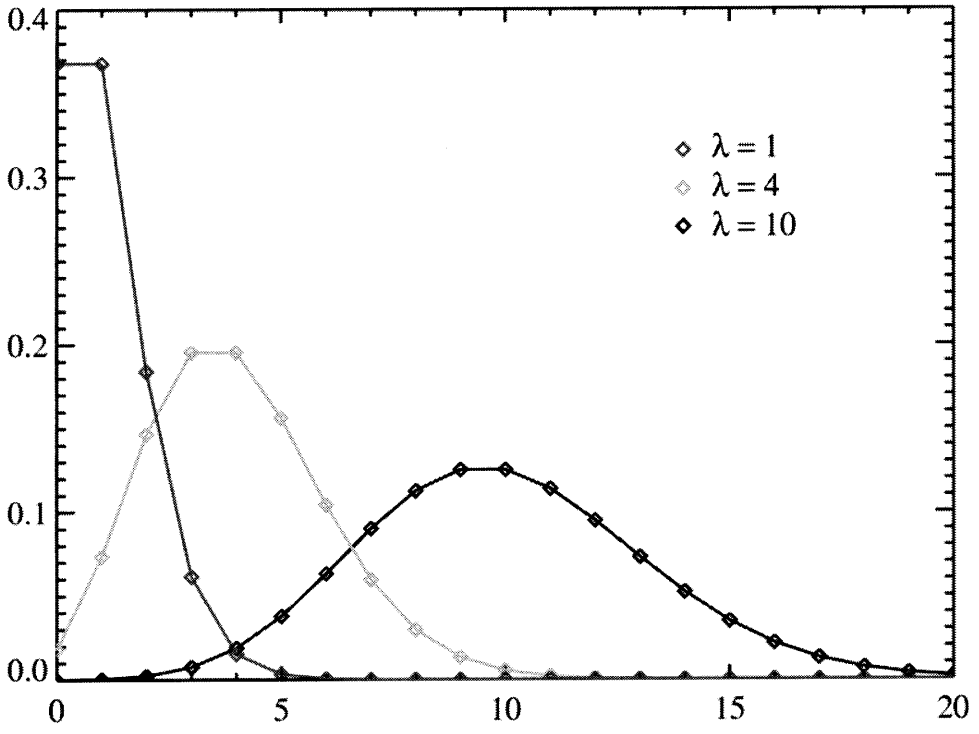

Figure A-1: Poisson distribution

- The Skellam distribution, the distribution of the difference between two independent Poisson-distributed random variables.
- The Yule-Simon distribution
- The zeta distribution has uses in applied statistics and statistical mechanics, and perhaps may be of interest to number theorists. It is the Zipf distribution for an infinite number of elements.

A.1.2 Continuous distributions

A.1.2.1 Supported on bounded interval

- The Beta distribution as shown in Equation A-3 and Figure A-2 on [0,1] differing in the values of their two non-negative shape parameters, α and β, of which the uniform distribution is a special case, and which is useful in estimating success probabilities.

$$f(x;\alpha,\beta) = \frac{1}{B(\alpha,\beta)} x^{\alpha-1}(1-x)^{\beta-1} \qquad \text{(A-3)}$$

where α, and β are non-negative shape parameters, Γ is gamma function as shown in Equation A-4, and B is beta function.

$$\Gamma(z) = \int_0^\infty t^{z-1} e^{-t}\, dt \qquad \text{(A-4)}$$

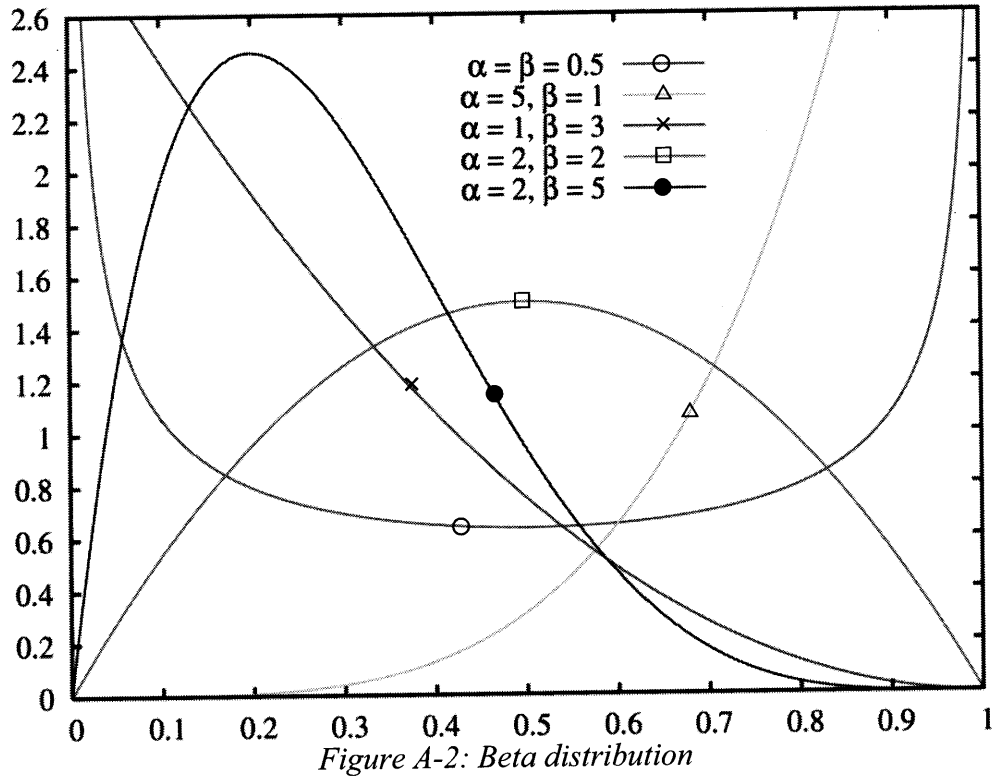

Figure A-2: Beta distribution

- The continuous uniform distribution on [a,b] as shown in Equation A-5 and Figure A-3, where all points in a finite interval are equally likely.

$$f(x) = \begin{cases} \dfrac{1}{b-a} & \text{for} \quad a < x < b \\ 0 & \text{for} \quad x < a \text{ or } x > b \end{cases} \tag{A-5}$$

- The rectangular distribution is a uniform distribution on [-1/2,1/2].
- The Dirac delta function although not strictly a function, is a limiting form of many continuous probability functions. It represents a discrete probability distribution concentrated at 0 — a degenerate distribution — but the notation treats it as if it were a continuous distribution.
- The Kumaraswamy distribution is as versatile as the Beta distribution but has simple closed forms for both the cdf and the pdf.
- The logarithmic distribution (continuous)
- The triangular distribution on [a, b] as shown in Equation A-6 and Figure A-4, a special case of which is the distribution of the sum of two uniformly distributed random variables (the convolution of two uniform distributions).

$$f(x) = \begin{cases} \dfrac{2(x-a)}{(b-a)(c-a)} & for \quad a \le x \le c \\ \dfrac{2(b-x)}{(b-a)(b-c)} & for \quad c \le x \le b \end{cases} \qquad \text{(A-6)}$$

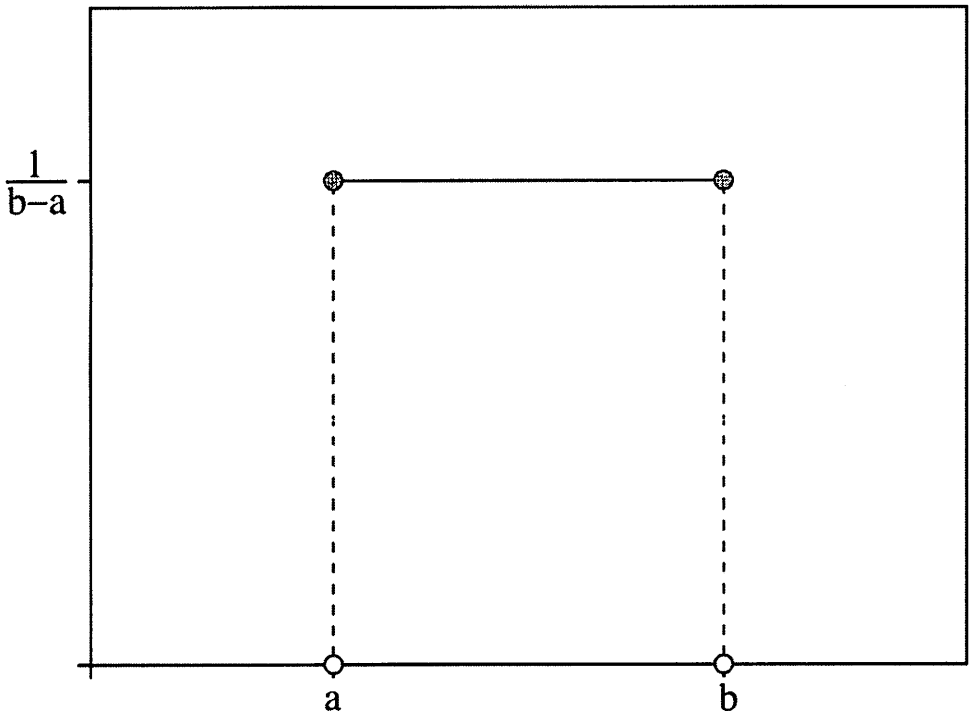

Figure A-3: Continuous uniform distribution

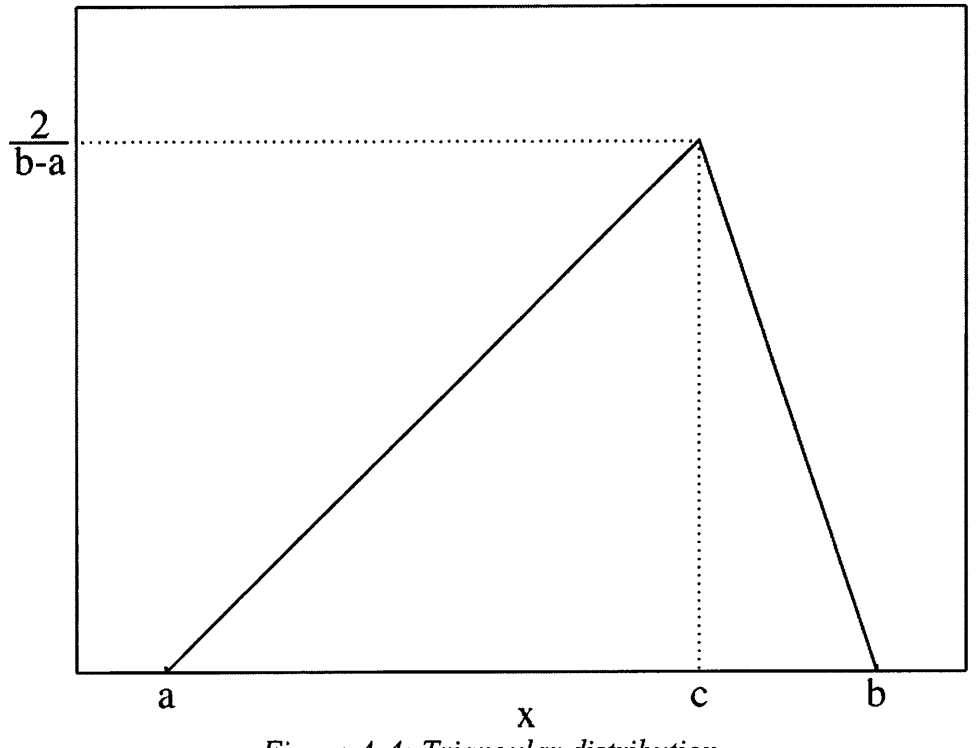

Figure A-4: Triangular distribution

- The von Mises distribution on the circle.
- The von Mises-Fisher distribution on the N-dimensional sphere has the von Mises distribution as a special case.
- The Kent distribution on the three-dimensional sphere.
- The Wigner semicircle distribution is important in the theory of random matrices.

A.1.2.2 Supported on semi-infinite intervals, usually [0,∞]

- The chi distribution
- The noncentral chi distribution
- The chi-square distribution as shown in Equation A-7 and Figure A-5, which is the sum of the squares of n independent Gaussian random variables. It is a special case of the Gamma distribution, and it is used in goodness-of-fit tests in statistics.

$$f(x;k) = \frac{0.5^{k/2}}{\Gamma(k/2)} x^{k/2-1} e^{-x/2} \qquad \text{(A-7)}$$

where, k is a parameter that is a positive integer and specifies the number of degrees of freedom.

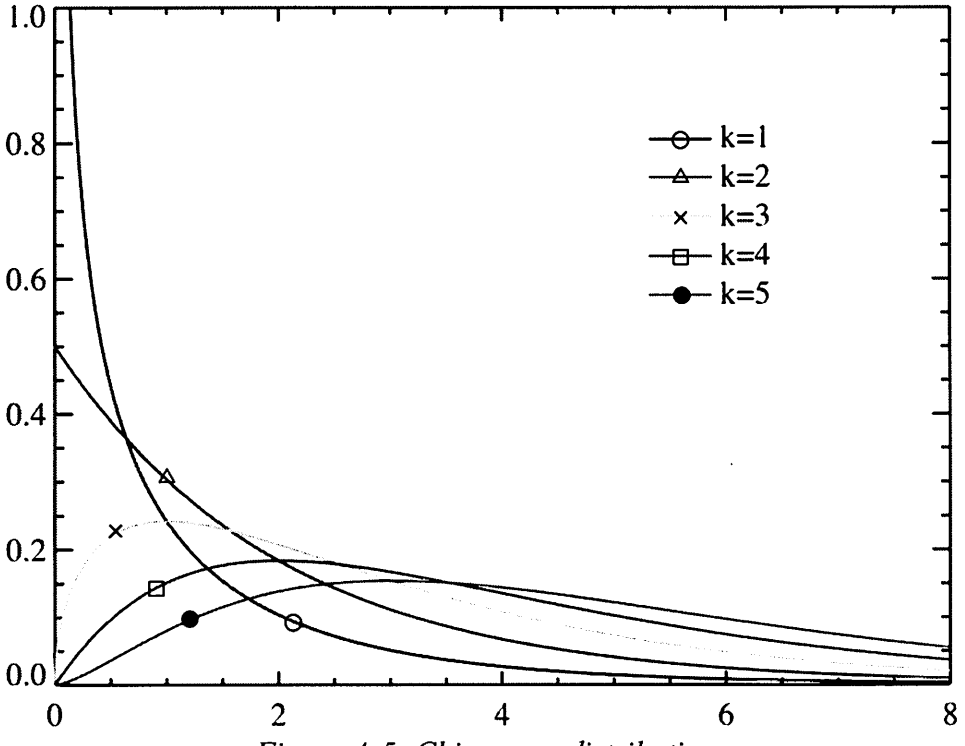

Figure A-5: Chi-square distribution

- The inverse-chi-square distribution
- The noncentral chi-square distribution
- The scale-inverse-chi-square distribution

- The exponential distribution as shown in Equation A-8 and Figure A-6, which describes the time between consecutive rare random events in a process with no memory.

$$f(x;\lambda) = \begin{cases} \lambda e^{-\lambda x}, x \geq 0 \\ 0 \quad , x < 0 \end{cases} \tag{A-8}$$

where $\lambda > 0$ is a parameter of the distribution, often called the rate parameter.

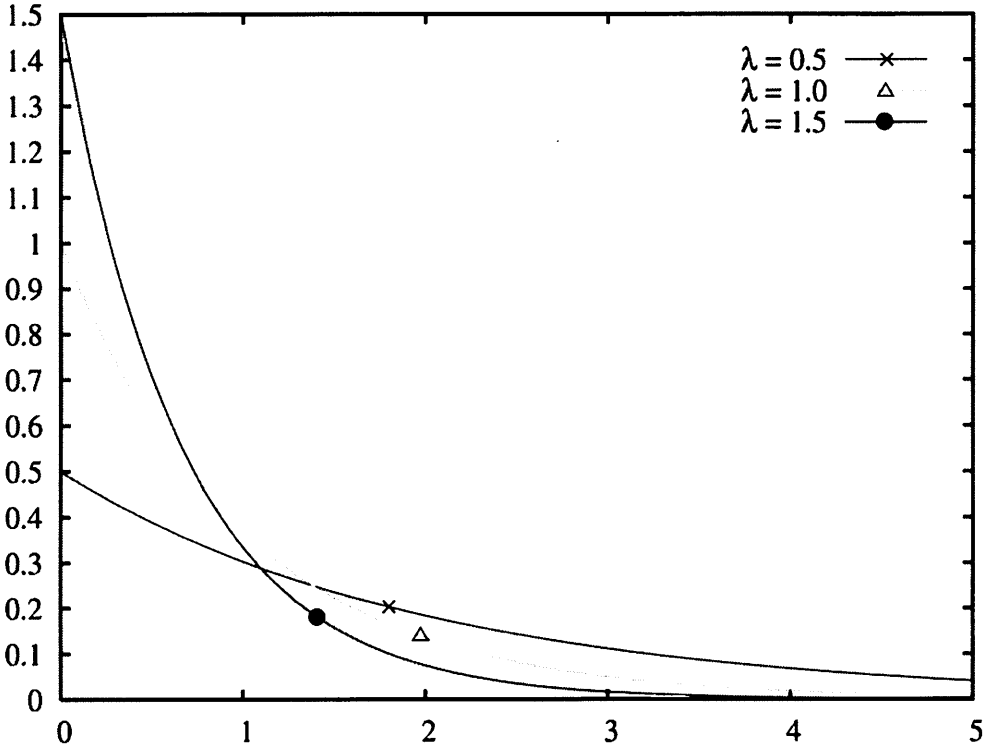

Figure A-6: Exponential distribution

- The F-distribution, which is the distribution of the ratio of two (normalized) chi-square distributed random variables, used in the analysis of variance. (Called the beta prime distribution when it is the ratio of two chi-square variates which are not normalized by dividing them by their numbers of degrees of freedom.)
- The noncentral F-distribution
- The Gamma distribution as shown in Equation A-9 and Figure A-7, is a two-parameter family of continuous probability distributions that represents the sum of k exponentially distributed random variables, each of which has mean θ .

$$f(x:k,\theta) = x^{k-1}\frac{e^{-x/\theta}}{\theta^k \Gamma(k)} \quad for \quad x > 0 \tag{A-9}$$

where k > 0 is the shape parameter and θ > 0 is the scale parameter of the gamma distribution.

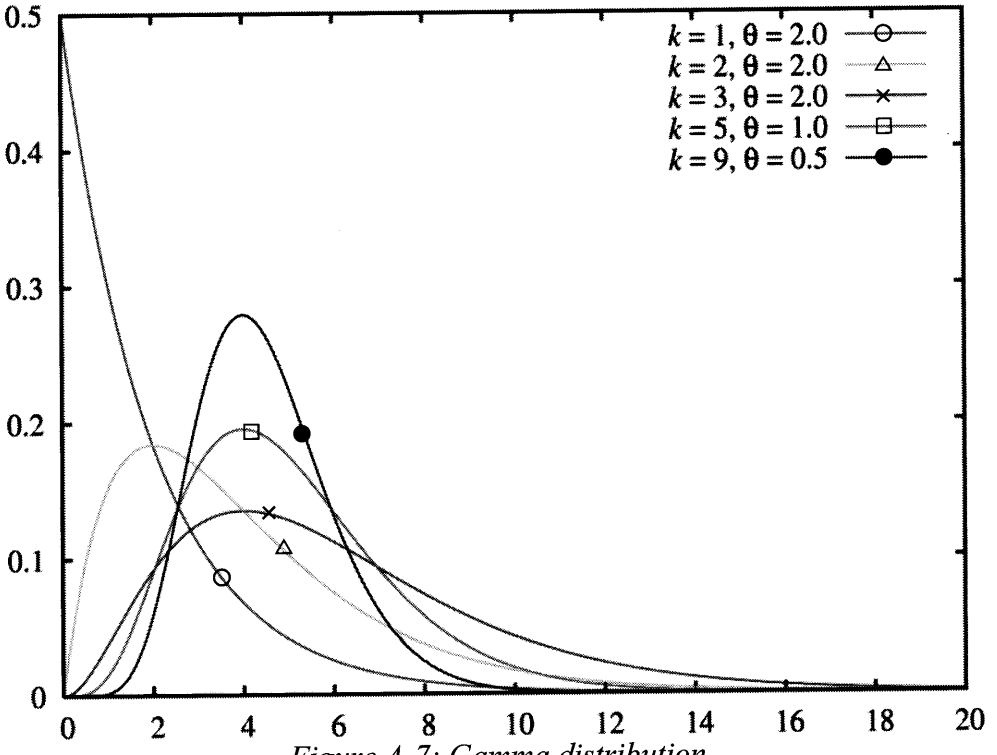

Figure A-7: Gamma distribution

- The Erlang distribution as shown in Equation A-10 and Figure A-8, which is a special case of the gamma distribution with integral shape parameter, developed to predict waiting times in queuing systems. The distribution is a continuous distribution, which has a positive value for all real numbers greater than zero, and is given by two parameters: the shape k, which is an integer, and the rate λ, which is a real. The distribution is sometimes defined using the inverse of the rate parameter, the scale θ. When the shape parameter k equals 1, the distribution simplifies to the exponential distribution. The Erlang distribution is a special case of the Gamma distribution where the shape parameter k is an integer. In the Gamma distribution, this parameter is a real.

$$f(x;k,\lambda) = \frac{\lambda^k x^{k-1} e^{-\lambda x}}{(k-1)!} \quad for \quad x > 0 \qquad \text{(A-10)}$$

The parameter k is called the shape parameter and the parameter λ is called the rate parameter.

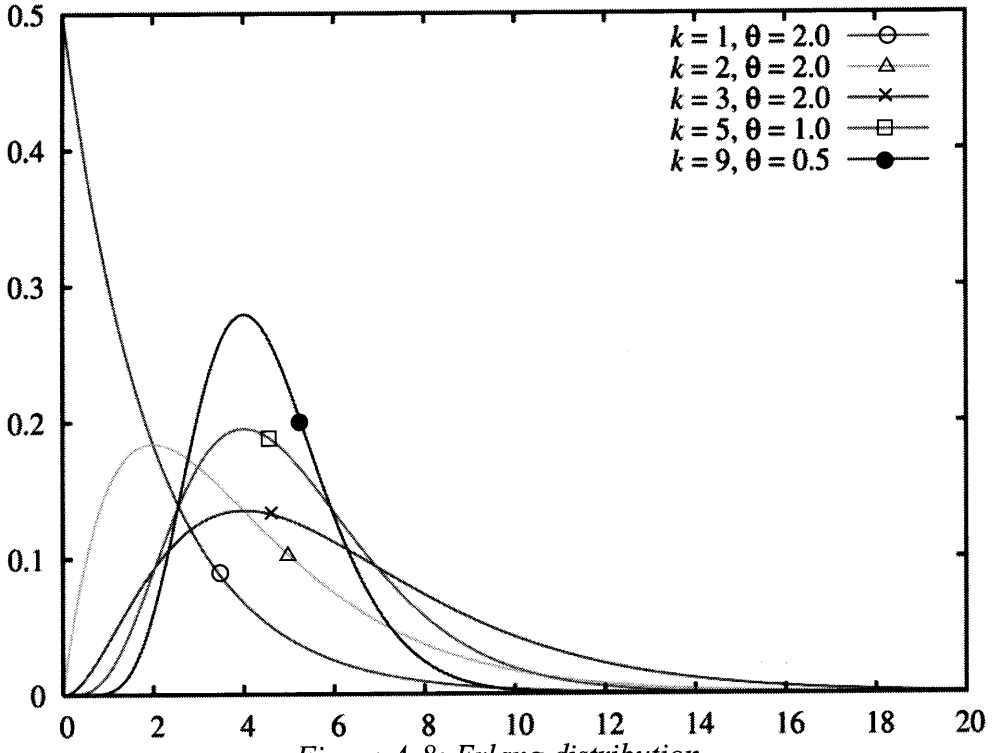

Figure A-8: Erlang distribution

- The inverse-gamma distribution as shown in Equation A-11 and Figure A-9

$$f(x;\alpha,\beta) = \frac{\beta^{\alpha}}{\Gamma(\alpha)} x^{-\alpha-1} \exp\left(-\frac{\beta}{x}\right) \qquad \text{(A-11)}$$

where α is the shape parameter and β is the scale parameter.

- The inverse Gaussian distribution as shown in Equation A-12 and Figure A-10

$$f(x;\mu,\lambda) = \left[\frac{\lambda}{2\pi x^3}\right]^{1/2} \exp\frac{-\lambda(x-\mu)^2}{2\mu^2 x} \qquad \text{(A-12)}$$

- The half-normal distribution
- The Lévy distribution
- The logistic distribution as shown in Equation A-13 and Figure A-11. This distribution has longer tails than the normal distribution and a higher kurtosis of 1.2 (compared with 0 for the normal distribution).

$$f(x;\mu,s) = \frac{e^{-\left(x-\mu/s\right)}}{s\left[1+e^{-\left(x-\mu/s\right)}\right]^2} \qquad \text{(A-13)}$$

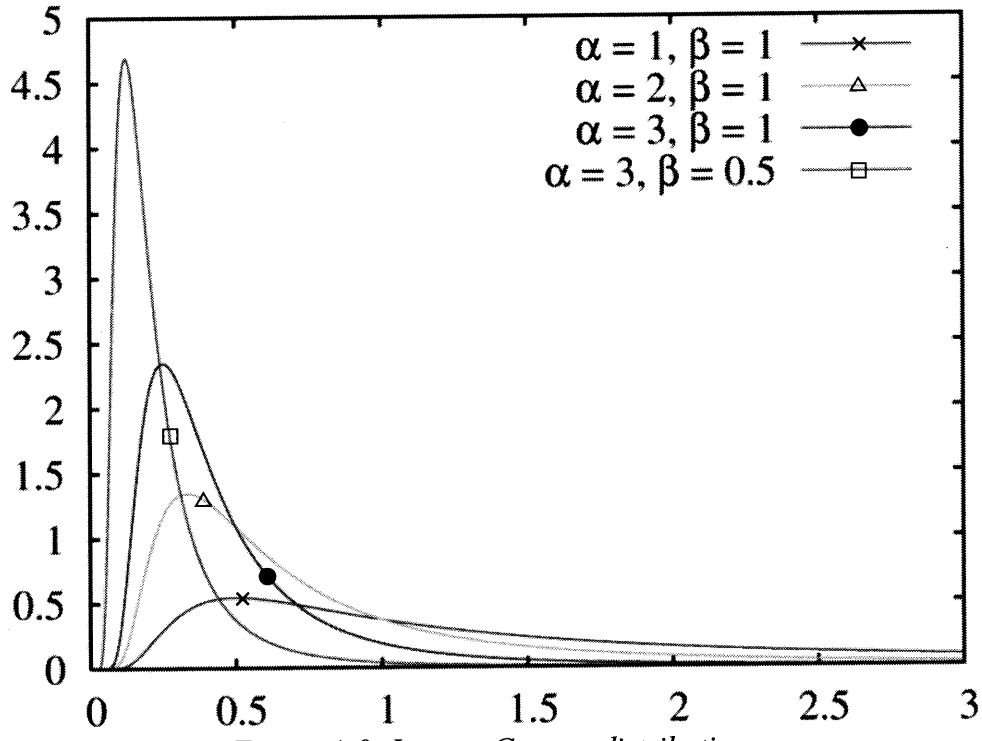

Figure A-9: Inverse Gamme distribution

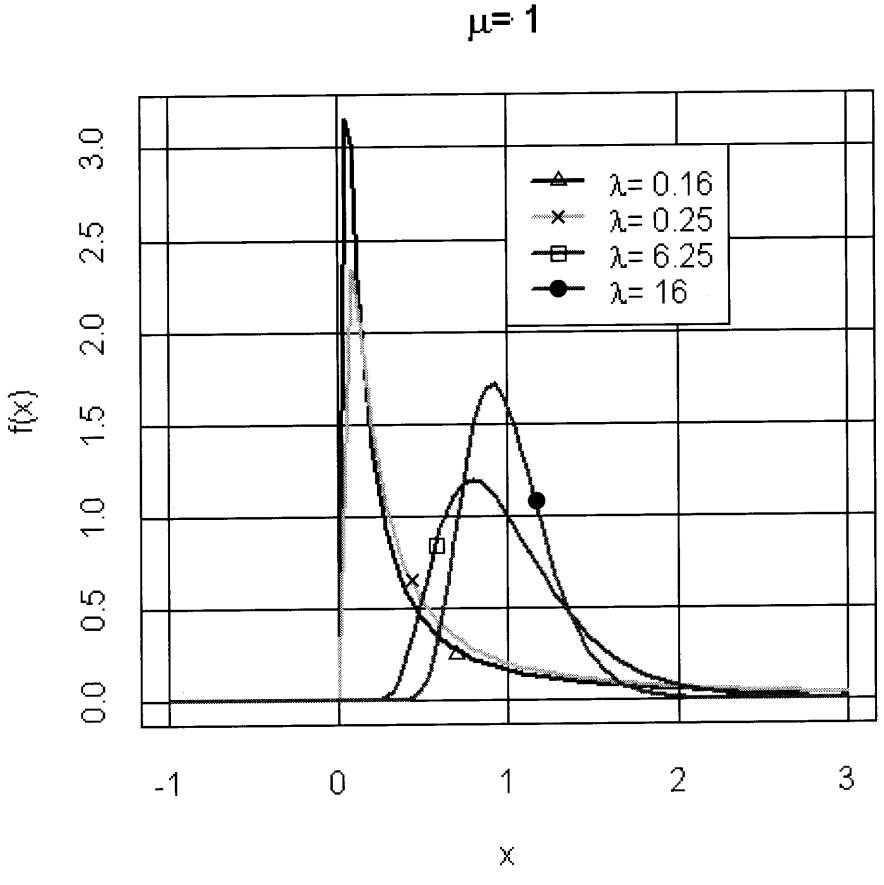

Figure A-10: Inverse Gaussian distribution

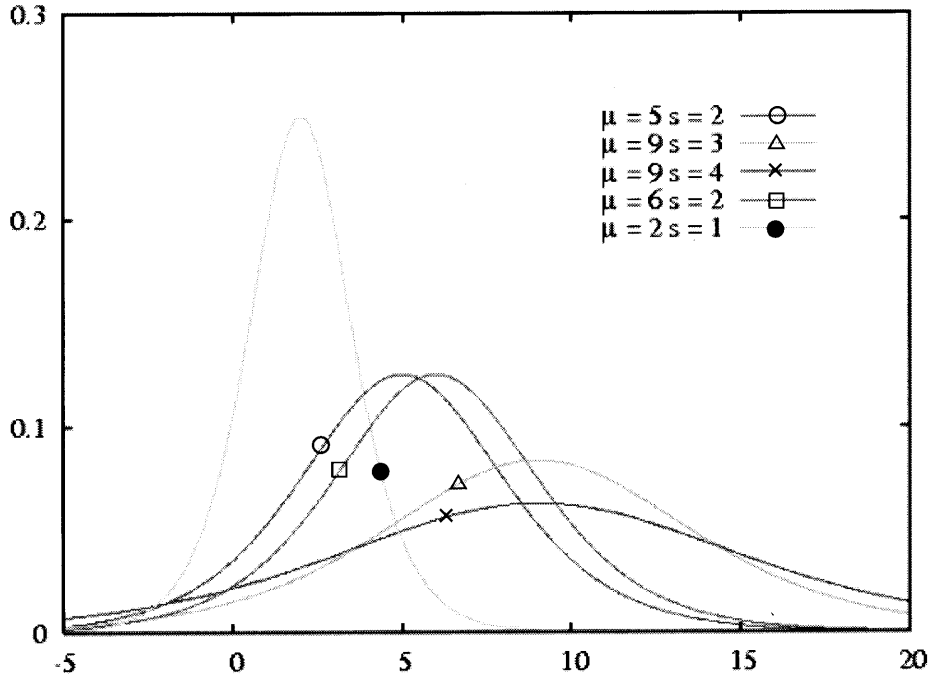

Figure A-11: Logistic distribution

- The log-logistic distribution
- The log-normal distribution as shown in Equation A-14 and Figure A-12, describing variables which can be modeled as the product of many small independent positive variables. This is the probability distribution of any random variable whose logarithm is normally distributed. If X is a random variable with a normal distribution, then exp(X) has a log-normal distribution; likewise, if Y is log-normally distributed, then log(Y) is normally distributed.

$$f(x;\mu,\sigma) = \frac{e^{-(\ln x-\mu)^2/(2\sigma)^2}}{x\sigma\sqrt{2\pi}} \qquad \text{(A-14)}$$

where μ and σ are the mean and standard deviation of the variable's logarithm.

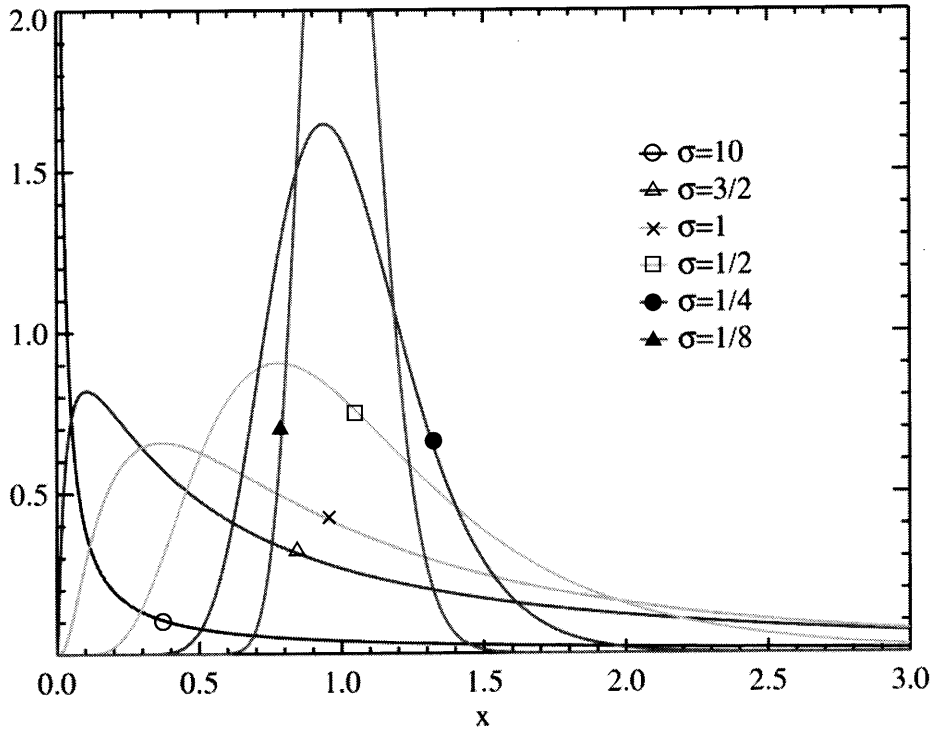

Figure A-12: Lognormal distribution

- The Pareto distribution as shown in Equation A-15 and Figure A-13, or "power law" distribution, used in the analysis of financial data and critical behavior.

$$f(x;k,x_m) = k\frac{x_m^k}{x^{k+1}} \quad for \quad x > x_m \tag{A-15}$$

where x_m is the (necessarily positive) minimum possible value of X, and k is a positive parameter.

- The Pearson distribution
- The Rayleigh distribution as shown in Equation A-16 and Figure A-14

$$f(x|\sigma) = \frac{x \cdot \exp\left(-\frac{x^2}{2\sigma^2}\right)}{\sigma^2} \tag{A-16}$$

- The Rayleigh mixture distribution
- The Rice distribution
- The type-2 Gumbel distribution
- The Wald distribution

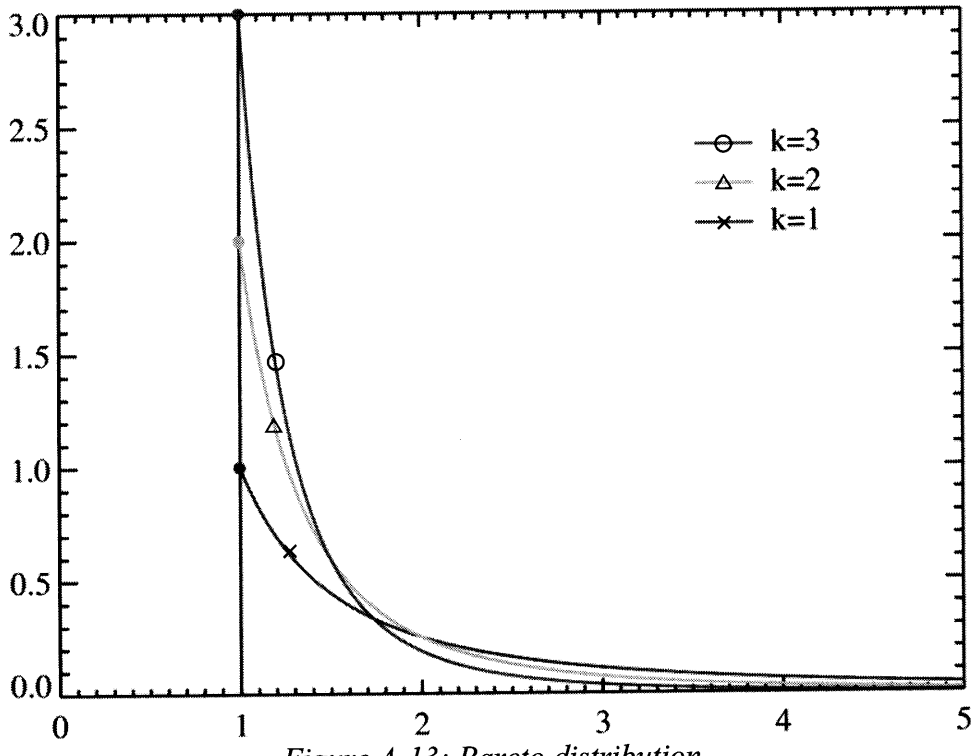

Figure A-13: Pareto distribution

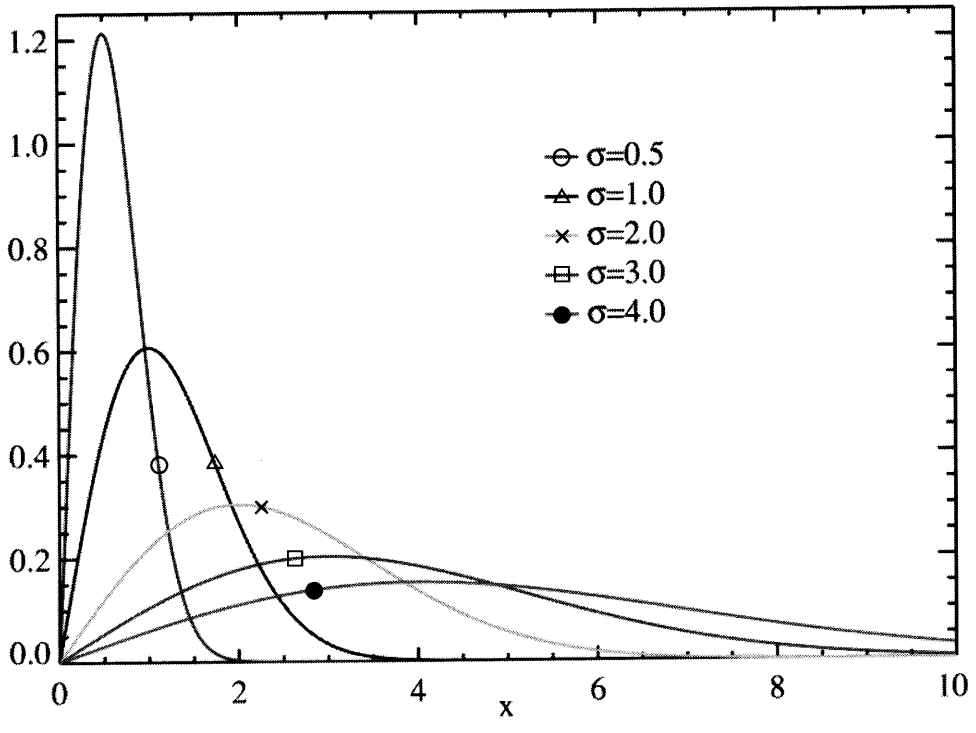

Figure A-14: Rayleigh distribution

- The Weibull distribution as shown in Equation A-17, of which the exponential distribution is a special case, is used to model the lifetime of technical devices.

$$f(x;k,\lambda)=\frac{k}{\lambda}\left(\frac{x}{\lambda}\right)^{k-1}e^{-(x/\lambda)^k} \qquad \text{(A-17)}$$

where k > 0 is the shape parameter and λ > 0 is the scale parameter of the distribution.

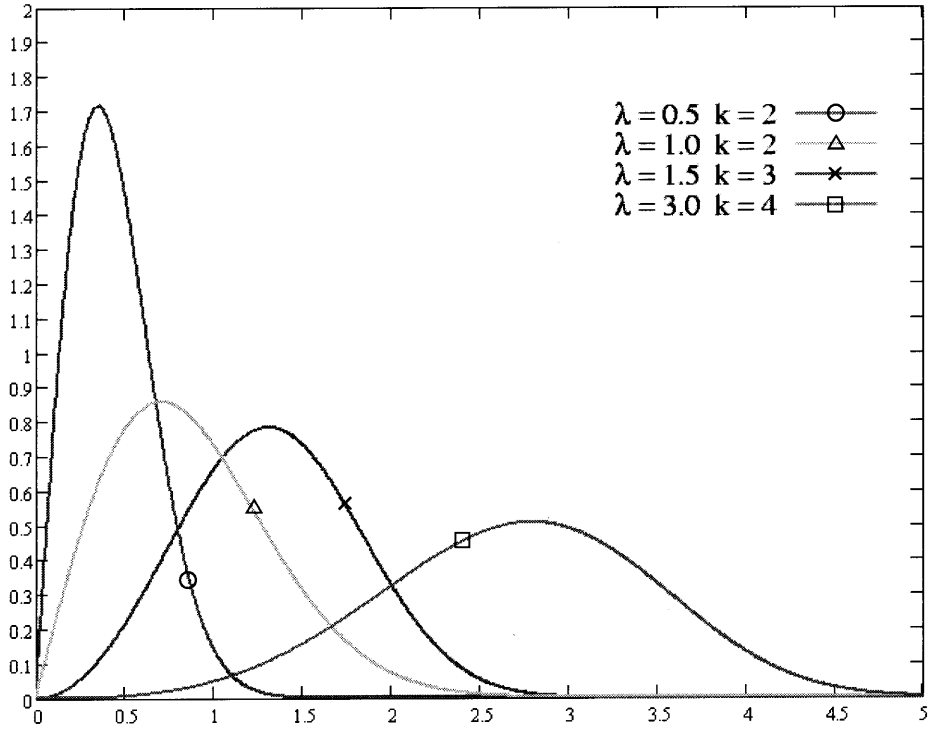

Figure A-15: Weibull distribution

A.1.2.3 Supported on the whole real line

- The Cauchy distribution, an example of a distribution which does not have an expected value or a variance. In physics it is usually called a Lorentzian profile, and is associated with many processes, including resonance energy distribution, impact and natural spectral line broadening and quadratic stark line broadening.
- The Fisher-Tippett, extreme value, or log-Weibull distribution
- The Gumbel distribution, a special case of the Fisher-Tippett distribution
- Fisher's z-distribution
- The generalized extreme value distribution as shown in Equation A-18: is a family of continuous probability distributions developed within extreme value theory to combine the Gumbel, Fréchet and Weibull families also known as type I, II and III extreme value distributions. Its importance arises from the fact that it is the limit distribution of the maxima of a sequence of independent and identically distributed random variables. Because of this, the GEV is used as an approximation to model the maxima of long (finite) sequences of random variables.

$$f(x;\mu,\sigma,\xi)=\frac{1}{\sigma}\left[1+\xi\left(\frac{x-\nu}{\sigma}\right)\right]^{-1/\xi-1}\exp\left\{-\left[1+\xi\left(\frac{x-\mu}{\sigma}\right)\right]^{-1/\xi}\right\} \quad \text{(A-18)}$$

where μ is the location parameter, σ is the scale parameter, and ξ is the shape parameter.

- The hyperbolic distribution
- The hyperbolic secant distribution
- The Landau distribution
- The Laplace distribution
- The Lévy skew alpha-stable distribution is often used to characterize financial data and critical behavior.
- The map-Airy distribution
- The normal distribution as shown in Equation A-19, also called the Gaussian or the bell curve. It is ubiquitous in nature and statistics due to the central limit theorem: every variable that can be modelled as a sum of many small independent variables is approximately normal.

$$f(x;\mu,\sigma)=\frac{1}{\sigma\sqrt{2\pi}}e^{\frac{(x-\mu)^2}{2\sigma^2}} \quad \text{(A-19)}$$

where σ is the standard deviation, and, μ is the mean.

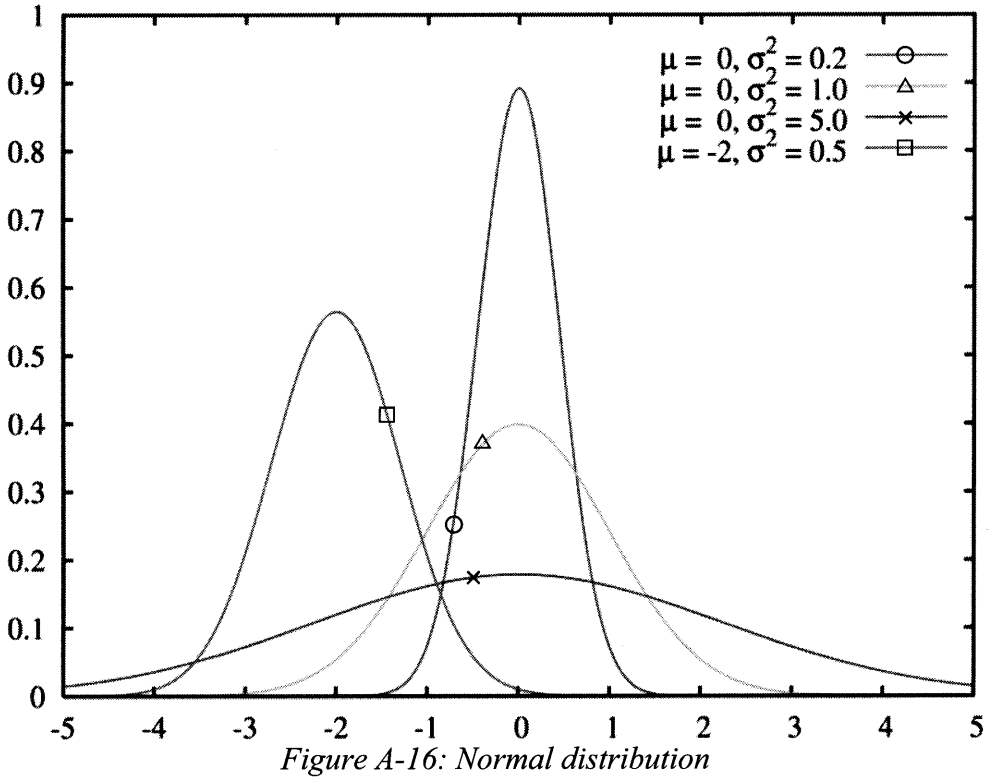

Figure A-16: Normal distribution

- The Pearson Type IV distribution
- Student's t-distribution as shown in Equation A-20, useful for estimating unknown means of Gaussian populations when the sample size is small.

$$f(t) = \frac{\Gamma\left((\nu+1)/2\right)}{\sqrt{\nu\pi}\,\Gamma(\nu/2)}\left(1+t^2/\nu\right)^{-(\nu+1)/2} \qquad \text{(A-20)}$$

The parameter ν is conventionally called the number of degrees of freedom. The distribution depends on ν , but not μ or σ ; the lack of dependence on μ and σ is what makes the t-distribution important in both theory and practice. Γ is the Gamma function.

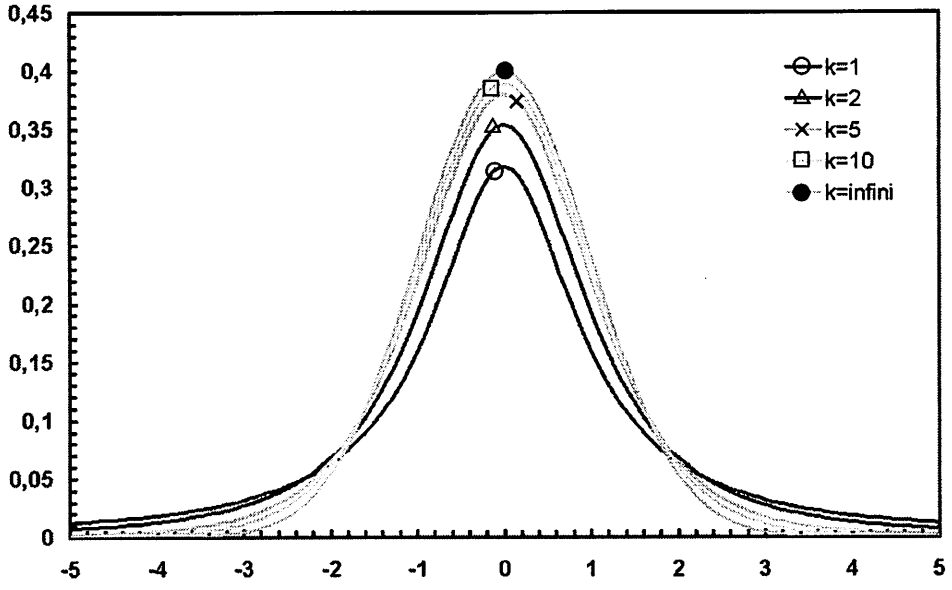

Figure A-17: Student's t-distribution

- The noncentral t-distribution
- The type-1 Gumbel distribution
- The Voigt distribution, or Voigt profile, is the convolution of a normal distribution and a Cauchy distribution. It is found in spectroscopy when spectral line profiles are broadened by a mixture of Lorentzian and Doppler broadening mechanisms.

However, only 38 different famous discrete and continuous distributions are available in the "BestFit" software as shown below.

Discrete distribution functions include Binomial, Discrete, Discrete uniform, Geometric, Hypergeometric, IntUniform, Negative Binomial, and Poisson.

Continuous distribution functions include Beta, Beta General, Chi square, Error function, Erlang, Exponential, Extreme Value, Gamme, Inverse Gaussian, Logistic, Log logistic, Lognormal, Lognormal2, Normal, Pareto, Pareto2, Pearson Type 5, Pearson Type 6, Rayleigh, Student's t, Triangular, Uniform, and Weibull.

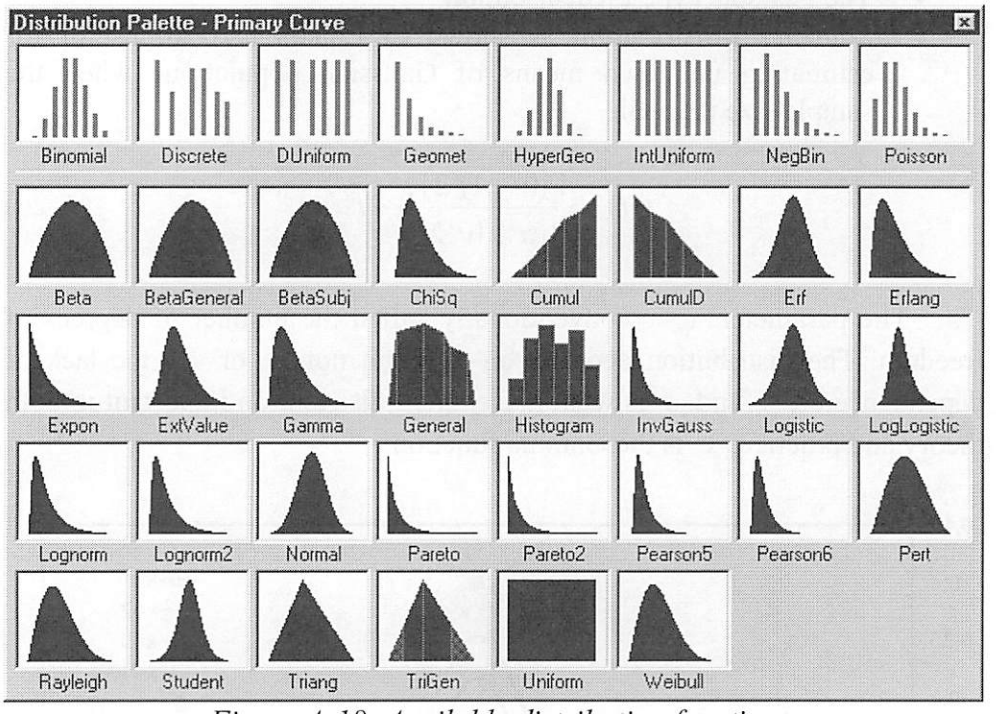

Figure A-18: Available distribution function

In order to determine the most suitable probability density function for the observed data, the goodness of fit test has to be conducted that will be explained in the next section. The most suitable probability density function is the function that can simulate the data and minimize the error with the observed data.

A.2 GOODNESS OF FIT TEST

Goodness of fit means how well a statistical model fits a set of observations. Measures of goodness-of-fit typically summarize the discrepancy between observed values and the values expected under the model in question. Four famous tests are Chi-Square test, Kolmogorov-Smirnov test, Anderson-Darling test, and root mean squared error.

A.2.1 Chi-square goodness of fit test

The Chi-Square test is the most common goodness-of-fit test. It can be used with sample input data and any type of distribution function (discrete or continuous). A weakness of the Chi-Square test is that there are no clear guidelines for selecting intervals or bins. An attractive feature of the chi-square goodness-of-fit test is that it can be applied to any univariate distribution for which you can calculate the cumulative distribution function. The chi-square goodness-of-fit test is applied to binned data (i.e., data put into classes). This is actually not a restriction since for non-binned data you can simply calculate a histogram or frequency table before generating the chi-square test. However, the value of the chi-square test statistic is dependent on how the data is binned. Another disadvantage of the chi-square test is that it requires a sufficient sample size in order for the chi-

square approximation to be valid. The chi-square test is an alternative to the Anderson-Darling and Kolmogorov-Smirnov goodness-of-fit tests. The chi-square goodness-of-fit test can be applied to discrete distributions such as the binomial and the Poisson. The Kolmogorov-Smirnov and Anderson-Darling tests are restricted to continuous distributions. For the chi-square goodness-of-fit computation, the data are divided into k bins and the test statistic is defined as shown in Equation A-21.

$$\chi^2 = \sum_{i=1}^{k} (O_i - E_i)^2 / E_i \qquad \text{(A-21)}$$

where O_i is the observed frequency for bin i and E_i is the expected frequency for bin i. This test is sensitive to the choice of bins. There is no optimal choice for the bin width (since the optimal bin width depends on the distribution). Most reasonable choices should produce similar, but not identical, results. Dataplot uses 0.3*s, where s is the sample standard deviation, for the class width. The lower and upper bins are at the sample mean plus and minus 6.0*s, respectively. For the chi-square approximation to be valid, the expected frequency should be at least 5. This test is not valid for small samples, and if some of the counts are less than five, you may need to combine some bins in the tails.

A.2.2 Kolmogorov-Smirnov goodness of fit test (K-S test)

The Kolmogorov-Smirnov test does not depend on the number of bins, which makes it more powerful than the Chi-Square test. This test can be used with sample input data but cannot be used with discrete distribution functions. A weakness of the Kolmogorov-Smirnov test is that it does not detect tail discrepancies very well. The Kolmogorov-Smirnov (K-S) test is based on the empirical distribution function (ECDF). Given N ordered data points Y1, Y2, ... , YN, the ECDF is defined as shown in Equation A-22.

$$E_N = n(i)/N \qquad \text{(A-22)}$$

where n(i) is the number of points less than Y_i and the Y_i are ordered from smallest to largest value. This is a step function that increases by 1/N at the value of each ordered data point.

Figure A-19 shows a plot of the empirical distribution function with a normal cumulative distribution function for 100 normal random numbers. The K-S test is based on the maximum distance between these two curves.

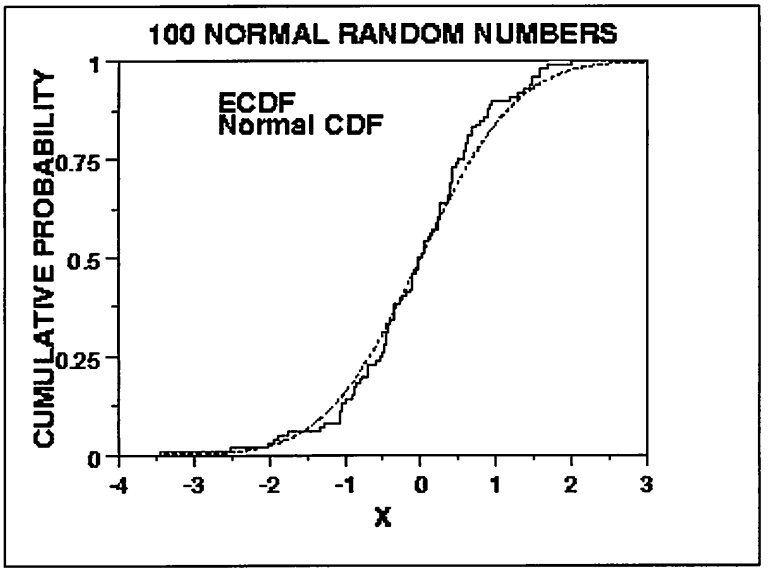

Figure A-19: Comparison between Empirical and Normal cumulative density function

An attractive feature of this test is that the distribution of the K-S test statistic itself does not depend on the underlying cumulative distribution function being tested. Another advantage is that it is an exact test (the chi-square goodness-of-fit test depends on an adequate sample size for the approximations to be valid). Despite these advantages, the K-S test has several important limitations:

- It only applies to continuous distributions.
- It tends to be more sensitive near the center of the distribution than at the tails.
- Perhaps the most serious limitation is that the distribution must be fully specified. That is, if location, scale, and shape parameters are estimated from the data, the critical region of the K-S test is no longer valid. It typically must be determined by simulation.

Due to limitations 2 and 3 above, many analysts prefer to use the Anderson-Darling goodness-of-fit test. However, the Anderson-Darling test is only available for a few specific distributions. The Kolmogorov-Smirnov test statistic is defined as shown in Equation A-23.

$$D = \max_{1 \le i \le N} \left[F(Y_i) - \frac{i-1}{N}, \frac{i}{N} - F(Y_i) \right] \qquad \text{(A-23)}$$

where F is the theoretical cumulative distribution of the distribution being tested which must be a continuous distribution (i.e., no discrete distributions such as the binomial or Poisson), and it must be fully specified (i.e., the location, scale, and shape parameters cannot be estimated from the data).

A.2.3 Anderson-Darling goodness of fit test (A-D test)

The Anderson-Darling test is very similar to the Kolmogorov-Smirnov test, but it places more emphasis on tail values. It does not depend on the number of intervals. The K-S test is distribution free in the sense that the critical values do not depend on the specific distribution being tested. The Anderson-Darling test makes use of the specific distribution in calculating critical values. This has the advantage of allowing a more sensitive test and the disadvantage that critical values must be calculated for each distribution. Currently, tables of critical values are available for the normal, lognormal, exponential, Weibull, extreme value type I, and logistic distributions. We do not provide the tables of critical values in this Handbook (see Stephens 1974, 1976, 1977, and 1979) since this test is usually applied with a statistical software program that will print the relevant critical values. The Anderson-Darling test is an alternative to the chi-square and Kolmogorov-Smirnov goodness-of-fit tests. The Anderson-Darling test statistic is defined as shown in Equation A-24 and A-25.

$$A^2 = -N - S \tag{A-24}$$

$$S = \sum_{i=1}^{N} \frac{(2i-1)}{N} \left[\ln F(Y_i) + \ln(1 - F(Y_{N+1-i}))\right] \tag{A-25}$$

where F is the cumulative distribution function of the specified distribution. Note that the Y_i are the ordered data.

A.2.4 Root mean squared error test (RMSE)

If the input data type is Density Curve or Cumulative Curve, only the RMS Error test is used to fit distributions. The mean squared error or MSE of an estimator is the expected value of the square of the "error." The error is the amount by which the estimator differs from the quantity to be estimated. The difference occurs because of randomness or because the estimator doesn't account for information that could produce a more accurate estimate. The MSE of an estimator θ_i with respect to the estimated parameter θ_c is defined as shown in Equation A-26.

$$MSE(\theta_i) = E\left[(\theta_i - \theta_e)^2\right] \tag{A-26}$$

The root mean squared error (RMSE) (or root mean squared deviation (RMSD)) is then simply defined as the square root of the MSE as shown in Equation A-27.

$$RMSE(\theta_i) = \sqrt{MSE(\theta_i)} \tag{A-27}$$

REFERENCES

[1] http://en.wikipedia.org/wiki/Main_Page
[2] http://www.palisade.com

APPENDIX B

B.1 COVERING DEPTH OF REINFORCING STEEL

B.1.1 Bridge No.1

Table B-1: Reinforcing steel covering depth of Bridge No.1 in mm.

114	19	139	100	102	118	93	92	79	92
99	20	104	104	99	107	92	88	85	87
100	57	106	93	79	82	88	92	78	89
96	67	120	86	86	92	98	85	74	92
88	63	102	79	80	89	89	78	80	76
91	60	90	114	76	95	104	75	84	77
88	60	88	100	75	88	94	81	77	78
82	62	86	112	77	97	107	77	76	83
95	56	52	114	73	95	91	84	77	92
74	60	49	125	71	96	99	85	82	81
82	49	45	128	77	101	117	99	87	78
93	51	44	41	71	87	109	89	111	72
88	48	38	110	106	106	93	93	92	66
75	97	105	92	86	84	104	106	82	91
76	108	98	103	74	101	107	86	70	118
79	84	92	103	72	91	100	99	102	91
85	97	106	125	98	106	120	108	112	106
110	92	92	102	76	143	115	95	103	87
93									

B.1.2 Bridge No. 2

Table B-2: Reinforcing steel covering depth of Bridge No.2 in mm.

33	18	18	18	31	29	19	24	20	18
29	20	14	17	36	24	19	33	16	19
42	19	17	17	51	29	17	20	18	18
37	20	16	18	48	30	16	16	17	17
30	18	13	15	34	27	17	18	15	24
40	20	16	16	27	27	16	19	16	24
37	20	14	16	16	19	16	17	18	28
38	23	19	17	19	20	16	20	14	16
37	25	14	14	16	19	19	19	15	21
32	25	17	20	18	17	22	20	24	29
22	26	20	21	18	15	25	44	21	31
19	28	16	20	21	16	26	34	26	31
14	31	20	17	23	17	20	33	23	28
13	30	19	17	21	17	20	40	20	29
16	20	28	15	30	16	25	41	20	30
17	20	20	17	25	16	26	33	20	31
15	17	23	11	37	16	24	36	17	31

18	13	21	30	31	15	26	25	19	18
92	20	24	20	26	38	23	21	26	19
101	20	26	19	23	37	24	22	23	18
29	17	28	19	19	35	19	18	21	18
34	19	31	22	19	51	16	19	23	25
29	25	28	23	18	36	19	19	22	26
28	23	25	20	18	48	20	19	16	31
26	18	28	29	21	38	16	16	21	32
23	20	25	23	25	39	17	19	17	25
29	20	31	41	23	36	17	19	20	25
29	20	31	39	20	32	15	19	95	23
30	20	24	41	20	34	17	20	110	23
31	20	23	39	22	32	16	19	66	20
30	19	26	26	20	33	18	17	75	18
32	24	29	43	20	33	30	18	79	17
29	24	30	42	19	18	30	17	33	19
27	18	39	43	21	23	42	22	42	18
30	20	48	40	19	16	31	20	44	19
28	19	25	27	20	25	19	30	35	23
25	19	23	18	18	25	29	24	58	25
21	17	25	18	18	29	29	25	58	29
22	18	24	14	19	26	23	23	36	28
24	19	27	15	20	20	28	22	26	17
22	16	22	17	23	23	21	18	23	18
24	14	23	17	22	21	30	17	21	19
16	18	25	18	19	23	33	17	20	20
20	19	32	16	18	21	33	17	18	18
20	20	31	14	24	18	23	18	19	18
17	20	24	15	46	20	41	14	20	17
18	16	24	16	44	20	41	16	20	17
27	20	26	15	86	19	29	19	21	20
26	21	24	17	39	21	32	29	22	18
23	19	21	18	35	21	35	23	25	22
22	18	20	18	35	21	29	25	25	21
20	20	21	15	36	21	21	19	18	29
20	22	29	19	31	23	28	25	19	84
20	32	25	18	36	23	25	22	18	65
22	34	22	37	15	26	25	28	20	23
20	33	29	21	16	30	27	11	17	22
23	27	23	20	17	38	17	11	16	19
22	27	20	20	16	28	18	12	13	19
23	18	29	18	18	23	19	13	14	19
21	18	24	18	18	24	21	10	15	21
20	18	26	21	18	21	20	11	14	21
22	17	24	20	16	20	22	10	16	33
23	13	22	22	18	18	19	12	11	82
24	17	18	25	19	17	22	8	17	87
25	17	21	19	22	17	19	15	12	75

26	17	19	22	24	18	22	14	15	65
26	17	21	21	31	16	23	17	14	73
25	28	18	19	21	16	20	19	15	28
23	22	20	25	19	17	18	22	12	23
23	21	21	24	19	21	22	18	14	20
24	13	21	23	18	19	30	51	14	20
22	17	27	18	20	16	69	40	15	20
22	16	31	21	23	19	58	42	15	21
21	16	23	22	13	25	111	54	16	23
24	17	23	20	12	26	62	44	17	26
24	15	19	23	11	27	48	24	18	30
18	17	19	20	12	25	41	26	17	25
22	16	20	23	11	20	37	25	18	26
16	17	20	21	8	78	44	21	19	26
21	19	17	19	27	81	32	23	18	26
20	19	23	20	23	94	41	17	17	30
19	19	40	18	25	25	19	17	16	30
20	18	24	18	23	20	16	16	18	23
22	24	20	19	21	31	18	18	17	22
24	23	21	20	21	32	19	17	16	21
37	24	20	26	15	25				

B.1.3 Bridge No. 3

Table B-3: Reinforcing steel covering depth of Bridge No.3 in mm.

40	41	29	61	41	56	24	23	52	46
44	42	33	65	44	68	52	20	51	56
49	48	30	68	41	61	60	26	46	55
49	50	32	64	45	59	61	26	54	55
54	47	31	64	43	46	52	33	59	57
61	46	30	71	39	45	64	28	57	60
62	50	25	42	34	46	64	24	60	73
57	53	28	36	44	29	63	23	62	52
73	48	33	28	37	25	87	29	76	50
54	60	50	34	29	27	65	28	54	45
62	55	44	28	29	22	65	27	49	66
61	53	48	31	36	19	62	26	51	51
69	60	48	28	31	50	58	21	33	51
61	62	46	24	25	19	48	37	41	44
59	62	46	39	32	42	44	36	38	45
71	67	44	31	31	49	45	37	39	38
63	58	46	29	47	49	46	32	39	32
56	68	34	24	45	59	49	35	36	32
54	45	65	22	54	66	45	29	40	35
51	49	54	22	42	70	47	32	45	30
51	49	49	19	55	68	47	28	35	35
48	45	61	20	48	82	39	66	46	28
46	33	63	49	49	87	31	58	45	30

42	45	62	49	46	42	36	56	49	28
36	44	59	60	39	37	33	63	49	31
87	43	69	55	44	29	29	53	47	27
59	35	65	60	47	34	31	59	52	31
72	49	52	64	52	29	29	57	38	35
73	47	60	61	49	31	50	62	44	40
57	52	32	67	35	28	43	61	56	39
59	24	25	34	33	40	81	55	47	58
51	27	42	32	28	40	55	43	49	54

B.1.4 Bridge No. 4

Table B-4: Reinforcing steel covering depth of Bridge No.4 in mm.

31	59	31	35	19	44	24	37	49	53
28	53	54	37	16	26	46	39	47	15
22	26	38	34	15	12	27	44	56	39
26	35	45	37	14	19	27	49	42	25
26	35	30	38	12	17	27	54	41	33
24	33	26	36	42	29	35	57	14	56
26	36	14	28	43	44	35	53	29	22
18	32	20	13	48	25	31	19	14	41
24	28	24	9	38	28	30	19	21	19
25	18	34	11	45	45	44	9	47	20
52	17	40	19	42	47	43	18	37	59
52	26								

B.1.5 Bridge No.5

Table B-5: Reinforcing steel covering depth of Bridge No.5 in mm.

49	20	34	45	51	63	15	66	39	54
42	41	30	40	43	68	16	70	36	58
31	44	24	37	47	76	19	66	37	64
24	51	15	40	36	67	19	64	27	71
38	17	27	31	35	68	27	73	16	54
27	24	37	27	32	64	29	74	10	65
48	26	12	18	39	77	25	69	26	66
35	24	32	21	35	72	25	65	29	67
22	18	57	24	27	67	29	65	29	65
35	17	49	36	26	72	23	60	30	55
33	25	50	40	26	66	27	67	26	65
37	34	22	47	37	69	29	68	29	60
42	40	29	54	52	77	24	76	53	55
26	45	22	62	35	71	25	98	29	54
32	50	15	54	16	62	27	65	28	51
29	28	12	46	24	73	31	69	24	47
30	29	14	49	45	74	26	70	29	44
36	35	21	41	47	73	46	73	28	43
36	20	21	37	44	68	47	63	40	45

20	18	27	21	45	66	39	69	28	50
16	23	34	29	30	66	36	60	32	83
20	26	34	8	30	64	31	63	34	81
19	43	29	16	30	70	53	71	19	69
20	46	35	14	27	24	35	76	17	74
43	30	34	33	29	17	21	72	20	71
29	16	34	35	26	14	31	83	20	57
27	39	32	26	26	46	36	79	21	66
32	38	23	17	27	36	34	76	23	59
40	35	28	13	27	37	35	112	26	57
34	39	18	10	24	33	9	81	39	57
36	38	15	18	49	41	31	67	37	54
33	45	11	41	33	24	38	76	48	54
31	44	6	59	29	37	34	72	49	63
33	44	7	56	26	40	24	69	54	66
11	43	13	69	37	37	30	66	40	71
48	36	15	62	28	37	20	72	44	65
18	36	15	51	51	40	25	72	40	67
17	34	17	53	27	74	44	66	42	66
33	35	36	54	30	54	23	70	39	75
39	30	47	57	22	58	27	63	46	68
39	42	31	51	33	57	31	61	35	70
51	34	34	64	27	59	26	53	29	81
55	31	37	66	29	64	28	57	27	62
61	31	54	65	27	67	30	62	27	59
44	29	38	67	26	70	25	64	27	63
38	21	36	116	29	75	19	65	29	61
60	19	36	64	35	67	18	68	40	65
48	26	43	74	39	77	15	66	32	62
46	22	43	56	33	76	18	80	32	51
46	25	29	54	34	78	14	70	46	61
48	27	35	55	34	57	18	81	28	63
57	40	26	59	37	50	26	71	24	58
52	40	24	61	39	54	36	66	25	64
45	41	32	61	42	60	49	64	31	64
39	46	29	66	41	69	10	85	27	54
31	43	37	58	41	34	34	66	27	75
39	47	44	62	42	64	28	42	33	82
40	38	17	20	55	35	29	32	29	70
31	56	18	25	47	40	25	35	31	69
31	58	15	28	43	21	50	31	18	64
29	62	31	31	44	20	30	36	16	60
30	61	14	31	49	31	18	49	20	61
35	62	21	26	49	36	25	35	29	59
17	59	23	25	44	35	30	34	36	57
37	55	28	28	26	34	36	40	36	61
38	64	39	34	23	46	28	44	36	64
33	65	64	32	19	25	43	44	35	61

34	66	28	34	16	42	29	38	47	69
34	73	26	30	11	43	50	35	47	120
38	67	26	16	37	44	38	28	39	84
26	65	36	16	24	44	38	36	28	77
35	66	25	29	45	35	39	35	19	9
34	76	27	24	43	44	45	36	41	19
86	68	27	17	49	37	31	38	42	31
78	66	11	18	41	23	32	28	41	44
62	68	11	24	52	26	34	29	39	29
59	71	39	37	44	30	35	28	36	30
60	85	28	36	44	37	36	28	36	36
67	72	21	40	45	38	50	30	35	42
80	68	19	36	39	38	41	32	35	35
73	76	16	45	33	31	42	41	37	38
68	81	16	35	32	33	43	35	32	36
72	74	24	40	19	41	43	34	20	40
65	72	27	34	44	40	40	30	19	25
67	71	32	35	44	46	29	32	24	20
61	72	38	37	32	35	27	31	25	16
79	73	33	40	26	39	27	81	32	33
78	60	35	42	32	43	37	103	33	35
75	54	33	10	20	33	43	95	31	30
74	57	43	7	11	28	47	100	32	23
61	56	41	9	11	31	36	96	37	18
65	57	42	16	17	40	41	100	36	31
98	60	50	37	17	36	33	90	92	33
111	65	45	32	34	33	37	93	49	42
63	58	27	31	20	29	26	100	48	37
14	61	27	31	30	30	27	95	44	42
18	55	29	37	32	30	29	106	57	41
20	56	17	32	35	30	32	97	50	47
25	26	19	60	47	35	44	123	54	38
28	23	19	29	23	34	25	76	31	39
34	41	11	30	18	52	15	78	24	33
43	38	16	34	14	40	16	83	21	27
22	24	23	34	37	41	26	79	48	26
29	44	25	29	37	41	24	88	18	38
20	32	39	54	47	39	23	81	20	39
25	46	27	35	40	40	35	77	23	14
36	34	20	30	32	47	49	69	31	8
44	28	18	29	49	41	15	63	42	9
48	28	14	27	43	62	22	58	49	18
50	24	38	25	49	45	32	64	46	21
73	32	45	36	44	46	28	15	43	84
33	31	50	42	35	26	36	65	44	66
20	31	41	37	25	29	33	86	48	72
77	32	41	51	26	36	32	59	43	81
46	26	28	40	27	35	36	64	15	67

36	36	33	36	27	32	34	67	38	70
35	36	33	30	31	36	32	64	30	69
74	32	35	90	39	35	33			

B.2 REBOUND NUMBER OF SCHMIDT HAMMER

B.2.1 Bridge No.1

Table B-6: Rebound number of Bridge No.1

32	43	47	45	33	57	34	44	42	34
39	46	44	45	37	54	46	50	34	36
41	46	44	45	38	59	51	46	37	37
37	44	46	47	40	54	35	44	36	44
34	52	43	48	41	47	39	41	31	36
42	43	43	50	32	48	53	38	47	49
34	44	45	44	45	46	42	44	34	32
52	46	44	46	42	47	32	34	35	42
54	43	53	44	37	49	31	24	30	45
54	49	41	43	45	41	41	48	39	43
54	49	47	44	36	46	47	46	33	46
44	50	46	43	36	42	41	45	34	55
43	49	47	43	32	46	43	45	30	47
37	44	47	41	36	38	47	42	32	50
31	44	41	55	33	49	42	40	32	46
42	43	43	49	35	48	33	46	32	44
33	46	45	48	31	43	33	46	35	44
35	45	45	41	32	28	46	45	35	47
31	43	45	45	33	38	46	44	30	46
31	46	39	44	32	38	38	49	30	48
36	44	47	41	36	46	31	45	36	44
42	34	39	46	30	46	32	45	35	43
43	33	40	30	31	50	42	45	34	35
32	34	43	42	41	54	41	47	37	40
38	37	46	51	30	35	41	46	29	41
32	36	37	49	35	38	33	43	44	41
36	36	43	51	34	55	43	51	37	46
49	36	47	44	41	46	36	44	30	46
42	38	47	45	33	45	39	44	35	39
51	44	41	46	36	50	29	40	29	41
52	39	36	44	43	46	43	45	36	42
54	32	39	45	43	41	44	46	42	41
45	38	44	31	44	41	40	45	35	44
33	36	39	40	44	46	44	43	33	41
33	36	45	41	39	49	37	43	41	44
33	42	53	48	44	45	43	44	33	28
28	54	46	37	46	47	50	44	31	40
36	50	36	54	46	38	45	42	32	52

36	43	31	50	35	38	42	46	33	43
41	38	44	49	42	53	31	46	43	40
30	45	36	46	42	51	34	38	32	41
31	43	41	47	44	52	34	39	42	43
32	48	31	50	43	53	38	41	37	33
35	42	31	45	47	57	43	41	36	46
36	40	32	48	40	43	41	42	33	37
36	42	37	55	42	45	39	41	31	41
42	44	34	51	34	54	39	42	38	47
37	47	35	54	47	47	43	39	37	47
31	44	44	46	38	48	32	39	36	41
50	35	41	52	34	47	31	43	34	43
43	50	34	46	42	33	31	44	45	50
38	48	32	43	37	41	44	44	46	43
43	43	28	42	42	42	47	45	45	44
44	43	32	40	33	37	45	52	44	53
47	46	31	46	39	43	45	50	44	44
50	47	32	45	42	42	46	47	46	34
44	45	40	50	37	31	46	47	41	33
46	47	32	46	34	33	40	52	44	36
51	54	39	45	36	28	44	57	43	44
46	53	33	50	45	27	42	52	43	46
47	52	31	41	49	30	44	47	44	55
35	44	33	49	45	35	43	48	47	53
34	31	33	51	50	33	40	51	55	46
42	43	38	32	45	28	36	41	50	44
45	53	41	43	58	33	44	43	29	38
43	47	35	35	46	27	45	40	33	51
42	41	35	32	38	20	45	42	35	52
41	43	33	42	40	29	42	43	44	55
40	49	34	47	49	29	42	31	44	50
38	44	33	51	34	35	43	41	29	46
46	48	34	36	37	31	45	38	47	52
50	46	36	37	38	29	44	39	35	45
45	53	33	37	43	43	45	44	33	43
42	47	33	35	38	30	45	41	47	45
45	45	38	37	47	36	35	51	45	54
46	44	36	37	34	34	50	41	46	40
44	44	34	34	36	43	45	46	42	43
53	45	33	35	31	43	49	48	43	51
49	36	28	37	46	42	43	36	46	43
55	38	31	38	51	44	42	35	34	28
46	44	36	43	32	44	44	44	42	51
38	37	44	42	45	43	42	53	42	43
44	48	35	33	46	42	45	53	40	50
38	43	40	34	46	44	45	55	42	43
30	40	40	36	41	42	38	54	44	46
33	36	40	29	38	43	43	51	57	32

32	38	43	36	37	41	43	51	43	43
40	35	43	32	37	53	44	46	45	37
42	39	46	37	53	45	45	47	43	34
38	50	49	36	39	43	41	51	44	41
40	49	52	32	34	42	39	50	45	45
52	44	44	31	46	43	44	44	38	42
32	34	46	42	44	36	44	55	40	42
45	48	44	33	43	37	38	52	60	41
46	44	39	32	43	50	30	45	43	35
37	45	46	40	32	45	45	46	45	36
51	44	44	36	23	45	40	46	43	38
47	34	33	29	25	49	41	54	46	32
31	46	48	45	33	46	45	52	45	50
40	44	41	45	33	50	44	52	47	55
52	46	48	52	41	46	45	50	48	55
54	49	40	45	44	45	43	44	30	51
51	52	46	44	39	47	45	49	54	57
53	55	44	35	36	48	42	53	44	59
50	45	42	36	36	52	45	55	44	46
52	48	37	46	36	54	44	46	49	49
52	51	33	39	50	39	44	51	43	53
53	53	46	42	44	44	42	51	46	54
54	49	39	45	38	44	45	49	45	53
50	51	40	42	39	33	39	51	50	52
43	53	44	41	55	35	44	50	46	45
44	46	41	42	54	35	42	52	47	37
47	58	42	38	56	33	45	47	40	50
43	49	41	44	51	28	44	52	54	56
45	49	43	39	51	40	36	48	48	53
38	54	42	38	36	41	43	48	49	56
39	52	43	39	41	45	40	47	51	55
47	51	43	43	36	44	44	53	46	59
48	50	36	42	47	50	42	56	45	38
44	45	44	41	38	37	43	54	42	48
35	53	41	41	44	40	43	49	45	36
32	48	41	39	42	36	42	57	44	55
41	48	41	43	49	41	31	51	44	55
34	49	40	38	41	42	44	53	52	48
40	50	43	39	35	42	45	56	46	43
31	60	41	39	41	43	38	53	38	45
40	49	42	35	39	46	42	47	43	47
49	46	43	41	45	45	45	51	38	32
47	47	46	37	38	53	47	57	46	49
47	59	38	32	45	37	35	59	46	45
53	38	51	36	43	54	44	59	47	47
43	46	44	30	43	48	38	58	45	54
44	48	41	50	45	45	33	56	51	53
43	53	28	50	41	46	47	56	50	45

43	54	30	50	41	51	39	37	44	47
46	43	37	52	44	50	43	58	44	35
45	41	44	50	43	46	44	51	45	38
51	42	42	45	44	49	44	56	47	42
53	41	38	48	47	52	44	54	46	45
47	41	31	51	45	44	35	55	47	48
41	46	31	50	45	43	50	55	53	38
41	43	41	45	42	47	44	33	50	40

B.2.2 Bridge No.2

Table B-7: Rebound number of Bridge No.2

30	36	52	33	43	49	47	45	47	57
43	47	47	36	54	48	44	52	43	56
43	46	32	33	38	43	45	47	44	57
45	47	45	43	33	54	40	42	53	59
38	44	42	43	41	38	43	43	50	40
44	42	50	43	39	42	39	54	51	55
36	46	39	29	43	41	45	57	56	57
43	46	48	28	47	50	45	36	49	59
55	43	45	41	44	44	44	49	56	57
47	42	51	37	44	41	50	46	46	56
57	44	40	37	33	35	41	48	45	60
42	59	43	36	38	43	46	46	40	57
49	44	43	34	45	45	46	42	56	41
37	46	48	39	38	45	44	51	36	55
45	44	33	40	51	59	51	42	42	57
32	42	40	46	33	49	44	49	51	39
43	31	46	34	44	59	47	51	47	44
52	32	48	36	41	42	51	46	38	44
56	49	36	39	38	46	43	47	42	41
34	56	40	32	30	55	49	41	53	42
46	46	42	35	40	43	48	45	44	41
44	44	40	44	37	42	50	50	39	43
43	52	46	43	36	38	49	44	34	41
54	43	39	46	37	50	47	52	45	47
47									

B.2.3 Bridge No.3

Table B-8: Rebound number of Bridge No.3

32	56	44	40	47	53	57	50	56	45
36	46	47	32	44	55	56	46	57	52
31	55	52	33	53	53	56	51	53	53
34	52	46	36	52	47	56	49	57	46
37	52	56	42	52	49	47	49	60	48
34	54	47	34	45	52	55	51	60	60
42	53	44	33	45	46	49	45	57	54

33	55	39	37	48	50	57	51	56	50
34	50	46	42	45	53	50	52	58	55
29	54	48	40	48	53	51	58	59	53
36	55	46	35	51	50	48	52	55	56
37	54	49	47	51	51	47	47	59	46
44	53	49	55	50	51	29	48	52	51
55	57	45	46	52	54	52	56	55	52
58	39	47	46	54	48	50	47	56	50
50	56	50	50	48	54	51	47	56	56
55	54	53	50	49	44	52	49	57	54
55	54	50	53	60	43	46	55	58	52
58	52	52	52	57	54	54	52	50	52
56	51	45	47	54	25	50	45	53	55
58	56	54	48	55	47	49	56	50	56
57	54	56	47	42	48	46	56	57	52
61	42	54	44	49	44	52	44	32	51
58	52	49	52	55	51	54	48	30	55
56	51	48	48	55	41	55	55	33	42
57	53	48	51	50	45	57	55	35	56
58	54	39	54	54	46	57	52	29	52
59	55	48	51	52	45	56	49	31	59
60	52	46	50	50	45	54	53	34	64
57	55	45	54	55	49	48	45	35	55
57	53	49	46	55	47	49	54	29	56
53	53	51	52	54	44	53	54	34	53
61	56	48	42	57	46	41	32	30	55
43	56	59	55	56	53	58	57	57	39
34	35	35	34						

B.2.4 Bridge No.4

Table B-9: Rebound number of Bridge No.4

47	46	45	53	39	55	47	44	56	46
55	46	41	48	37	49	49	45	53	45
54	45	45	51	43	50	41	43	59	42
53	50	47	52	42	50	48	44	47	47
52	48	43	46	44	56	44	45	54	43
58	54	41	48	41	45	51	47	53	49
43	40	46	48	42	47	49	47	49	44
54	48	42	51	45	45	50	46	59	46
56	52	39	47	43	57	47	45	58	42
53	52	44	46	55	51	48	48	54	47
54	58	43	55	56	46	43	49	56	44
42	46	48	56	41	54	49	55	54	45
47	58	41	49	55	57	46	58	51	53
56	46	44	45	55	56	43	52	51	46
56	54	49	47						

B.2.5 Bridge No.5

Table B-10: Rebound number of Bridge No.5

47	46	45	53	39	55	47	44	56	46
50	55	50	43	47	49	54	53	37	50
47	54	48	47	51	52	52	44	40	51
54	51	55	43	47	48	53	51	42	49
58	54	52	48	46	45	55	50	46	38
60	53	46	44	46	46	45	43	53	49
58	54	46	47	54	46	46	43	53	47
53	55	39	48	46	48	43	49	48	43
49	42	51	51	44	45	44	46	46	50
51	45	48	47	45	49	47	43	53	48
54	43	52	50	53	51	58	46	42	50
51	46	48	53	46	51	44	47	44	49
46	44	57	50	50	49	47	46	47	41
53	44	48	53	43	49	44	48	52	49
52	43	44	46	46	51	43	45	54	50
45	41	51	55	44	50	46	44	48	46
47	42	49	53	50	46	42	35	44	46
46	41	51	52	53	44	43	48	46	41
52	43	47	49	51	49	45	43	52	42
47	45	47	48	51	51	48	45	45	49
50	47	50	46	48	48	45	46	47	47
53	42	50	51	50	50	51	43	42	51
53	44	49	51	55	49	45	45	45	34
45	42	43	50	54	50	45	47	54	45
53	42	55	48	49	50	42	41	45	50
52	43	43	53	53	45	45	68	55	51
52	46	52	51	53	44	47	60	59	52
52	51	46	54	46	44	45	52	54	52
39	55	50	53	52	49	46	50	54	48
47	55	44	59	46	47	48	51	52	54
50	53	51	41	51	50	43	61	55	54
45	52	42	51	58	17	47	51	50	55
54	52	42	42	57	51	35	55	51	52
53	52	53	50	53	51	44	50	50	51
48	51	43	51	51	42	43	51	59	55
53	45	46	51	51	47	53	43	52	54
55	38	37	60	43	49	48	39	49	46
52	51	43	52	53	48	50	50	58	54
52	53	43	49	53	51	35	53	49	54
51	48	58	50	54	49	41	40	42	49
56	46	49	50	48	47	33	52	51	40
54	50	35	48	51	45	57	52	51	50
51	51	38	53	45	51	48	47	45	46
57	47	49	49	51	50	50	45	46	43
57	46	51	44	54	44	49	43	47	44

38	51	50	44	51	47	47	46	51	47
51	48	51	46	53	55	36	52	43	58
52	48	51	49	49	53	54	49	51	46
51	48	58	44	51	50	49	51	52	46
54	58	45	46	51	40	49	47	54	47
52	51	47	50	51	52	55	50	55	41
61	46	50	47	52	50	46	46	43	51
49	50	55	47	46	49	47	47	48	51
65	48	53	49	48	50	49	43	49	46
51	55	47	36	51	53	43	41	51	48
52	48	46	45	40	40	45	35	55	52
51	54	50	50	47	52	49	40	46	49
52	49	47	49	43	54	48	45	51	46
52	48	52	50	45	47	53	44	44	52
54	48	46	49	42	52	47	46	48	49
52	49	47	47	52	55	49	38	51	54
51	55	52	49	55	56	50	42	53	48
53	51	50	49	51	51	54	35	42	49
52	57	56	52	49	49	44	44	49	50
50	48	47	50	51	59	53	44	45	55
46	49	46	37	47	48	43	42	50	53
51	46	53	43	48	48	51	44	49	51
52	49	47	47	47	50	49	53	52	48
53	49	48	46	47	49	44	45	46	48
50	49	41	52	49	57	46	44	51	51
49	50	52	43	46	48	48	43	50	49
52	48	52	43	54	53	45	43	52	52
57	48	53	46	48	43	51	45	48	45
45	51	51	38	53	45	46	60	46	47
52	48	49	52	48	50	45	43	50	45
52	47	51	47	52	42	47	45	51	53
47	52	52	49	51	53	50	54	52	49
43	51	58	51	47	51	56	44	50	53
49	45	54	52	48	46	45	47	44	41
50	48	50	37	54	49	52	48	54	47
44	42	46	47	43	44	42	48	37	45

INTERNATIONAL CENTER FOR URBAN SAFETY ENGINEERING
Institute of Industrial Science, The University of Tokyo
4-6-1 Komaba, Meguro-ku,
Tokyo 153-8505, Japan
http://icus.iis.u-tokyo.ac.jp/
E-mail: icus@iis.u-tokyo.ac.jp

Tel: (+81-3)5452-6472

Fax: (+81-3)5452-6476